

Copyright
by
Kriti Kapoor
2013

**The Dissertation Committee for Kriti Kapoor Certifies that this is the approved
version of the following dissertation:**

**Modeling and Optimization for Energy Efficient Large Scale Cooling
Operation**

Committee:

Thomas Edgar, Supervisor

John Stuber

Michael Baldea

Erhan Kutanoglu

Dragan Djurdjanovic

Isaac Sanchez

**Modeling and Optimization for Energy Efficient Large Scale Cooling
Operation**

by

Kriti Kapoor, B.Tech.

Dissertation

Presented to the Faculty of the Graduate School of

The University of Texas at Austin

in Partial Fulfillment

of the Requirements

for the Degree of

Doctor of Philosophy

The University of Texas at Austin

December 2013

Dedicated to my parents and teachers.

Acknowledgements

I am extremely grateful to Prof. Thomas F Edgar for being a wonderful adviser and a constant well-wisher. Despite his many commitments, Prof. Edgar was always available for discussion and provided valuable support and guidance. His mature supervision enabled me to make independent decisions and take my projects forward on my own.

I am thankful to my committee members – Dr. Stuber, Prof. Baldea, Prof. Djurdjanovic, Prof. Kutanoglu and Prof. Sanchez for giving constructive inputs towards making wiser project selections. I was also fortunate to learn about the subjects “Statistical Methods in Semiconductor Manufacturing” (by Prof. Djurdjanovic), “Scheduling” (by Prof. Kutanoglu) and “Advanced Analysis for Chemical Engineers” (by Prof. Sanchez) by taking their courses. The expert comments and suggestions provided by Dr. Stuber and Jeff Hanson (TI, Dallas) during our monthly project review meetings have proved very valuable to my research. Ever since Prof. Baldea joined the department, I have been learning from his discussions and observations during our weekly Edgar-Baldea group meetings.

I would like to thank Cockrell School of Engineering at UT Austin and Texas Instruments Inc. for funding my research. Without the financial support they offered, it would not have been possible for me to pursue graduate studies and research. Dr. Stuber has played a vital role in getting TI sponsorship for my project.

My undergraduate institute, IIT Bombay, has also had a significant contribution in my success. Some of the courses taught by the Chemical Engineering faculty at IIT Bombay strengthened my concepts while improving my analytical skills.

It has been a great learning experience to be in the company of my research group members. My seniors, Gill, Xiaojing, Anh, Ramiro, Ivan and Doug, have helped me at some point or the other in learning different aspects of research, relevant courses and the group culture. Kody and Jong who joined the group same year as me, have been great companions and collaborators. Wesley and Kody have inspired me through their immense dedication towards their research while wonderfully taking care of their respective families. Wesley has also provided inputs as a co-author which helped me improve my technical writing and correspondence skills.

I am grateful for the chance to work closely with the Utilities and Energy Management staff for a major part of this dissertation. On many occasions, they have taken time out of their schedules to help me and my group members pursue our goals. I am particularly thankful to Ryan Thompson and Juan Ontiveros for repetitively providing large amount of plant data, taking me on power plant and chiller plant tours, and providing valuable insights on their operation.

I feel absolutely blessed to have been surrounded by some amazing friends outside my research group – Kiran, Guneet, Shatam, Pradeep, Madhu, Tanvi, Priyanka, Poolkeshi, Sahana, Sindhu, Shweta, Akhilesh, Gunja, Amey, Rachit, Sarabjot, Aditya, Geetha, Gill, Karthik, Ramya, Harpreet, Donia, Anish, Apurv, Pranav, Neeraj, Janani – to name a few. Some of them have been like my family away from home. Kiran has always motivated me, through his own example, to aim higher and give my best to whatever I undertake. Apart from discussing day to day research issues, I have learnt several tips on improving presentation in articles/reports from Guneet who is also a graduate student at UT Austin. Harpreet has been a source of inspiration. My roommates, Sahana, Sindhu and Shweta, have been fun companions and I have shared good times with all of them.

Prashant Agarwal, a friend from India, helped me extensively in one of my projects with his expertise in using Microsoft Excel Macro.

Above all, I want to whole heartedly thank my parents for motivating me to pursue my goals and supporting me in every possible way while physically being thousands of miles away from me. My siblings, Iti and Adarsh, an important part of my family support system, have always been there for me with their unconditional love. I feel blessed to be part of such a loving family.

Modeling and Optimization for Energy Efficient Large Scale Cooling Operation

Kriti Kapoor, Ph.D.

The University of Texas at Austin, 2013

Supervisor: Thomas Edgar

Optimal chiller loading (OCL) is described as a means to improve the energy efficiency of a chiller plant operation. It is formulated as a multi-period constrained mixed integer non-linear optimization problem to optimize the total cooling load distribution through accurate chiller models. OCL is solved as a set of quadratic programs using sequential programming algorithm (SQP) in MATLAB. Based on application of the methodology to chiller systems at UT Austin and a semiconductor manufacturing facility, OCL can result in an annual energy savings of about 8%. However, the savings may reduce considerably in case of additional physical constraints on overall plant operation. With the addition of thermal energy storage (TES) to the system, OCL can reduce the daily cooling costs in the case of time varying electricity prices by 13.45% on an average.

The energy efficiency of a chiller plant as a function of its chiller arrangement is studied by using fitted chiller models. If all other variables are kept same, chillers operating in parallel consume up to 9.62% less power as compared to when they are operated in series. Otherwise, chillers may operate up to 12.26% more efficiently in series depending on their chilled water outlet temperature values. The answer to the optimal chiller arrangement can be straightforward in some cases or can be a complex optimization problem in others.

Table of Contents

List of Tables	xii
List of Figures	xiii
Nomenclature	xvii
Chapter 1: Introduction	1
Chapter 2: Modeling of Centrifugal Chillers	6
2.1 Introduction	6
2.2 Existing models in literature	8
2.3 Modifications to Gordon-Ng model for centrifugal chillers	11
2.3.1 Dependence of internal energy losses on cooling load	11
2.3.2 Dependence of internal energy losses on water flow rate	12
2.4 Implicit chiller modeling	14
2.4.1 Stoecker's equation [25]	18
2.4.2 Energy balance equation	20
2.5 Comparison of model fits	23
2.5.1 Gordon-Ng model versus Modified Gordon-Ng model 1	24
2.5.2 Modified Gordon-Ng model 2 versus Modified Gordon-Ng model 1	26
2.5.3 Implicit chiller model versus Modified Gordon-Ng model 1	30
2.6 Conclusions	36
Chapter 3: Optimal Chiller Loading for Energy Efficient Operation	39
3.1 Introduction	39
3.2 Optimal chiller loading (OCL) – A constrained optimization problem	41
3.3 Case studies	43
3.3.1 Equal loading rate (ELR) method [27]	46
3.3.2 Lagrangian method [7]	46
3.3.3 Optimal chiller loading	47
3.4 Results and discussion	47
3.5 Optimization versus intuitive cooling load distribution	52

3.6 Conclusions.....	56
Chapter 4: Energy Optimization of Large Cooling Systems through Multi-period Optimal Chiller Loading.....	59
4.1 Introduction.....	59
4.2 System overview.....	60
4.3 Model development.....	63
4.3.1 Chiller models.....	64
4.3.2 Auxiliary equipment models.....	68
4.4 Multi-period cooling system optimization.....	70
4.4.1 Case study 1 – UT Austin cooling system.....	71
4.4.1.1 Cooling system optimization without storage.....	71
4.4.1.2 Cooling System Optimization with Storage.....	73
4.4.2 Case study 2 – DMOS6, Texas Instruments Inc., Dallas.....	76
4.4.2.1 OCL – Part 1.....	77
4.4.2.2 OCL – Part 2.....	77
4.5 Results and discussion for System 1.....	79
4.5.1 Time-varying electricity prices.....	85
4.6 Results and discussion for System 2.....	88
4.7 Conclusions.....	93
Chapter 5: Energy Efficient Chiller Configuration – A Design Perspective.....	97
5.1 Introduction.....	97
5.2 Chiller arrangements.....	97
5.2.1 Chillers in series.....	98
5.2.2 Chillers in parallel.....	99
5.3 Comparison of energy efficiency – series versus parallel.....	100
5.3.1 Difference in chilled water flow rate.....	101
5.3.2 Difference in chilled water outlet temperature.....	103
5.4 Conclusions.....	105

Chapter 6: Conclusions and Future Work.....	107
References.....	112

List of Tables

Table 2.1: MGN1 model fitting parameters for Chiller 12	27
Table 2.2: MGN1 model fitting parameters for Chiller 32	28
Table 2.3: MGN1 model vs. MGN2 model fitting for Chiller 12.....	29
Table 2.4: MGN2 model fitting parameters.....	30
Table 2.5: MGN1 model vs. implicit chiller model (Chiller 6.2, Day 1)	33
Table 2.6: MGN1 model vs. implicit chiller model (Chiller 6.2, Day 2)	34
Table 3.1: Model parameters for System 1	43
Table 3.2: Model parameters for System 2	44
Table 3.3: Optimization results for System 1	48
Table 3.4: Optimization results for System 2	49
Table 3.5: Optimal chiller loading results for System 2 at 90% cooling load	53
Table 3.6: Suboptimal chiller loading results for System 2 at 90% cooling load	55
Table 4.1: Error analysis for centrifugal chiller modeling (System 1)	65
Table 4.2: Error analysis for centrifugal chiller modeling (System 2)	66
Table 4.3: Error analysis for auxiliary component modeling	69
Table 4.4: Effect of OCL with thermal energy storage on the frequency of cold starts	84

List of Figures

Figure 2.1: Refrigeration cycle in a vapor compression chiller [8]	7
Figure 2.2: Energy and material flow in a centrifugal chiller [22]	10
Figure 2.3: Two different non-zero ΔT values across one chiller at TI, Dallas....	13
Figure 2.4: Chillers, cooling towers and pumps in a typical chiller plant schematic. E1 and C1 represent the evaporator and condenser units, respectively, of chiller 1. The black/gray loop is known as condenser water loop, while the red/blue loop is known as chilled water loop.....	15
Figure 2.5: Variation of condenser water temperature over a year	16
Figure 2.6: Chiller power consumption as a function of the condenser water temperature	17
Figure 2.7: Schematic of the condenser water loop in cooling station 6, UT Austin	18
Figure 2.8: Stoecker's model fit for the cooling tower data from Station 6, UT Austin	19
Figure 2.9: Heat flows in the network of a centrifugal chiller (assembled in the dotted box) and a cooling tower. Solid and dashed arrows represent liquid and vapor streams respectively. Blue and red arrows represent cold and hot streams respectively.	20
Figure 2.10: Energy balance equation fit for the chiller plant data from Station 6, UT Austin.....	22
Figure 2.11: Gordon-Ng model predicted chiller power consumption vs. data for Chiller 6.1	25
Figure 2.12: MGN1 model predicted chiller power consumption vs. data.....	26

Figure 2.13: MGN1 model predicted chiller power ($T_c = 302$ K) vs. data for Day 1	32
Figure 2.14: Implicit chiller model predicted chiller power vs. data for Day 1	33
Figure 2.15: MGN1 model predicted chiller power ($T_c = 302$ K) vs. data for Day 2	34
Figure 2.16: Implicit chiller model predicted chiller power vs. data for Day 2	35
Figure 3.1: Schematic of a multi-chiller arrangement [7]	40
Figure 3.2: Energy efficiency curves for all chillers in System 1	45
Figure 3.3: Energy efficiency curves for all chillers in System 2	45
Figure 3.4: Comparison of power consumption in System 1 from different chiller loading methods	50
Figure 3.5: Comparison of power consumption in System 2 from different chiller loading methods	51
Figure 3.6: Estimated percentage energy savings from using OCL over ELR in System 2	52
Figure 3.7: The optimal solution marked on energy efficiency curves	54
Figure 3.8: The sub-optimal solution marked on energy efficiency curves	56
Figure 4.1: District cooling network at the University of Texas at Austin campus [24]	61
Figure 4.2: Screenshot from the chiller plant at fab DMOS6 (TI, Dallas)	62
Figure 4.3: Electric power consumed by Chiller 6.1 (System 1) in the month of September– Model vs. data	65
Figure 4.4: Fitted energy efficiency curves for chillers in System 2 at $TWB, i = 270$ K	67

Figure 4.5: Fitted energy efficiency curves for chillers in System 2 at $TWB, i = 300$ K.....	68
Figure 4.6: Total power consumed by the auxiliary equipment in the cooling station 6 – Model vs. data.....	70
Figure 4.7: Hourly campus cooling load values (left axis) and ambient wetbulb temperature values (right axis) over 24 hour period. This data is from 11th July 2012. It serves as an example for days with more than one maxima in the cooling load profile.	74
Figure 4.8: Schematic of chiller layout in System 2.....	76
Figure 4.9: Cooling load distribution among 24 hours (Day 1) from different optimization conditions for System 1	81
Figure 4.10: Cooling load distribution among 24 hours (Day 2) from different optimization conditions for System 1	81
Figure 4.11: Comparison of power consumption values from a) plant data, b) static optimization and c) dynamic optimization for System 1	82
Figure 4.12: Comparison of the variations in the total number of operating chillers under different cooling load profiles (System 1).....	85
Figure 4.13: Variation in the hourly real-time prices in the ERCOT wholesale market over the year 2012 in Austin, TX.....	86
Figure 4.14: Comparison of the cooling cost in case of time varying electricity prices – With TES ($\alpha = 0$) vs. without TES (System 1).....	87
Figure 4.15: Comparison of hourly power consumption values over the year 2012 from a) plant data, b) OCL – Part 1 for System 2	88
Figure 4.16: Predicted hourly energy savings from OCL – Part 1 for System 2..	89

Figure 4.17: Comparison of hourly power consumption values over the year 2012 from a) plant data, b) OCL – Part 2 for System 2	91
Figure 4.18: Predicted hourly energy savings from OCL – Part 2 for System 2..	91
Figure 4.19: Comparison of the total annual power consumption of System 2 from data, OCL – Part 1 and OCL – Part 2	92
Figure 5.1: Schematic of a two-chiller system in series configuration.....	98
Figure 5.2: Schematic of a two-chiller system in parallel configuration.....	99
Figure 5.3: Chiller power variation with cooling load (series vs. parallel) for Chiller 12.....	102
Figure 5.4: Chiller power variation with cooling load (series vs. parallel) for Chiller 32.....	102
Figure 5.5: Chiller efficiency variation with cooling load for Chiller 11 for constant T_e	104
Figure 6.1: Simplified schematic of the Hal C. Weaver power plant complex at UT Austin [39]	109

Nomenclature

Symbol	Description*	Units**
T_{WB}	Ambient wet-bulb temperature	K
δ	Binary variable representing chiller on/off status	Dimensionless
T_H	Chilled water inlet temperature	K
F	Chilled water mass flow rate	kg/sec
T_e	Chilled water outlet temperature	K
X	Chiller cooling load assuming on status; $X \in [L, U]$	Tons or kW
Q	Chiller cooling load; $Q \in \{0\} \cup [L, U]$	Tons or kW
Cap	Chiller design capacity	Tons or kW
P	Chiller power consumption	kW
COP	Coefficient of performance	Tons/kW
\dot{m}	Condenser water mass flow rate	kg/sec
T_c	Condenser water return temperature	K
T_s	Condenser water supply temperature	K
C_p	Heat capacity	J·kg ⁻¹ ·K ⁻¹
M_c	Heat transfer coefficient of condenser	WK ⁻¹
M_e	Heat transfer coefficient of evaporator	WK ⁻¹
L	Lower bound on chiller cooling load	Tons or kW
M	Number of chillers in a plant	Dimensionless
p	Number of cooling towers	Dimensionless
PLR	Part load ratio	Dimensionless
Q_T	Rate of heat rejection by the cooling tower	kW

Q_C	Rate of heat transfer at the condenser	kW
q_c	Rate of internal condenser heat loss	kW
q_e	Rate of internal evaporator heat loss	kW
\dot{W}_C	Rate of work done by the compressor	kW
D	Total cooling demand	Tons or kW
U	Upper bound on chiller cooling load	Tons or kW
E	Amount of stored thermal energy	kWh
E_{max}	Maximum capacity of the thermal energy storage (TES) tank	kWh
P_{AUX}	Power consumed by the auxiliary equipment	kW
$P_{station}$	Total power consumed by a chilling station	kW
R_{max}	Maximum charging/discharging rate of TES tank	kW
γ	Real time market rate of electric energy	\$/kWh
DBT	Dry bulb temperature	K
r	Total number of chilling stations	Dimensionless
m_k	Total number of chillers upto the k^{th} station; $m_0 = 0, m_r = M$	Dimensionless
n	Number of hours in the optimization horizon	Dimensionless
RH	Relative humidity	Dimensionless
WBT	Wet bulb temperature	K
SL	Total station cooling load	kW
α	Penalty coefficient	Dimensionless
Pdata	Actual power consumed by the cooling system in a day	MWh
Popt	Estimated power consumption by the cooling system in a day for the cooling load profile resulted from solving optimization	MWh

- *Any symbol with j subscript represents a variable corresponding j^{th} chiller.
- *Any symbol with i subscript represents a variable corresponding i^{th} hour.
- *Any symbol with k subscript represents a variable corresponding k^{th} station.
- *Any symbol with l subscript represents a variable corresponding l^{th} cooling tower.
- **Units are the same as given in this table unless specified otherwise in the text.
- **Units for cooling loads are considered to be “tons” in Chapter 3 and “kW” everywhere else.

Chapter 1: Introduction

As global energy demand escalates and climate change concerns grow ever larger, the importance of using energy more efficiently continues to intensify. A large fraction of global electrical energy consumption belongs to various manufacturing industries and building systems, which consume nearly 40% of the primary energy in the United States [1]. Energy efficient manufacturing has emerged as an important part of the solution to the problem of rising energy demand. Current manufacturing processes can be modified to be energy efficient and environmentally friendly. Energy efficient manufacturing not only saves energy, but also has the potential to reduce pollutant emissions, reduce carbon footprint, improve yields and hence make the overall process more profitable and sustainable. Many companies are now starting to implement energy conservation policies and processes, which makes this an exciting new field with huge potential for exploration and growth.

Considering the semiconductor industry as an example, an excerpt from the SEMI website (www.semi.org) in October 2001 mentioned “Slashing energy consumption has become an unquestioned semiconductor industry goal.” Energy efficiency was never a high priority for the semiconductor industry in the past due to the high overall operating costs as compared to energy costs. But increased energy costs, coupled with energy intensive manufacturing processes, have caused the industry to revisit the issues. Based on surveys, even the most efficient semiconductor fabs use over 450 kWh of energy for every 200 mm of wafer processed, and a typical semiconductor factory spends over \$1,000,000 per month for electricity during peak usage periods [2]. An important contributor to energy usage in fabs is the chiller plant. More than 20% of the total energy

is consumed by the chiller plant, which takes the cooling load from different parts of the fabs [2, 3].

Large scale cooling systems account for a significant portion of the electrical energy consumed by most industrial, residential and university campuses. By some estimates, the cooling of buildings contributes up to 35% of the total electrical demand in United States [4]. Depending on a building's heating ventilation and air conditioning (HVAC) system, a building may require heating and cooling year round. In the summer, air may be cooled to lower than required room temperatures in order to remove humidity, and then reheated to bring it back up to the desired temperature. In the winter, thermal zones in the middle of large buildings require cooling because they are not exposed to ambient conditions, so the thermal needs are driven by the internal gains of the zone. Chillers are generally used to meet building cooling needs, and boilers are often used to provide heating.

The operation of a typical chiller plant has enough flexibility to encourage a wide range of optimization approaches with respect to its power consumption. One method of improving energy efficiency of a complex process is to create an accurate system model, and then use optimization algorithms to determine more efficient operating strategies for the system. The processes involved in a chiller plant operation are fairly complex but can be numerically optimized to improve the energy efficiency of the plant. The energy efficiency can also be improved by optimally designing the plant configuration while installing or retrofitting it. This dissertation discusses both these approaches that lead to a sustainable large scale cooling operation.

Optimal chiller loading (OCL) can be described as a method to optimize the total cooling load distribution at regular time intervals through multi-period constrained optimization problems. Chiller models are important in solving these optimization

problems to get accurate and implementable results [5]. Different models may be suitable for different cooling systems. Addition of thermal energy storage (TES) to the OCL problem can significantly reduce the energy costs associated with the cooling system, especially in the case of time varying electricity prices by shifting the cooling load from more expensive hours to the less expensive ones. The ability to shift cooling load across time using TES can also help generate a cooling load profile with least fluctuations and cold starts. This can further reduce the electricity cost by reducing the number of times a chiller operates in the transient, hence less efficient cooling load range.

The energy efficiency of a chiller plant also depends on the way its chillers are arranged with respect to one another. Even though a parallel arrangement of chillers is most popular, some chiller plants may employ a series or hybrid (mix of series and parallel) arrangement for several reasons. The analysis of the effect of chiller arrangement on its energy efficiency can be quite useful from a design perspective. An outline of the dissertation, based on the topics discussed above is explained in the following paragraphs.

Chapter 2 discusses various centrifugal chiller models developed from the Gordon-Ng model [6] to compute chiller power consumption. Modified Gordon-Ng model – 1 is developed by adding the dependence of rates of internal energy loss in a chiller on its cooling load to the original Gordon-Ng model equations. Similarly, Modified Gordon-Ng model – 2 includes the dependence of rates of internal energy loss on the chilled water flow rate. The third model is named as implicit chiller model which aims at evaluating variables like condenser water return and supply temperatures in addition to the chiller power consumption. The chapter also throws light on the motivation behind devising these new model equations by analyzing real year-long plant

data from the chiller plants at UT Austin and TI, Dallas campuses. The accuracy of these models are then compared with the Gordon-Ng model [6] using the same sets of data.

Chapter 3 introduces the concept of optimal chiller loading (OCL) as a way to improve the energy efficiency of chiller plant operation with minimal capital investment. OCL is formulated as a constrained optimization problem with a different objective function used from the one in Lagrangian method [7]. Three different methods of chiller loading are compared in terms of the resulting total power consumed by two chiller plant systems in Taiwan. The coefficients used to characterize the chiller efficiencies of the systems under consideration are obtained from [7]. This chapter also highlights the importance of optimal chiller loading for a more sustainable cooling operation.

Chapter 4 illustrates the application of multi-period optimal chiller loading for large and complex chiller plants. The chiller plants at UT Austin and TI, Dallas are used as case studies to show the varied complexity and structure in large scale cooling systems. Year-long data obtained from each of these systems are fitted to the models presented in Chapter 2 which are then used in the OCL formulation for that system. Case study 1, based on the UT Austin cooling system, demonstrates the modeling of a district cooling system which has several chiller plants with different sets of auxiliary equipment contributing to a significant fraction of the power consumption. It also explores the advantages of using thermal energy storage (TES) in reducing the overall cooling cost (\$) in case of time varying electricity prices. The effect of using TES is also analyzed on the overall cooling load profile and the frequency of cold starts. Case study 2 based on TI, Dallas chiller plant is solved for two scenarios – hypothetical and real. The comparison of results from these two scenarios in case study 2 leads to some significant recommendations for the concerned chiller plant layout and operation.

Chapter 5 describes some of the common chiller configurations used in large scale chiller plants. Series and parallel chiller arrangements are compared for the overall plant energy efficiency. Models of chillers at the DMOS6 chiller plant at TI, Dallas are used to quantitatively study the effect of chiller arrangement on plant energy efficiency. This chapter highlights the importance of such an analysis as an essential step in designing energy efficient and sustainable chiller plant.

Chapter 6 summarizes the results gathered throughout the study and lists probable future steps to further the current research.

Chapter 2: Modeling of Centrifugal Chillers

2.1 INTRODUCTION

Chiller plants are widely used in university campuses, residential areas with district cooling, and various industrial plants, such as semiconductor manufacturing and pharmaceutical plants, to provide cooling. Industrial chiller plants are usually employed to keep the processes and tools at the desired temperature level and also to provide air conditioning. Therefore, chiller plants are essential for the smooth operation of industrial plants and campuses, accounting for about 20-30% of the total electricity usage [3]. In a typical chiller plant, its chillers are the most energy consuming machines. So to minimize the overall power consumption of a plant or campus, its chiller power consumption needs to be optimized. This chapter focuses on modeling the overall power consumption of chillers, which will then be used to estimate and optimize the chiller plant operation in the following chapters.

Chillers usually work on the basis of either an absorption refrigeration cycle or a vapor compression cycle (Figure 2.1), to cool down water, which is then used to remove heat from buildings and/or manufacturing tools. Vapor compression chillers, also known as electric chillers, are preferred over absorption chillers due to their higher energy efficiency. Electric chillers can be of several types based on the type of compressor used in them – centrifugal, reciprocating or screw-driven. The type of compressor used is chosen on the basis of the amount of cooling requirement, also known as cooling load, on the chiller. Cooling load (kW) on a chiller is defined by Equation 2.1.

$$Q = F * C_p * (T_H - T_e) \quad (2.1)$$

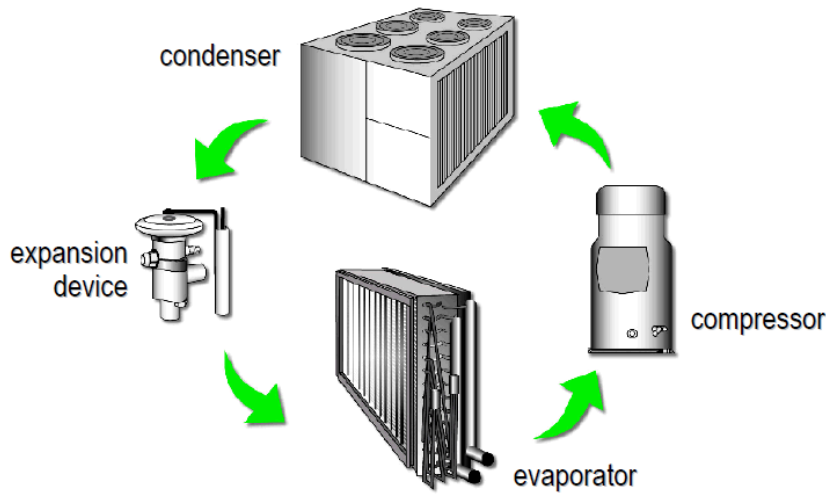


Figure 2.1: Refrigeration cycle in a vapor compression chiller [8]

Typically, reciprocating compressors are used for small size chillers ($Q < 50$ tons), screw compressors for mid-sized chillers ($50 \text{ tons} < Q < 300 \text{ tons}$) and centrifugal compressors for large chillers ($Q > 300 \text{ tons}$) [1 ton = 1 refrigeration ton = 3.516 kW]. Hence, centrifugal chillers are commonly used in most large scale chiller plants. The electric power consumed by a centrifugal chiller, and by extension its energy efficiency, depends on several variables such as cooling load, chilled water temperature and condenser water temperature. The condenser water temperature in turn depends on the ambient weather conditions. Accurate models or correlations that compute the power consumption of a centrifugal chiller as a function of these variables are required to perform any energy optimization study for such chiller plants.

The power consumption of a chiller is usually derived from its energy efficiency, which is technically described by a dimensionless term called coefficient of performance (COP). COP of a chiller is defined as the ratio of the heat removed (i.e., cooling load) to the power input to its compressor:

$$COP = \frac{Q}{P} \quad (2.2)$$

The next section presents a literature review on the existing empirical, first principles and hybrid models developed for various types of chillers. In later sections, the Gordon-Ng model for centrifugal chillers [6] is modified or combined with additional physical equations to develop more general physical models. These models are then fitted to a set of real plant data collected from the University of Texas at Austin cooling system and compared with the Gordon-Ng model fit.

2.2 EXISTING MODELS IN LITERATURE

Steady-state chiller models have been used extensively for a variety of chiller types and sizes. Chiller models can be based on first-principles [9,10] or on purely empirical relationships [11-17], such as neural networks [18]. Purely empirical models, also known as black box models, are easy to fit but cannot be extrapolated over a wide range of data [19]. Often, models developed for one chiller type work for other chiller types. For example, in [6] the authors found that model equations developed for reciprocating [20] and absorption chillers [21] also worked very well for centrifugal chillers. Lee *et al.* [22] identified eleven types of centrifugal chiller models that have been used in the literature:

- (i) Simple linear regression model
- (ii) Bi-quadratic regression model
- (iii) Multivariate polynomial regression model
- (iv) Simpler multivariate polynomial regression model
- (v) DOE-2 model
- (vi) Modified DOE-2 model

- (vii) Gordon-Ng universal model (based on the evaporator inlet water temperature)
- (viii) Gordon-Ng universal model (based on the evaporator outlet water temperature)
- (ix) Modified Gordon-Ng universal model
- (x) Gordon-Ng simplified model
- (xi) Lee simplified model

All necessary equations for each model are included in Lee *et al.* [22] and hence not reproduced here. In comparing the different models against a total of 2401 chiller datasets, they found that most chiller models performed well under all scenarios, including the Gordon-Ng models, which are discussed in detail in this chapter.

Chiller models are increasingly being used to determine the best operating conditions for a chiller, as illustrated by Ng *et al.* [23], where a thermodynamic chiller model is used to determine the optimal chiller operating points. Optimal operating conditions ensure efficient chiller operation, which in turn can lead to substantial savings in operating costs. It also potentially increases the chiller lifetime by avoiding operating regions that quickly degrade the chiller.

Apart from the semi-empirical universal models described by Lee *et al.* [22], Gordon *et al.* [6] have developed a first principles model for centrifugal chillers that is based on an energy balance equation around the refrigerant's vapor compression cycle (Figure 2.2). This model is referred to as the Gordon-Ng model in the rest of the chapter. It computes the power consumed by a chiller (P) as a function of its cooling load (Q), condenser water return temperature (referred to as condenser water temperature for simplicity) (T_c), and chilled water temperature setpoint (T_e) (see Equations 2.3 and 2.4). The parameters represented in bold font in Equation 2.3 are the four model parameters

(M_c , M_e , q_c and q_e) that are assumed to have different values for different chillers. M_c and M_e are the condenser and evaporator heat exchanger coefficients ($W K^{-1}$) respectively, while q_c and q_e are the rates of internal energy losses (kW) at condenser side and evaporator side respectively. All variables in the Gordon-Ng model equations are in SI units.

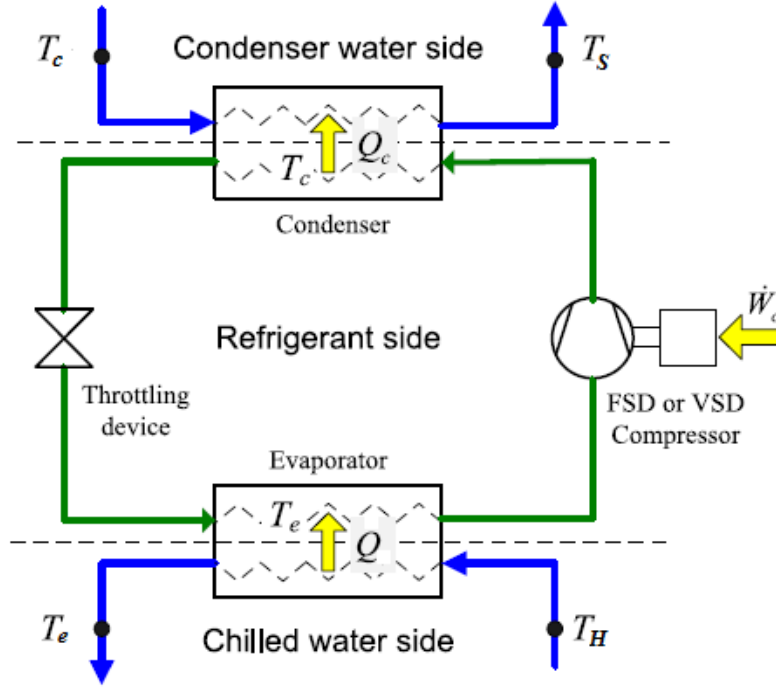


Figure 2.2: Energy and material flow in a centrifugal chiller [22]

$$\frac{1}{COP} = -1 + \frac{T_c}{T_e} + \left(\frac{1}{Q}\right) \left(\frac{q_e T_c}{T_e} - q_c\right) + \left(\frac{1}{Q}\right) \left(\frac{q_e}{M_c T_e}\right) \left(\frac{q_e T_c}{T_e} - q_c\right) + \left(\frac{Q}{T_e}\right) \frac{T_c}{T_e} \left(\frac{1}{M_c} + \frac{1}{M_e}\right) + \frac{\frac{q_c}{M_e} + \frac{q_e T_c}{T_e M_c} + \left(\frac{T_c q_e}{T_e} - q_c\right) \left(\frac{1}{M_c} + \frac{1}{M_e}\right)}{T_e} \quad (2.3)$$

$$P = Q * (1/COP) \quad (2.4)$$

The Gordon-Ng model, being a first principles model, provides a good fit for almost all real datasets obtained from a centrifugal chiller over its entire operating range. However, while fitting the Gordon-Ng model to the data obtained from chillers at UT

Austin and Texas Instruments Inc. (TI), Dallas, several limitations were observed. The next section discusses the observed limitations and proposes modifications to the original Gordon-Ng model to overcome them.

Models in this chapter are validated against two distinct datasets collected from the cooling systems at UT Austin and a fab at TI, Dallas.

2.3 MODIFICATIONS TO GORDON-NG MODEL FOR CENTRIFUGAL CHILLERS

The Gordon-Ng model assumes that its four model parameters (M_c , M_e , q_c and q_e) are constant for a given chiller. The purpose of using a chiller model is to determine the power consumption of a chiller as a function of ambient weather conditions and its cooling load. Therefore, the model parameters are assumed to be constant with respect to the key variables, i.e., chiller cooling load and ambient conditions. However, a more general model was proposed that includes these parameters differently.

2.3.1 Dependence of internal energy losses on cooling load

Data from nine centrifugal chillers (UT Austin) were independently fitted against the Gordon-Ng model. The model and data seemed to be in good agreement for each chiller for most of the operating range, except at the two extremes of the cooling load range (Figure 2.11). To explain this behavior, it was hypothesized that the rate of internal energy losses is a function of the chiller cooling load, and not a constant parameter. This dependence was assumed to be linear for simplicity. Therefore, the following equations represent the proposed addition to the Gordon-Ng model equations:

$$q_e = q_{e_m} + a * Q \quad (2.5)$$

$$q_c = q_{c_m} + b * Q \quad (2.6)$$

With the proposed additional equations, this model is referred to as the Modified Gordon-Ng model 1 (MGN1) in this chapter. Hence, MGN1 model is given by Equations 2.3, 2.4, 2.5 and 2.6. All symbols represented in bold font are model parameters.

2.3.2 Dependence of internal energy losses on water flow rate

In most large scale chiller plants, all chillers are operated in parallel mode. That is, the temperature difference ($\Delta T = T_H - T_e$), is the same across all chillers. Therefore, the cooling load across any chiller is directly proportional to the rate at which chilled water flows through its evaporator. Models for multi-chiller systems with chillers working in parallel do not consider cooling load (Q) and chilled water flow rate (F) as independent variables.

However, in some chiller plants (for instance at TI, Dallas) some of the chillers are arranged in series. For chillers in series, the chilled water flow rate remains the same and hence the cooling load is divided among them by proportionally reducing the total ΔT . For cooling systems with mixed (both series and parallel) chiller arrangements, the cooling load and chilled water flow rate should be treated as independent variables. Chiller cooling load, temperature difference across the chiller, and chilled water flow rate are all related to each other by Equation 2.1. In other words, such systems may have one additional degree of freedom in chiller operation.

Data from nine chillers (TI, Dallas) were studied and it was found that the ΔT values were nearly constant (range ~ 0.5 °F) for five of them. However, for the rest of the four chillers ΔT was observed to be within two distinct ranges of values (Figure 2.3). These four chillers were operated independently at various times and operated in series with another chiller at other times. The data from each of these four chillers was divided into two parts based on its mode of operation. The original Gordon-Ng model was fitted

separately against the two datasets for each of the four chillers using minimization of least squares. Different values of fitting parameters were obtained for different datasets regarding each individual chiller (Tables 2.1 and 2.2 in Section 2.5). In other words, two separate models described each chiller's behavior depending on whether its mode of operation was independent or in series with another chiller. It was concluded that a chiller performs differently in terms of energy efficiency when operated independently versus when operated in series with another chiller. Data also confirmed that for the same values of cooling load, condenser water temperature and chilled water temperature, a chiller always consumed more energy when operated in series than when operated independently.

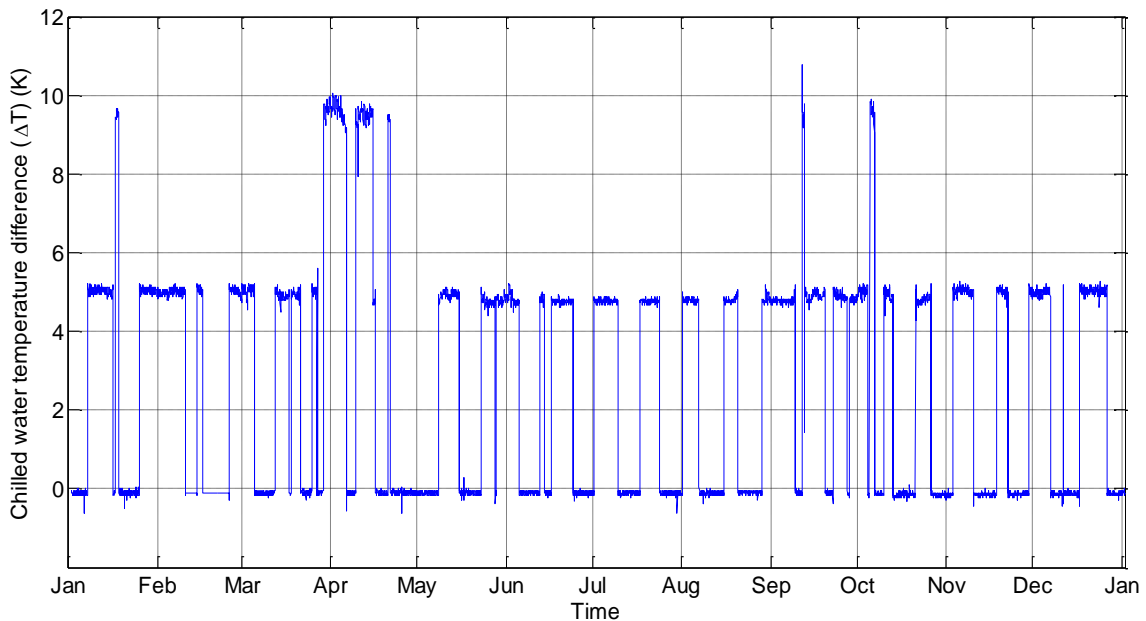


Figure 2.3: Two different non-zero ΔT values across one chiller at TI, Dallas

A new modification to the Gordon-Ng model was proposed in order to make the model more comprehensive such that a single model is able to explain a chiller's

behavior in all circumstances. The energy losses at condenser and evaporator sides, i.e., q_c and q_e , are generated from internal dissipation, including fluid friction among several other sources [6]. Therefore it was proposed that the internal losses vary as a function of the chilled water flow rate in addition to the cooling load. This leads to addition of one more term to Equations 2.5 and 2.6 as follows:

$$q_e = q_{e_m} + a * Q + d_1 * F \quad (2.7)$$

$$q_c = q_{c_m} + b * Q + d_2 * F \quad (2.8)$$

Here q_{e_m} , q_{c_m} , a , b , d_1 , d_2 are fitting parameters.

The resulting chiller model based on the above hypothesis, which aims at modeling chillers for operation in a non-parallel arrangement, is referred to as the Modified Gordon-Ng model 2 (MGN2) in this chapter.

The two datasets regarding one chiller were combined and fitted against the MGN2 model, i.e., Equations 2.3, 2.4, 2.7 and 2.8. The resulted values of fitting parameters are presented in Table 2.4 and are discussed in section 2.5.

2.4 IMPLICIT CHILLER MODELING

The models discussed so far have one thing in common – they all have a certain set of inputs required for chiller power computation. The inputs are cooling load, chilled water temperature and condenser water temperature. The purpose of developing chiller models in this research was to determine an optimal cooling load distribution that minimizes the total power consumed by the cooling system (see Chapter 3). In order to use a model for this optimization study, either the model inputs should be decision variables for the optimization problem or their values should be known and they should be treated as optimization parameters. Chiller cooling loads are the decision variables,

while the chilled water temperature is maintained at a constant set point. Condenser water temperature is a variable whose value depends on a complex network of heat and mass transfer.

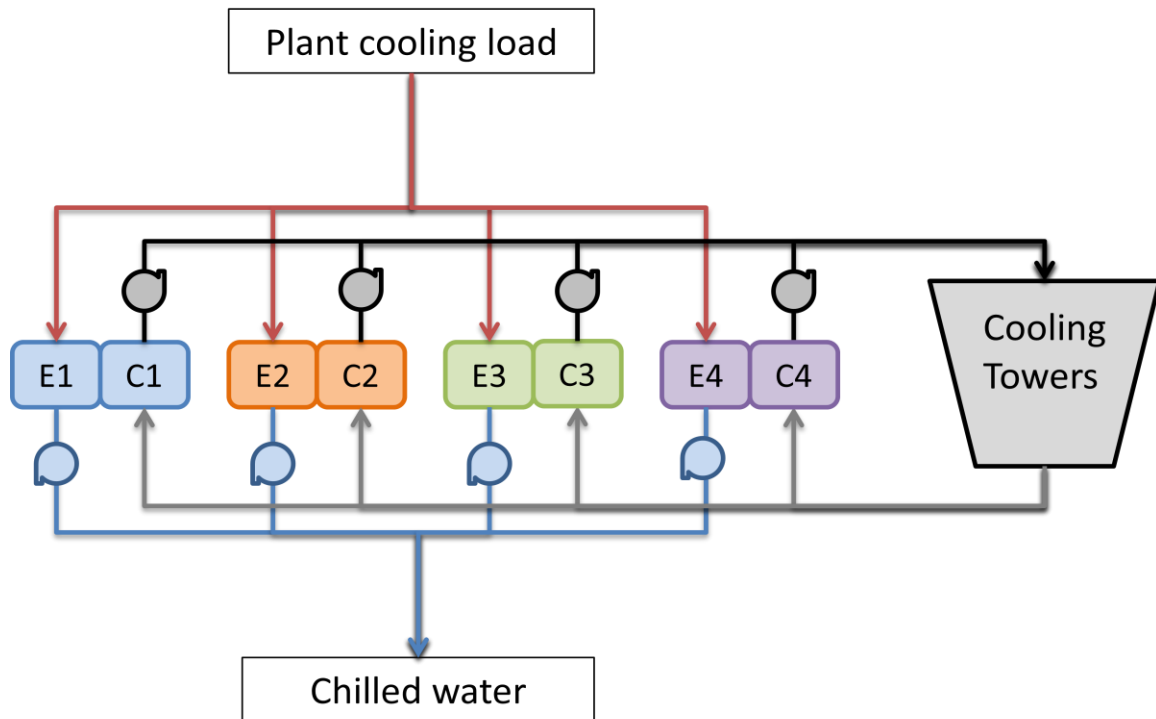


Figure 2.4: Chillers, cooling towers and pumps in a typical chiller plant schematic. E1 and C1 represent the evaporator and condenser units, respectively, of chiller 1. The black/gray loop is known as condenser water loop, while the red/blue loop is known as chilled water loop.

Chillers are normally operated as part of a complex and bigger cooling system (Figure 2.4). There are three kinds of loops (named after the type of material flowing through them) of heat and mass transfer in any large scale cooling system. The refrigerant loop connects different parts of a centrifugal chiller assembly, i.e., evaporator, condenser, compressor and the expansion valve. The chilled water loop connects the plant or buildings with the evaporators of several chillers. The condenser water loop connects their condensers with the cooling towers. The heat absorbed by the chiller is finally

rejected into the environment by cooling towers through evaporative cooling. The temperature of condenser water returning from cooling towers to a chiller is known as condenser water return temperature or condenser water temperature.

Condenser water temperature is neither a decision variable nor maintained at a constant setpoint. Its value depends on the ambient weather conditions as well as the cooling load on chillers, while the cooling load in turn depends on the ambient temperature and other stochastic variables such as the building occupancy. Optimization studies in the literature either assume T_c to have a constant value [7] or consider the chiller power to be independent of T_c [24].

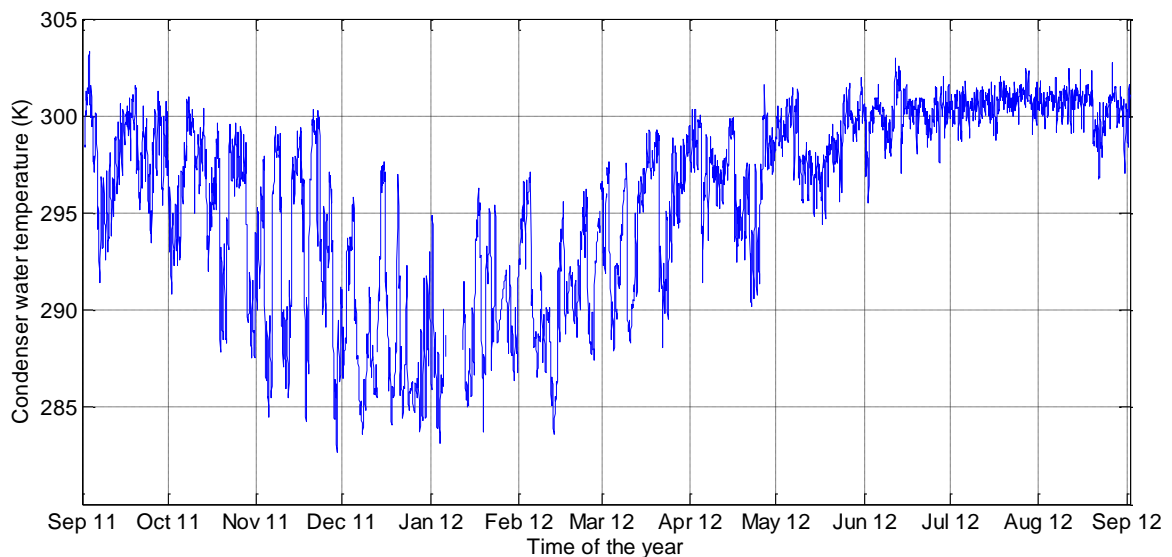


Figure 2.5: Variation of condenser water temperature over a year

One year of hourly data for T_c at a chiller plant (UT Austin) was plotted against time (Figure 2.5). It was observed from the data that T_c varies from about 283 K to 303 K during the year. The significance of this variation was quantified by plotting the model predicted power consumption of a chiller at UT Austin against T_c , keeping all other variables constant (Figure 2.6). From Equations 2.3 and 2.4, it is evident that Gordon-Ng

model predicts the power consumption to vary linearly with T_c . With T_c varying from 283 K to 303 K, the power consumption of this chiller is expected to rise by 77.8%, which is a significant rise. Hence, ignoring the variability of T_c or the correlation between T_c and chiller power consumption cannot be considered a reasonable assumption.

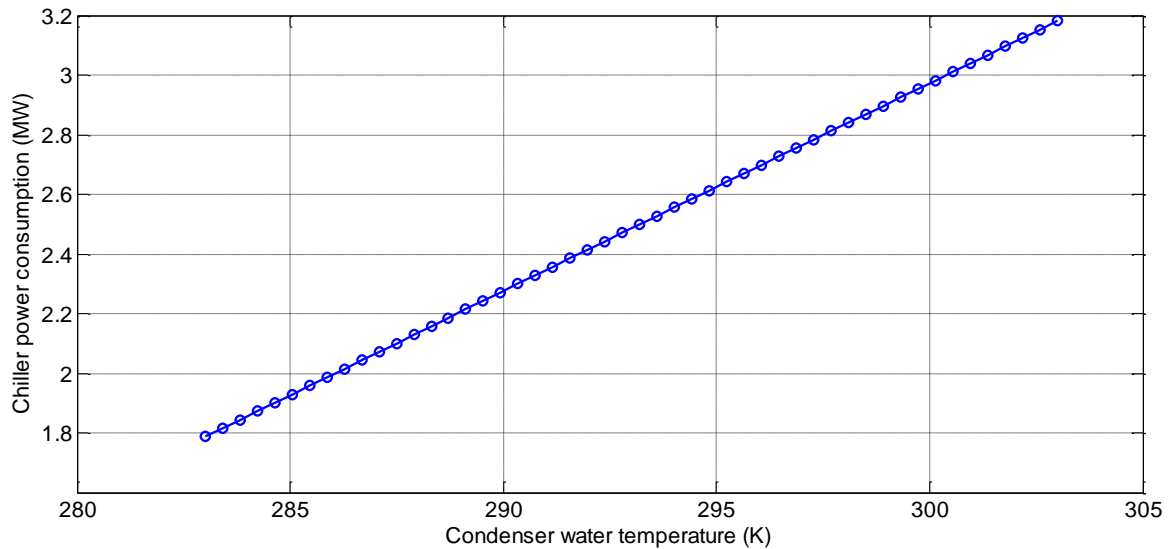


Figure 2.6: Chiller power consumption as a function of the condenser water temperature

With the idea of evaluating the condenser water temperature as a function of ambient wet-bulb temperature and the individual chiller load values, instead of assuming it as a constant, a new chiller model was developed. This model comprises of Gordon-Ng model (Equations 2.3 and 2.4) along with two additional equations (Equations 2.9 and 2.16). The output variables of this model (chiller power, condenser water return temperature and condenser water supply temperature) are obtained as a result of solving all model equations simultaneously. Since this model does not compute power as an explicit function of the input variables, it is named as the “implicit chiller model”.

The implicit chiller model equations were developed by considering the whole chiller plant as a system. For data and chiller plant layout, a chiller plant at UT Austin

(Station 6) was chosen as an example. This chiller plant consists of three centrifugal electric chillers which are all connected to a set of three cooling towers (Figure 2.7). The temperature of the condenser water flowing from chiller to cooling towers is called the condenser water supply temperature. For simplicity, the heat losses associated with mixing or splitting of condenser water streams are ignored in the development of this model.

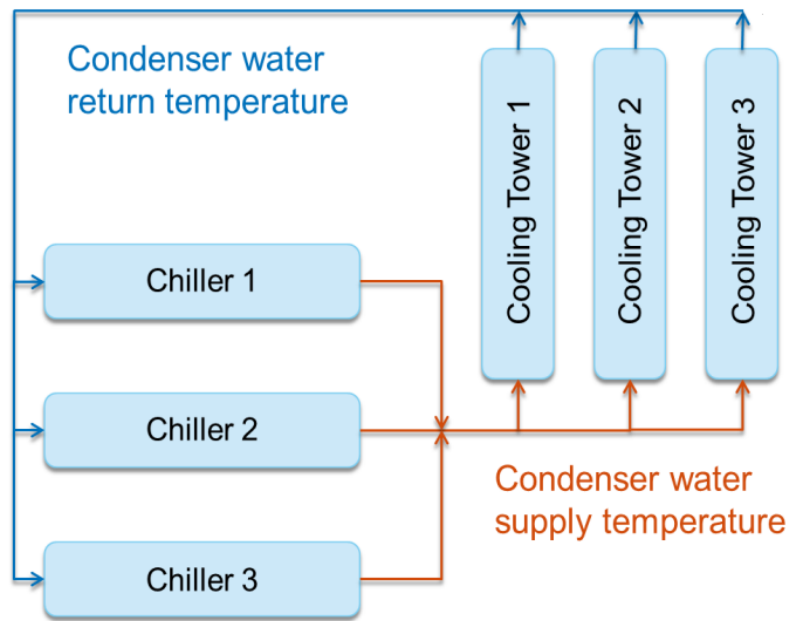


Figure 2.7: Schematic of the condenser water loop in cooling station 6, UT Austin

The equations included in the implicit chiller model in addition to the Gordon-Ng model equation, are derived and/or described point-wise as follows:

2.4.1 Stoecker's equation [25]

Stoecker's equation is a quadratic correlation between the ambient wet-bulb temperature, condenser water return temperature and condenser water supply temperature for any cooling tower (Equation 2.9). The ambient wet-bulb temperature is considered as

an input variable to the implicit chiller model. Weather forecasts from national database are used to obtain the predicted WBT values, which enable the model to also make predictions for chiller power consumption. All temperatures in Stoecker's equation are in degree Celsius.

$$T_c = c_1 + c_2 * T_{WB} + c_3 * T_{WB}^2 + c_4 * T_S + c_5 * T_S^2 + c_6 * T_{WB} * T_S + c_7 * T_{WB}^2 * T_S + c_8 * T_{WB} * T_S^2 + c_9 * T_{WB}^2 * T_S^2 \quad (2.9)$$

Stoecker's equation was fitted to the data collected over 12 months from cooling towers at Station 6, UT Austin and the unknown coefficients were fitted. Figure 2.8 plots the estimated values of condenser water temperature against the actual values obtained from data for one such cooling tower. It was observed that the correlation equation can be used to estimate the condenser water temperature with an accuracy of $\pm 2.8\%$.

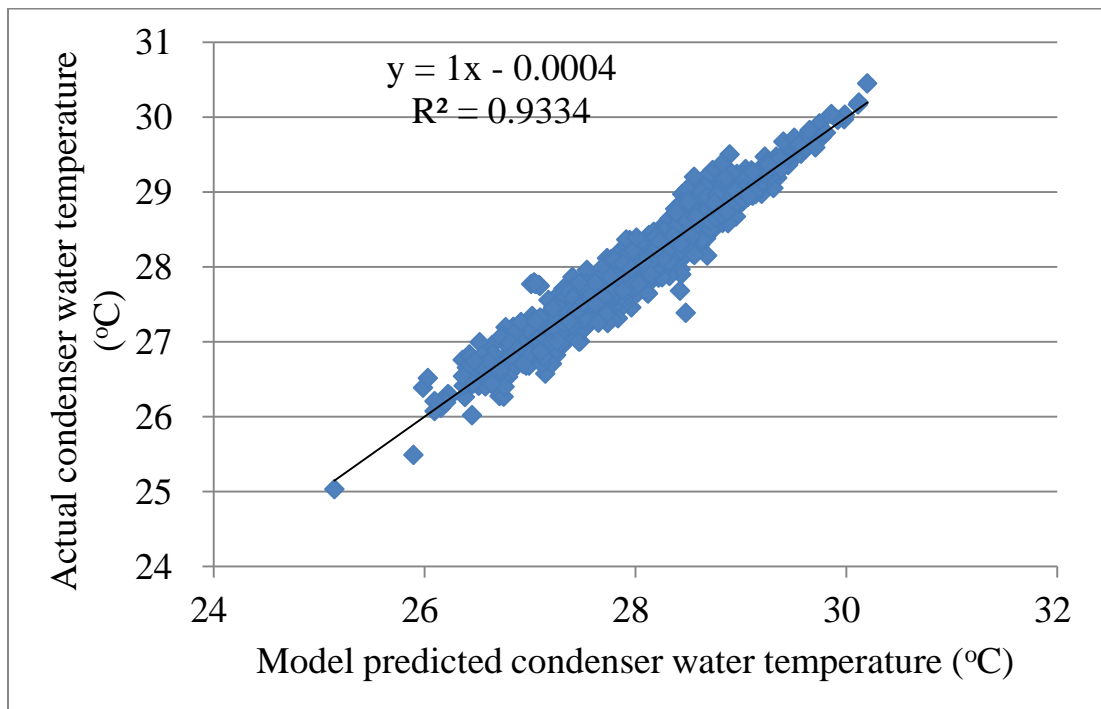


Figure 2.8: Stoecker's model fit for the cooling tower data from Station 6, UT Austin

2.4.2 Energy balance equation

The second equation was obtained by writing an energy balance equation around the condenser water loop. The heat flow across various components of a chiller plant is shown in the form of a simplified schematic in Figure 2.9. Q amount of heat is first transferred from chilled water to refrigerant at the evaporator. Then Q_c amount of heat is transferred from refrigerant to condenser water at the condenser of a chiller. The condenser water collects this heat from every chiller's condenser, which is then rejected into the environment at cooling towers. This heat rejection at cooling tower (Q_T) leads to the temperature drop of condenser water from T_s to T_c .

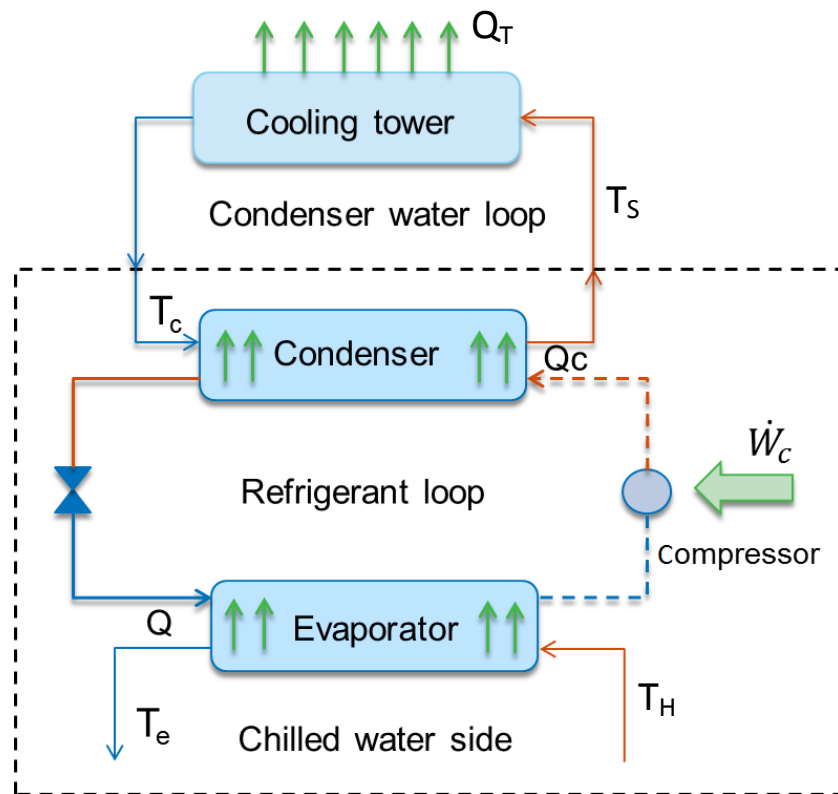


Figure 2.9: Heat flows in the network of a centrifugal chiller (assembled in the dotted box) and a cooling tower. Solid and dashed arrows represent liquid and vapor streams respectively. Blue and red arrows represent cold and hot streams respectively.

In a chiller plant with M number of chillers (therefore, M number of condensers) and p number of cooling towers, the overall energy balance around its condenser water loop can be expressed by the following equation.

$$\sum_{j=1}^M (Q_C)_j = \sum_{l=1}^p (Q_T)_l \quad (2.10)$$

The energy balance around the refrigerant loop inside j^{th} chiller, given by the first law of thermodynamics, can be written as follows:

$$(\dot{W}_C)_j + Q_j - (Q_C)_j = 0 \quad (2.11)$$

The rate of work done by the compressor is equal to its power consumption (by definition) and hence is equal to the chiller power consumption. Therefore, the rate of heat flow at the condenser of j^{th} chiller can be given by the following equation:

$$(Q_C)_j = Q_j + P_j \quad (2.12)$$

Combining Equations 2.12 and 2.4, we get the following:

$$(Q_C)_j = P_j * (1 + COP_j) \quad (2.13)$$

Equation 2.13 establishes the left hand side of the energy balance around the condenser water loop (Equation 2.10).

The rate of heat rejection at l^{th} cooling tower can be determined by the definition of sensible cooling (Equation 2.14). The loss in water flow rate due to evaporation is assumed to be negligible.

$$(Q_T)_l = \dot{m}_l * C_p * (T_S - T_C) \quad (2.14)$$

Substituting the values of left hand side and right hand side terms in Equation 2.10 from Equation 2.13 and Equation 2.14, the following equation is obtained for energy balance around the condenser water loop:

$$\sum_{j=1}^M (P_j * (1 + COP_j)) = (T_S - T_C) * \sum_{l=1}^p \dot{m}_l * C_p \quad (2.15)$$

Data suggest that the term $\sum_{l=1}^p \dot{m}_l * C_p$ cannot be assumed constant. Therefore, the right hand side of Equation 2.15 is modeled as a third order polynomial in $(T_S - T_C)$, T_{WB} and the total station cooling load (Equation 2.16).

$$\sum_{j=1}^M (P_j * (1 + COP_j)) = e_1 + (T_S - T_C) * \left(e_2 + e_3 * \sum_{j=1}^M Q_j + e_4 * T_{WB} + e_5 * T_{WB} * \sum_{j=1}^M Q_j \right) \quad (2.16)$$

where e_1, e_2, e_3, e_4 and e_5 are energy balance coefficients.

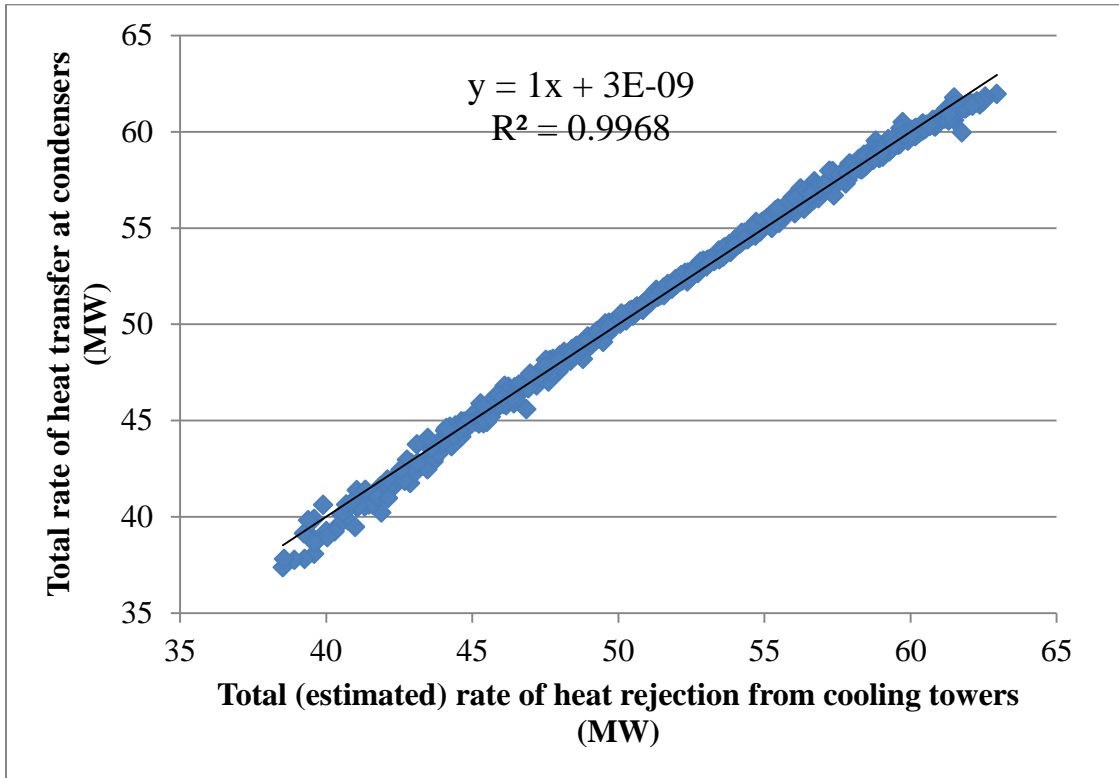


Figure 2.10: Energy balance equation fit for the chiller plant data from Station 6, UT Austin

In Equation 2.16, expression for the term $\sum_{j=1}^M Q_j$ can be obtained for each chiller in terms of P_j and COP_j by using the relation in Equation 2.4. Data from three chillers and three cooling towers were fitted against Equation 2.16 to estimate the value of the energy balance coefficients (e_1, e_2, e_3, e_4 and e_5). Figure 2.10 validates the energy balance equation by plotting its left hand side (LHS), i.e., the total rate of heat transfer (from data) at all the condensers, versus its right hand side (RHS), i.e., the estimated value of total rate of heat rejected by all cooling towers.

The implicit chiller model is unique as compared to other chiller models as it is developed for the whole chiller plant taken as a system. The inputs to this model are individual chiller loads and ambient wet-bulb temperature. It evaluates the individual power consumption values for every chiller in the plant, based on estimating the condenser water return temperature and the condenser water supply temperature. The model evaluates the outputs by solving a system of $(2M + 2)$ simultaneous equations, i.e. Equation 2.3 (M times, one for each chiller), Equation 2.4 (M times, one for each chiller), Equation 2.9 and Equation 2.16. The system of equations has $(2M + 2)$ number of unknown variables, i.e. P_j, COP_j, T_S and T_c . The system has zero degrees of freedom and therefore, can be solved to obtain a unique solution.

2.5 COMPARISON OF MODEL FITS

This section compares the chiller models described in earlier sections with respect to quality of their fits against real chiller plant data collected over a year. Two distinct datasets were obtained and used for this comparative study – (i) data from chiller plants at UT Austin and (ii) data from chillers in a semiconductor fab (DMOS6) at Texas Instruments Inc., Dallas. Each model was compared against the Gordon-Ng model (or

with MGN1 model), which is the most commonly used first principles model for centrifugal chillers.

2.5.1 Gordon-Ng model versus Modified Gordon-Ng model 1

Year-long chiller data collected from the UT Austin chiller plants was used for comparing the MGN1 model against the existing Gordon-Ng model. The UT Austin chiller plant consisted of nine separate electric centrifugal chillers with varying efficiencies and operating load ranges. They are numbered after their respective cooling stations – 6.1, 6.2 and 6.3 from Station 6; 5.1, 5.2 and 5.3 from Station 5 and; 3.1, 3.2 and 3.3 from Station 3. The data obtained from each chiller was fitted using the Gordon-Ng model and their respective fitting parameters were obtained by minimizing the sum of squared errors. The model demonstrated a good fit for the most part of the operating load range for all chillers. However, the predicted chiller power consumption deviated from the actual data for very low and very high cooling loads for all the chillers.

Figure 2.11 plots the model predicted chiller power versus the actual chiller power values for Chiller 6.1. In case of a perfect fit, all the points in such a plot should lie on the straight line $y = x$. However, in Figure 2.11 a large number of points, especially at the extremes, deviate from this straight line. It was observed that the model does not agree well with the actual data for power < 500 kW and for power > 2500 kW. This behavior is referred to as extreme load discrepancy in this work.

The Gordon-Ng model uses rate of internal heat losses as model parameters, suggesting that they are independent of the chiller cooling load. But the fact that Gordon-Ng model predicted values deviated from actual data for very low and very high load values suggested that internal heat losses should be higher for high cooling load and lower for low cooling load (accounted for in MGN1 model).

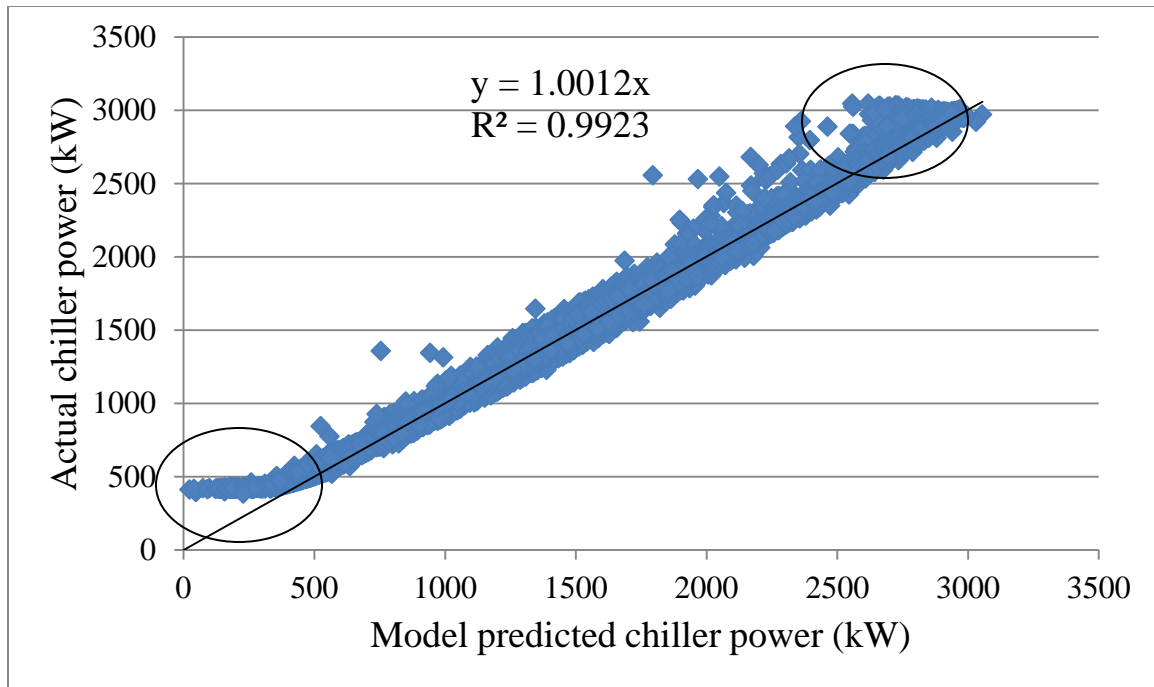


Figure 2.11: Gordon-Ng model predicted chiller power consumption vs. data for Chiller 6.1

Figure 2.12 illustrates the Modified Gordon-Ng model 1 fit for the same chiller 6.1. The comparison between Figure 2.11 and Figure 2.12 show that the MGN1 model fits much better to the data from Chiller 6.1. The data points in Figure 2.12 were fitted to a straight line using Microsoft Excel, which resulted in perfect $y = x$ line. It is also evident from Figure 2.12 that the MGN1 model has a good fit over the entire range of cooling load, thus avoiding the extreme load discrepancy behavior.

Similar comparisons were done by fitting data from rest of the eight chillers at UT Austin. Every chiller, when fitted to the Gordon-Ng model, exhibited extreme load discrepancy behavior similar to Figure 2.11. However, when using the MGN1 model, the discrepancies disappeared. The model fits resulted in coefficient of determination (R^2) values ranging from 0.94 to 0.999 with one exception of $R^2 = 0.84$ for Chiller 3.1.

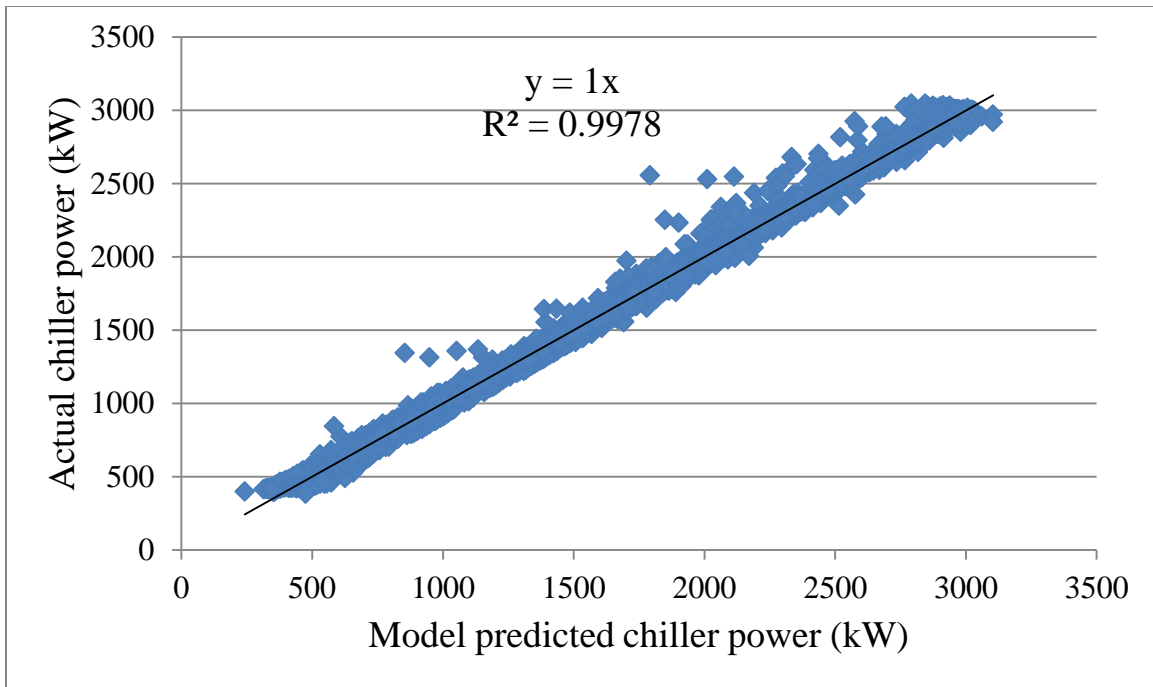


Figure 2.12: MGN1 model predicted chiller power consumption vs. data

2.5.2 Modified Gordon-Ng model 2 versus Modified Gordon-Ng model 1

Year-long data collected from nine separate chillers in DMOS6 fab at TI Dallas were used for comparing the two MGN models. These chillers are numbered as 11, 12, 21, 22, 31, 32, 42, 51 and 52. The chillers are arranged such that four pairs of chillers - 11 and 12, 21 and 22, 31 and 32, 51 and 52 - are operated in series with one another. Data collected from the chillers reveals that among the chillers in series pairs, the second chiller in each pair (Chiller 12, 22, 32 and 52) has been operated in two distinct modes – (i) when the first chiller among the pair (Chiller 11, 21, 31 and 41) is on and (ii) when the first chiller is off. But in both cases, the range of cooling load placed on the second chiller remained the same. In the first mode, both series chillers are on (say Chiller 11 and 12), the chilled water temperature difference is distributed between the two chillers. . While in the second mode, Chiller 11 is off and Chiller 12 is operated in parallel with all

other chillers, the chilled water temperature difference across Chiller 12 is greater because Chiller 11 is not contributing anything towards lowering the chilled water temperature. Hence, with the cooling load on Chiller 12 kept at a similar range in both modes, the chilled water flow rate is much lower in the second mode as compared to the first (see Equation 2.1). The two modes of operation, applicable for the second chiller in every series pair, are referred to as the series mode and the parallel mode respectively, in this dissertation.

Data from both operating modes of Chiller 12 was fitted using the MGN1 model and their respective modeling parameters were obtained (Table 2.1). Similarly, Table 2.2 shows two sets of fitting parameters obtained for the two modes of Chiller 32.

Fitting parameter	Series mode	Parallel mode
M_c	277.6358	277.6363
M_e	13.93207	13.93432
q_{e_m}	494.6412	307.7059
q_{c_m}	7.53E-09	7.53E-09
a	1.369754	0.514203
b	2.308691	0.94418

Table 2.1: MGN1 model fitting parameters for Chiller 12

Fitting parameter	Series mode	Parallel mode
M_c	803.635	803.635
M_e	195.578	195.578
q_{e_m}	0.0007	0.0007
q_{c_m}	2.8E-07	2.28E-07
a	2.206	1.736
b	1.955	1.489

Table 2.2: MGN1 model fitting parameters for Chiller 32

It is evident from Tables 2.1 and 2.2 that two different sets of fitting parameters characterize the energy efficiency curve for the same chiller operating in two different modes. However, an interesting observation is that the parameters that define the heat transfer coefficients for the evaporator and condenser (M_e and M_c) do not vary between series and parallel modes. This observation is consistent with the fact that heat transfer coefficient of a heat exchanger is a constant and does not vary with fluid flow rate or rate of heat transfer. On the other hand, the set of parameters which describe the rate of energy losses at evaporator and condenser have different values for different modes. The values of the fitting parameters suggest that internal losses are higher in series mode as compared to parallel mode. This can be explained by the fact that higher water flow rate in series mode leads to higher shear viscous dissipation, which is a contributor to internal energy losses.

The hypothesis suggesting that internal losses vary with chilled water flow rate, defined in Equation 2.7 and Equation 2.8, was validated by using data from Chiller 12 and Chiller 32. Data related to different modes of operation were combined to obtain one dataset for each chiller. This data was fitted against both MGN1 and MGN2 models. Table 2.3 presents the sum of squared errors (SSE), mean absolute error (MAE) and mean percentage error (MPE) in both cases to compare the accuracy of model fits for Chiller 12.

Error metric	MGN1	MGN2
SSE	76694 kW ²	33653 kW ²
MAE	7.07 kW	4.41 kW
MPE	1.32%	0.83%

Table 2.3: MGN1 model vs. MGN2 model fitting for Chiller 12

From Table 2.3, it is clear that MGN2 model estimates the chiller power more accurately than MGN1 model, without having prior knowledge about the mode of chiller operation. Table 2.4 presents the MGN2 model fitting parameters obtained after minimizing the sum of squared errors, for both Chiller 12 and Chiller 32. As expected, the heat transfer coefficients (M_e and M_c) obtained for MGN2 model for both Chiller 12 and Chiller 32 are similar to the ones from MGN1 models. However, the parameters involved in the estimation of internal energy losses have different values from Table 2.1 and Table 2.2. These observations support the hypothesis behind the development of MGN2 model.

Fitting parameter	Chiller 12	Chiller 32
M_c	277.7234	803.1358
M_e	14.02435	190.8316
q_{e_m}	304.4677	2.057007
q_{c_m}	7.53E-09	0
a	0.507089	1.677012
b	0.960825	1.472803
d_1	0.01816	0.153584
d_2	0	0.135811

Table 2.4: MGN2 model fitting parameters

2.5.3 Implicit chiller model versus Modified Gordon-Ng model 1

As discussed in the previous sections, the implicit chiller model was developed for an entire cooling station as a system. Results in this section are presented for Station 6 at UT Austin. It consists of three chillers (numbered as 6.1, 6.2 and 6.3) and three cooling towers as shown in Figure 2.7. Year-long data from Station 6 were used to obtain the fitting parameters for Stoecker's equation [25] and energy balance equation (Equation 2.16) (Figure 2.8 and Figure 2.10). These parameters were then used to solve a system of simultaneous non-linear equations (2.3, 2.4, 2.9 and 2.16) in order to compute individual chiller power consumptions. Hourly data for ambient wet-bulb temperature and individual chiller cooling loads were used as input variables. Therefore, the set of model

equations was solved every hour with different set of input variables. Microsoft Excel Solver was used to solve the system of simultaneous non-linear equations.

The implicit chiller model predictions were compared against MGN1 model predictions for the same time stamps. Two days having different cooling load profile and different ambient weather conditions were chosen from the month of July, 2011 and named as Day 1 and Day 2.

These models were developed to be used in an optimization problem where the value of condenser water temperature would not be known in advance. A constant value of condenser water temperature needed to be fed as an input parameter to the equations of MGN1 model. Mean of the previous year's hourly condenser water temperature values over the month of July ($T_{c,July}$) was used for this purpose. Therefore, while the implicit chiller model estimated the variable T_c from model equations, MGN1 model assumes a constant value of $T_{c,July} = 302$ K to estimate chiller power during the month of July.

Figures 2.13 and 2.14 show the comparison between model predicted and actual power consumption values for MGN1 model and implicit chiller model respectively, for Chiller 6.2 and Day 1. Table 2.5 compares these two model fits in terms of the sum of squared errors (SSE) and the integrated absolute error (IAE) over 24 points. It was observed from Figures 2.13 and 2.14 and Table 2.5 that the MGN1 model estimates the chiller power consumption closer to the real data as compared to implicit chiller model for Day 1.

The implicit chiller model has a larger modeling error when the cooling load is on the higher end of the range or when the cooling load profile undergoes large fluctuations (Figure 2.14). An important component of the implicit chiller model formulation is the steady-state energy balance equation. However, when the cooling load or ambient wet-bulb temperature fluctuates by an amount above certain level, the heat transfer processes

cannot be assumed to be in steady state. This hypothesis explains the large modeling errors occurring at certain times of Day 1 for implicit chiller model.

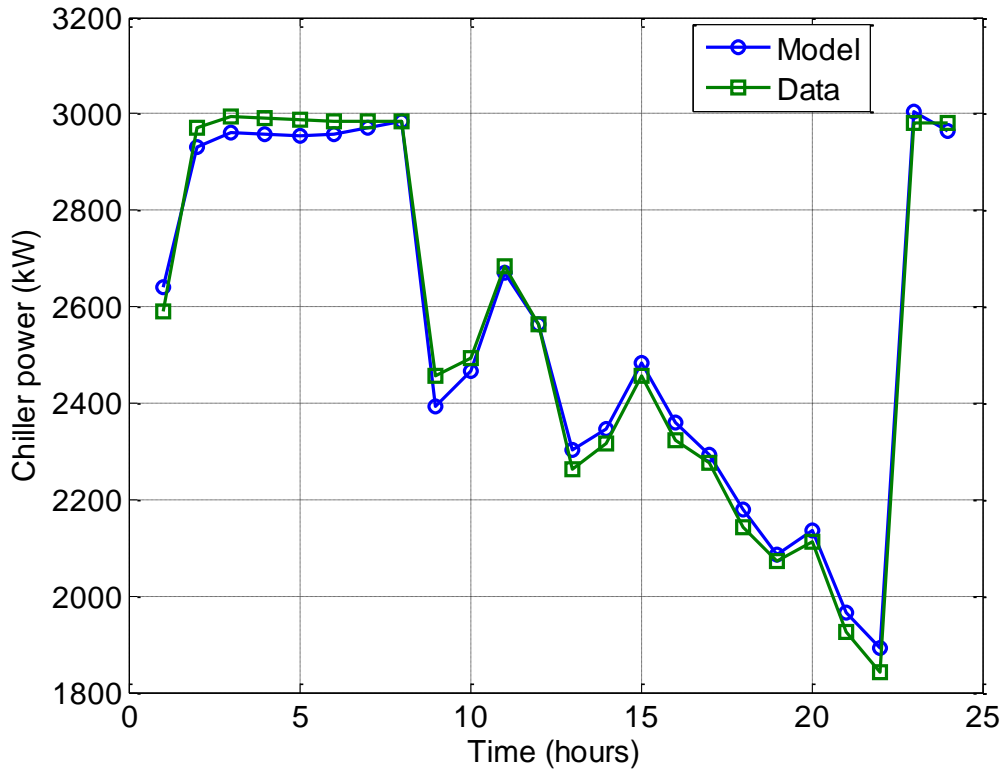


Figure 2.13: MGN1 model predicted chiller power ($T_c = 302$ K) vs. data for Day 1

It has been shown in the earlier sections that the MGN1 model gives quite accurate results if the values for all input variables are known. On Day 1, the actual condenser water temperature varies from 301.8 K (83.6 °F) to 302.5 K (84.8 °F). The assumed constant value for condenser water temperature (i.e., 302 K) happens to be quite close to the actual range for that day. Therefore, the modeling error from MGN1 model is relatively low for Day 1.

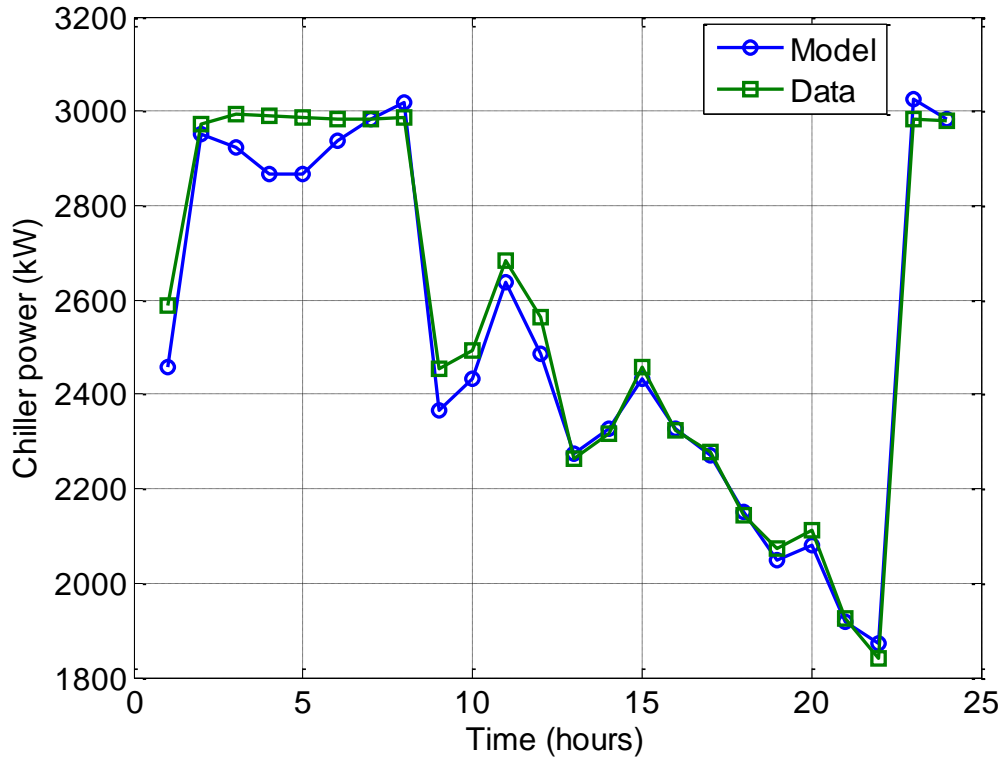


Figure 2.14: Implicit chiller model predicted chiller power vs. data for Day 1

Error metric	MGN1 model	Implicit chiller model
SSE	$0.25 \times 10^5 \text{ kW}^2$	$0.81 \times 10^5 \text{ kW}^2$
IAE	$0.69 \times 10^3 \text{ kWh}$	$1.02 \times 10^3 \text{ kWh}$

Table 2.5: MGN1 model vs. implicit chiller model (Chiller 6.2, Day 1)

Figure 2.15 and Figure 2.16 shows the plots for Day 2 which is a relatively cooler day in the same month. The average value of T_c over the 24 hours in Day 2 is 300.2 K. Qualitative comparison of these two figures makes it clear that the implicit chiller model performs better than the MGN1 model for this day. Table 2.6 supports this observation through quantitative comparison of modeling errors between the two models. Even though the implicit chiller model gives accurate estimation of chiller power at most data

points, it has relatively large modeling error ($\sim 7\%$) associated with 11th hour. This reinforces the hypothesis based on observations from Figure 2.14. Since the chiller cooling load undergoes sudden rise and drop at 11th hour, steady state energy balance equations do not represent the heat transfer taking place at the chiller heat exchangers (evaporator and condenser) accurately.

Error metric	MGN1 model	Implicit chiller model
SSE	$2.48 \times 10^5 \text{ kW}^2$	$0.57 \times 10^5 \text{ kW}^2$
IAE	$2.35 \times 10^3 \text{ kWh}$	$0.74 \times 10^3 \text{ kWh}$

Table 2.6: MGN1 model vs. implicit chiller model (Chiller 6.2, Day 2)

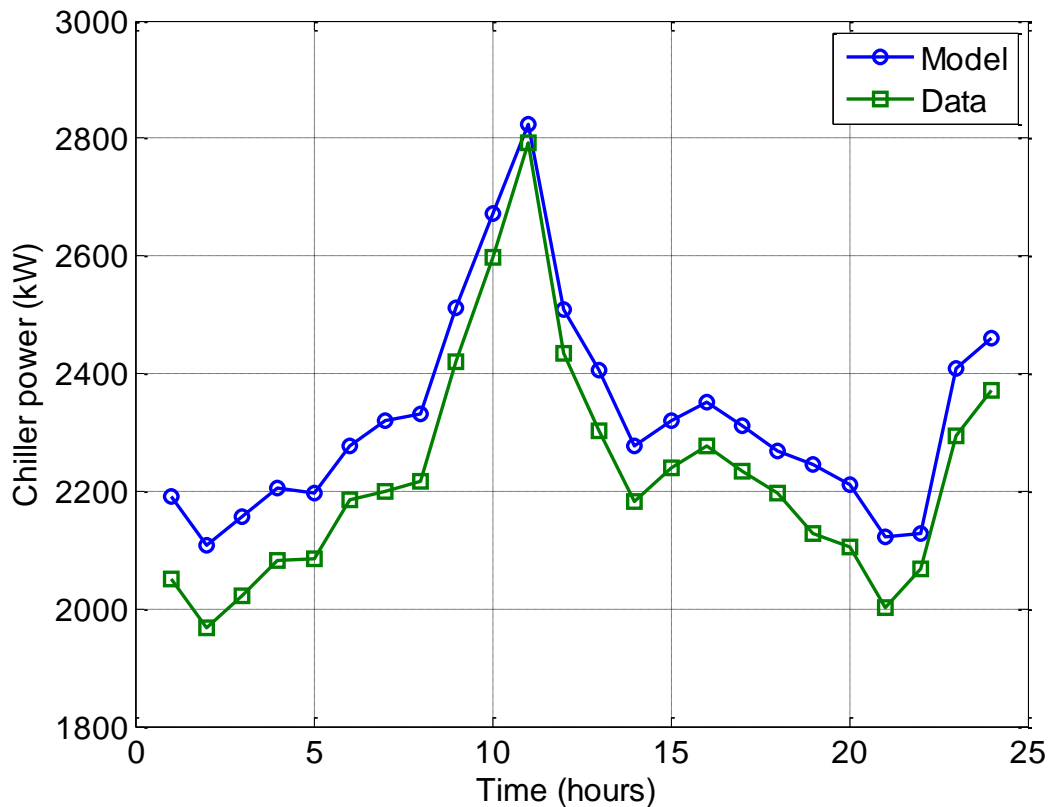


Figure 2.15: MGN1 model predicted chiller power ($T_c = 302 \text{ K}$) vs. data for Day 2

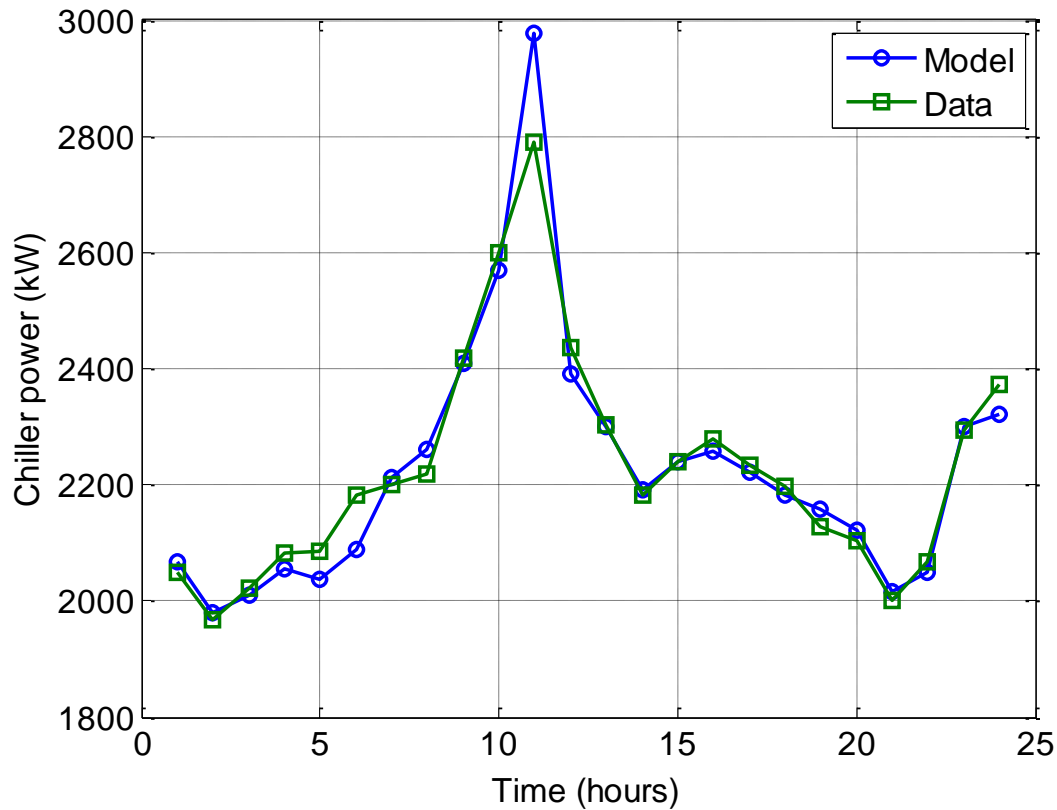


Figure 2.16: Implicit chiller model predicted chiller power vs. data for Day 2

The MGN1 model, in this case, does not compute the chiller power consumption as accurately as it does for Day 1. This is because the MGN1 model computes the power consumption by using $T_c = T_{c,July} = 302$ K, while the actual average value of T_c is around 300.2 K over Day 2. Figure 2.6 shows that according to Gordon-Ng model and MGN1 model, a rise of 1 K in the condenser water temperature can increase the chiller power consumption by about 3%. Hence, an error of 2 K in the value of condenser water temperature, used as an input to the model equation, can lead to a modeling error of about 6%.

Implicit chiller model, being a combination of MGN1 model equations, Stoecker's equation and energy balance equation, is a much more complex model with more number of output variables as compared to MGN1 model. The combination of errors associated with each equation can result in a much higher modeling error in the case of implicit model. Despite having more sources of error due to its complexity, this model results in pretty accurate estimation ($< 1\%$ deviation from data) of the chiller power consumption for most part of the cooling load range and irrespective of the ambient weather conditions. This accuracy is achieved because the model takes into account the effect of variation of the wet-bulb temperature (included in Equation 2.9 and Equation 2.16). On the other hand, a standalone MGN1 model works fine for certain ambient weather conditions but may produce relatively large modeling error for others (up to 5% deviation from data).

2.6 CONCLUSIONS

This chapter describes the development and performance of three models that compute the power consumption of an electric centrifugal chiller. The Gordon-Ng model for centrifugal chillers [6] is used as the base model, which is either modified or included as part of a bigger set of equations, to develop the three new models.

The Modified Gordon-Ng 1 (MGN1) model is conceptualized by redefining certain parameters (related to internal energy losses at evaporator and condenser) in the Gordon-Ng model equation as variables that depend linearly on the chiller cooling load. This modification leads to much better fits to a wider range of chiller data.

The Modified Gordon-Ng 2 (MGN2) model considers internal energy losses to vary with the cooling load as well as the chilled water flow rate linearly. This model is

proposed to represent chillers that are operated in series as well as in parallel with other chillers, such that the chilled water flow rate and cooling load can be treated as independent variables. The model fitting results show that MGN2 model can be used to describe a chiller's efficiency curve irrespective of its mode of operation.

The implicit chiller model is developed in order to compute the chiller power consumption without having to know or guess the condenser water temperature (T_c). This model is developed using a combination of MGN1 model, Stoecker's correlation, and energy balance around the condenser water loop of a chiller plant. This model accurately estimates the value of T_c , thus avoiding modeling errors that arise in MGN1 and MGN2 models due to incorrect assumption of T_c value. For a situation when T_c value is unknown, MGN1 model is compared against the implicit chiller model. Implicit model results in pretty accurate estimation (< 1% deviation from data) of the chiller power consumption for most part of the cooling load range irrespective of the ambient weather conditions. While MGN1 model accuracy is dependent on the ambient weather conditions and may produce relatively large modeling errors in some cases (up to 5% deviation from data).

In spite of the positives of implicit chiller model, results do reveal that improvements need to be made in modeling the heat transfer processes occurring in transient state conditions and for higher end of the chiller cooling load range. As seen from Figure 2.16, its chiller power estimate can deviate from actual data by up to 7% at certain times.

Having analyzed the advantages and shortcomings of various chiller models, it is easier to choose an appropriate model depending on the kind of system and the optimization problem under consideration. The optimization problem can be defined and solved in several ways. Next chapter introduces the concept of optimal chiller loading

(OCL) as a constrained optimization problem with multiple possible objective functions. While Chapter 3 uses a simple quadratic correlation [26] to compute chiller power consumption, Chapter 4 utilizes the models discussed in the current chapter to solve the OCL problem for large and complex cooling systems.

Chapter 3: Optimal Chiller Loading for Energy Efficient Operation

3.1 INTRODUCTION

Large cooling systems usually consist of chiller plants, cooling towers and pumps. Chiller plants often include a number of centrifugal chillers that cool the circulating chilled water, which in turn is used for providing air conditioning and preventing over heating of tools and processes. In most cases, multiple chillers are arranged in parallel in a chiller plant, as shown in Figure 3.1. The total plant cooling load is divided among several independent chillers by dividing the chilled water flow rate in such arrangements. Several methods are employed in such plants to determine an optimum cooling load distribution among the individual chillers for a given plant cooling load [27-28]. One of the most common methods is equal loading rate method [27], which is achieved through distributing the total load such that all the chillers have the same part load ratio (PLR), where part load ratio of j^{th} chiller is defined by the following equation.

$$PLR_j = \frac{Q_j}{Cap_j} \quad (3.1)$$

The individual chiller load resulting from the equal loading rate method is the total cooling load multiplied by a loading rate, where the loading rate is the ratio of individual chiller capacity to the total chiller capacity. Even though this is the simplest chiller loading method, it is suboptimal in two ways. One, it ignores the dependence of a chiller's energy efficiency on various factors including its own cooling load. Two, it ignores the difference between individual chillers with respect to their energy efficiency curves.

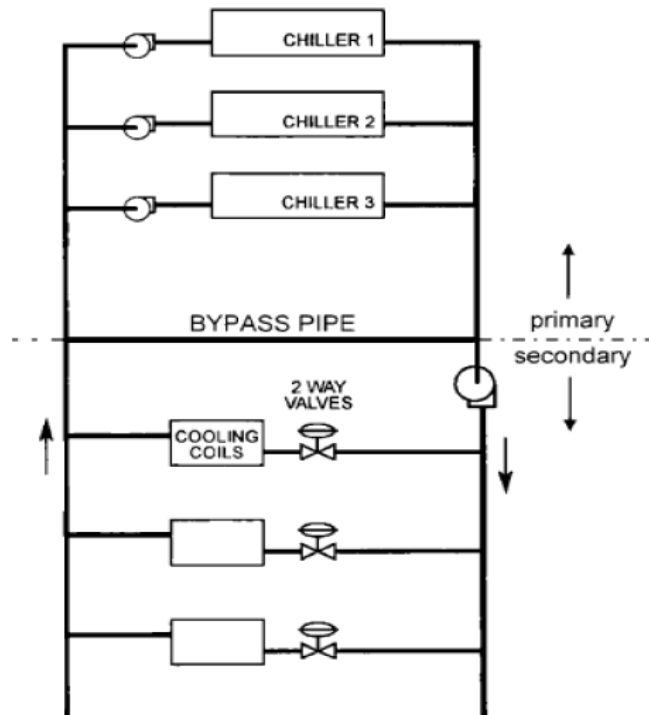


Figure 3.1: Schematic of a multi-chiller arrangement [7]

This chapter discusses the concept of optimal chiller loading (OCL) as an energy saving alternative to the equal loading rate method. Next section formulates OCL as a constrained optimization problem which can be solved with various objective functions, i.e., minimizing total power consumption or maximizing the sum of coefficients of performance (COP). Optimal chiller loading that aims at maximizing the sum of individual chiller COP values is called the Lagrangian method by Chang [7].

The second half of the chapter demonstrates the application of OCL with the help of two case studies performed on simple multi-chiller systems. These case studies compare the chiller plant energy consumption resulting from equal loading rate method, Lagrangian method, and OCL that minimizes the total power consumed by the multi-chiller system.

3.2 OPTIMAL CHILLER LOADING (OCL) – A CONSTRAINED OPTIMIZATION PROBLEM

Optimal chiller loading is one of the methods to determine the most efficient manner of distributing an overall cooling load among several chillers in a multi-chiller system. OCL is mathematically formulated as a constrained optimization problem. It aims at making two kinds of decisions – (i) which set of chillers to turn on, and (ii) amount of cooling load to be distributed to each of those chillers. To solve these questions, two decision variables are defined for each j^{th} chiller (i) δ_j - binary variable δ_j which represents the on or off status of a chiller (1 = “on”; 0 = “off”), and (ii) X_j - cooling load on each chiller assuming it is “on”. Hence, the actual cooling load on j^{th} chiller is given by Equation 3.2.

$$Q_j = \delta_j * X_j \quad (3.2)$$

Two different objective functions are discussed in this chapter. Lagrangian method [7] aims at maximizing the sum $\sum_{j=1}^M COP_j$ for a total of M number of chillers. On the other hand, the OCL problem proposed in this chapter (to find the optimum solution for minimizing overall chiller power consumption) can be formulated as the following:

$$\min_{\delta_j, X_j} \sum_{j=1}^M \delta_j * P_j(X_j) \quad (3.3)$$

Equation 3.3 illustrates an important application of models that compute chiller power consumption $P_j(X_j)$ as a function of the chiller cooling load. It thus emphasizes the importance of the work on various chiller models presented in Chapter 2.

This optimization problem aims at minimizing the sum of power consumed by all chillers which are “on”, while satisfying the cooling load demand. This leads to the following constraint:

$$\sum_{j=1}^M \delta_j * X_j \geq D \quad (3.4a)$$

Due to the finite nature of each chiller's design capacity, and operational constraints on physical variables such as chilled water flow rate, each chiller if turned on has a corresponding lower and upper limit on its cooling load value. This leads to a total of $2M$ inequality constraints which are represented by Equation 3.4b.

$$L_j \leq X_j \leq U_j \quad \forall j \in \{1, 2, \dots, M\} \quad (3.4b)$$

In addition to the above constraints, the decision variables defining the on/off status of each chiller are declared as binary variables.

$$\delta_j \in \{0,1\} \quad (3.4c)$$

Equation 3.4a states that the sum of cooling loads on all chillers has to be greater than or equal to the total cooling load demand. Since the objective function seeks to minimize power consumption, the constraint 3.4a will always hold with equality when no thermal storage is in place to store the excess amount of chilled water generated. So it could be replaced with an equality constraint and still achieve the same solution. However, it is left as an inequality constraint because (i) it provides a useful way to ensure that the model and algorithm are performing correctly (if the constraint ever does not hold with equality, there is an error somewhere), and (ii) it allows the addition of thermal energy storage without changing the formulation (as discussed later in Chapter 4), thus making the code more portable.

Optimal chiller loading is defined for a certain point in time as a steady state mixed integer non-linear program (MINLP), where the total number of decision variables is $2M$ for M number of chillers. In order to determine the optimal chiller loads over a certain span of time with variable cooling load demand (D), the time span is divided into smaller time intervals. Independent steady state optimization problems, defined by

Equations 3.3 and 3.4, are then solved for each time interval. This widely applicable methodology is also known as multi-period optimization and is discussed in detail in Chapter 4.

3.3 CASE STUDIES

The application of optimal chiller loading was simulated for two real systems – System 1 and System 2, both based in Taiwan. System 1 is a hotel while System 2 is a semiconductor manufacturing site. Chiller models for these systems are obtained from a previous paper by Chang [7], according to which each chiller follows quadratic correlation between its coefficient of performance (COP) and its part load ratio (PLR) (Equation 3.5) [26]. It is important to note that this correlation serves as a very simple chiller model which ignores the effect of chilled water temperature or condenser water temperature on coefficient of performance. Hence, it does not describe the behavior of most real cooling systems which are much more complex.

$$COP_j = \mathbf{a}_j + \mathbf{b}_j * PLR_j + \mathbf{c}_j * PLR_j^2 \quad (3.5)$$

The correlation coefficients (\mathbf{a}_j , \mathbf{b}_j and \mathbf{c}_j) are reproduced from [7] in Table 3.1 and Table 3.2. In System 2, all chillers have identical design capacities while in System 1 some chillers have lesser capacities than others.

Chiller	\mathbf{a}_j	\mathbf{b}_j	\mathbf{c}_j	\mathbf{Cap}_j
1	0.1561	3.7023	-2.5909	450
2	0.9000	1.8432	-1.4188	450
3	0.2932	3.0419	-2.0054	1000
4	0.1415	3.6376	-2.2469	1000

Table 3.1: Model parameters for System 1

Chiller	a_j	b_j	c_j	Cap_j
1	0.5703	3.1602	-2.0912	1250
2	0.3257	2.3513	-1.4265	1250
3	0.5438	1.8668	-1.2360	1250
4	0.7865	1.8473	-1.1633	1250
5	1.1191	1.0228	-0.7542	1250

Table 3.2: Model parameters for System 2

The chiller plant cooling capacity is the sum of cooling capacities of all working chillers in that plant. Therefore, the plant capacities for System 1 and System 2, as computed from the data tables, are 2900 tons and 6250 tons respectively. The upper limit (U_j) on each chiller's cooling load was assumed to be equal to its design capacity (Cap_j) while the lower limit (L_j) was assumed to be half of its design capacity. These assumptions were made in order to maintain consistency between the optimization problem formulation in this chapter and in [7] as this study aims at comparing the total power consumption resulting from these two formulations.

Figure 3.2 plots the energy efficiency curves for all chillers in System 1 over their respective cooling load ranges. Chiller efficiency is generally expressed in terms of kW per ton (kW/ton) and chiller cooling load in tons. Figure 3.2 clearly illustrates how energy efficiency curves of individual chillers can vary from one another and hence underlines the importance of employing an optimization algorithm to determine the most energy efficient cooling load distribution. Figure 3.3 plots chiller efficiency curves for chillers in System 2. It is evident from the plots that variation in chiller efficiency across chillers is even greater in System 2 as compared to System 1.

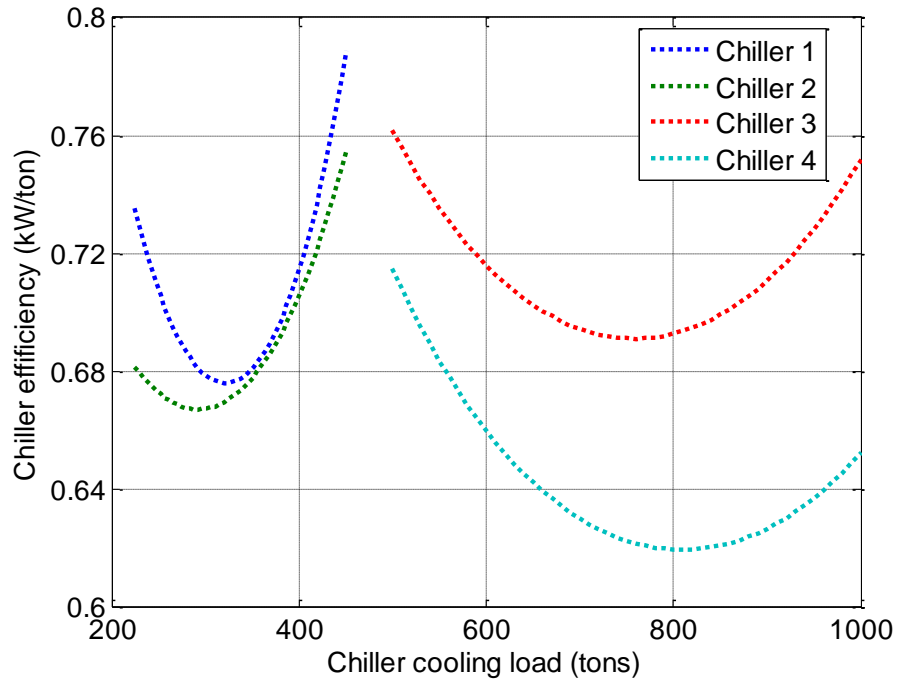


Figure 3.2: Energy efficiency curves for all chillers in System 1

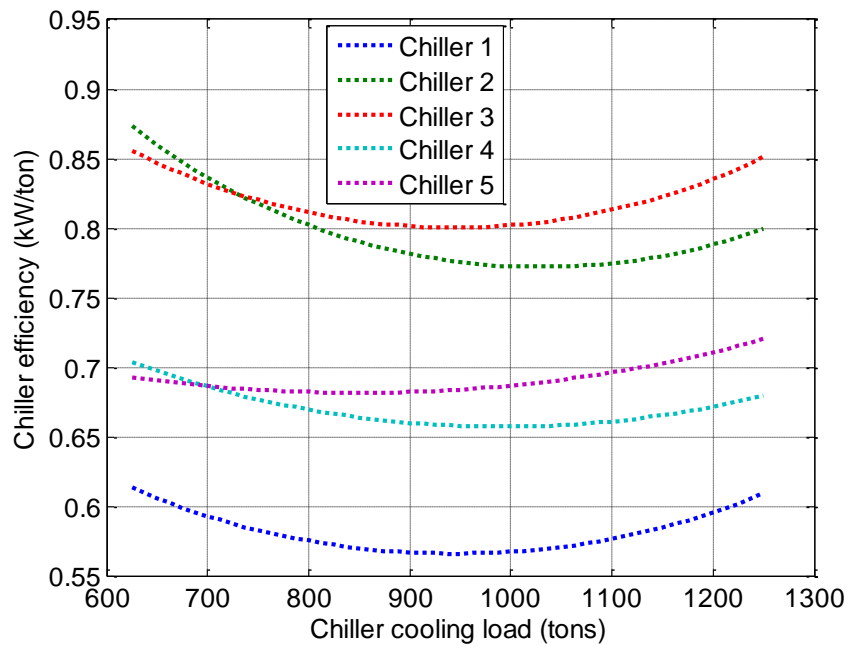


Figure 3.3: Energy efficiency curves for all chillers in System 2

Three different methods were used with both the systems to determine a method to optimally distribute the overall plant cooling load among its chillers. The comparison between the total resultant power consumption from these methods is presented in the following section. Computations were done for different values of total plant cooling load ranging from 70% to 95% of the overall plant cooling capacity. The methods used for each system are listed below:

3.3.1 Equal loading rate (ELR) method [27]

As the name suggests, load distribution was done such that all chillers have identical part load ratio, which was obtained from the following equation:

$$PLR_j = \frac{D}{\sum_{j=1}^M Cap_j} \quad (3.6)$$

Individual chiller power consumption was computed by using Equations 3.5 and 3.6 for each chiller in the system. Summing it over all chillers resulted in the total power consumption for the plant.

3.3.2 Lagrangian method [7]

The advantage of using Lagrangian method lies in the ability to compute optimal chiller loads analytically using Equation 3.7 [7]. The optimization problem is solved using Lagrange multipliers (λ). The optimal PLR_j of j^{th} unit can then be expressed as:

$$PLR_j = \frac{\lambda * Cap_j - b_j}{2c_j} \quad (3.7a)$$

$$\lambda = \frac{2D + \sum_{j=1}^M \frac{b_j}{c_j} Cap_j}{\sum_{j=1}^M \frac{Cap_j^2}{c_j}} \quad (3.7b)$$

The total power consumption was calculated from PLR_j in the same way as described in the equal loading rate method.

3.3.3 Optimal chiller loading

This constrained optimization problem, as described in the previous section, was solved for both systems with the help of Microsoft Excel solver, which uses the Generalized Reduced Gradient (GRG2) algorithm. The objective function (total power consumption) in this case is given by combining Equations 2.2, 3.1, 3.3 and 3.5.

$$\min_{\delta_j, X_j} \sum_{j=1}^M \left(\delta_j * \frac{X_j * Cap_j^2}{a_j Cap_j^2 + b_j Cap_j X_j + c_j X_j^2} \right) \quad (3.8)$$

The upper and lower bounds for cooling load are defined by the following relations:

$$U_j = Cap_j \quad \forall j \in \{1, 2, \dots, M\} \quad (3.9a)$$

$$L_j = 0.5 * Cap_j \quad \forall j \in \{1, 2, \dots, M\} \quad (3.9b)$$

This method involves numerically solving for optimal X_j and δ_j to minimize total power consumption (Equation 3.8) while satisfying the constraints of total cooling load and bounds on cooling load (Equations 3.4 and 3.9). The resulting X_j and δ_j values were substituted in the expression of objective function to compute the total power consumption.

3.4 RESULTS AND DISCUSSION

Chang [7] compares the total power consumption for each system from equal loading rate method and from Lagrangian method. The resulting values of Q_j (see Equations 3.1 and 3.2) and P_j from these two methods are reproduced in this section and compared with the results generated from solving optimal chiller loading as proposed and formulated in the previous sections (Equations 3.4, 3.8 and 3.9).

Table 3.3 compares the results for System 1 from all three methods. The shaded columns in the table represent the new results generated from this work. Similarly, Table

3.4 shows the comparison of results for System 2. All chiller load values are in tons and all power consumption values are in kW.

Total load	Chiller	Equal loading rate		Lagrangian		OCL	
		Q_j	P_j	Q_j	P_j	Q_j	P_j
2610 (90%)	1	405	291.5	350.3	238.6	373.4	258.5
	2	405	287.3	344.8	233.1	383.7	266.4
	3	900	639.9	941.8	682.9	882.7	623.5
	4	900	564.2	973.1	626.4	970.2	623.7
	Total	2610	1782.8	2610	1780.9	2610	1772.1
2465 (85%)	1	382.5	267.3	340.5	231	354.0	241.6
	2	382.5	265.3	327	219.4	353.6	240.2
	3	850	594.5	879.7	620.8	834.0	581.0
	4	850	527.9	917.7	578.2	923.4	582.8
	Total	2465	1655	2465	1649.4	2465	1645.6
2320 (80%)	1	360	246.6	330.8	223.9	335.2	227.1
	2	360	245.5	309.2	206.6	327.8	220.0
	3	800	554.3	817.6	567.9	781.4	540.5
	4	800	495.8	862.3	536.5	875.6	545.9
	Total	2320	1542.2	2320	1534.9	2320	1533.5
2175 (75%)	1	337.5	228.7	321.1	217.1	316.7	214.2
	2	337.5	227.4	291.5	194.5	287.4	191.8
	3	750	518.5	755.6	522.3	734.9	508.4
	4	750	467.1	806.9	500	836.0	518.5
	Total	2175	1441.7	2175	1433.9	2175	1432.9
2030 (70%)	1	315	213.1	311.3	210.7	340.4	230.9
	2	315	210.7	273.7	182.9	0	0
	3	700	486.2	693.5	482.2	798.2	553.0
	4	700	441.1	751.5	467.9	891.4	557.6
	Total	2030	1351.1	2030	1343.7	2030	1341.4

Table 3.3: Optimization results for System 1

Total load	Chiller	Equal loading rate		Lagrangian		OCL	
		Q_j	P_j	Q_j	P_j	Q_j	P_j
5625 (90%)	1	1125	664.2	1086.4	632.4	1182.2	700.1
	2	1125	932.7	1102.4	904	1097.5	850.5
	3	1125	1064.1	954.5	800.6	996.8	799.7
	4	1125	752.2	1250	861.4	1213.8	818.2
	5	1125	811.9	1231.6	924.4	1134.7	795.7
	Total	5625	4225.7	5625	4122.8	5625	3964.2
5312.5 (85%)	1	1062.6	614.1	1039.4	597.1	1140.4	665.8
	2	1062.6	856.8	1035.5	826.8	1043.4	806.1
	3	1062.6	952.6	899.9	738.1	929.6	744.6
	4	1062.6	704.1	1227.7	840.4	1152.0	767.6
	5	1062.6	753.4	1110.5	797.9	1047.1	723.8
	Total	5312.5	3881.0	5312.5	3800.4	5312.5	3707.7
5000 (80%)	1	1000	569.9	1001.6	570.9	1100.9	635.8
	2	1000	790	981.5	771.8	991.2	766.5
	3	1000	859.2	855.8	693	861.3	692.8
	4	1000	659.3	1148.3	771.1	1091.0	721.3
	5	1000	699.1	1012.8	709.9	955.5	654.3
	Total	5000	3577.6	5000	3516.8	5000	3470.7
4688 (75%)	1	937.6	530.6	963.8	546.6	1192.5	709.1
	2	937.6	731	927.7	722.2	1110.2	861.5
	3	937.6	780.4	811.9	651.9	0	0
	4	937.6	617.5	1069.2	709.0	1229.4	831.7
	5	937.6	648.6	915.4	631.4	1155.8	813.9
	Total	4688	3308.1	4688	3261.2	4688	3216.2
4375 (70%)	1	875	495.3	926	523.8	1157.2	679.2
	2	875	677.9	873.7	676.8	957.3	742.3
	3	875	712.2	767.8	614	0	0
	4	875	577.9	989.8	652.3	1177.1	787.6
	5	875	600.9	817.7	559.5	1083.3	752.8
	Total	4375	3064.1	4375	3026.5	4375	2961.9

Table 3.4: Optimization results for System 2

Careful analysis of the numbers in Tables 3.3 and 3.4 reveals that the optimal chiller load values are largely consistent with the notion of individual chiller efficiencies as perceived from Figures 3.2 and 3.3. The chillers having higher chiller efficiency (i.e., lower kW/ton) end up with higher cooling load values in the optimized cooling load

distribution resulting from OCL or Lagrangian method. For example, Figure 3.3 illustrates that Chiller 3 is the least energy efficient chiller in System 2 for most part of the cooling load range. This observation is consistent with the fact that for each value of total load in Table 3.4, OCL and Lagrangian method result in Chiller 3 having the lowest cooling load. Due to the MINLP formulation, OCL allows a chiller to be turned off (zero cooling load) by setting δ_j equal to zero. Therefore, Chiller 3 is shown to be turned off in Table 3.4 when the total load is less than or equal to 75% of the plant capacity.

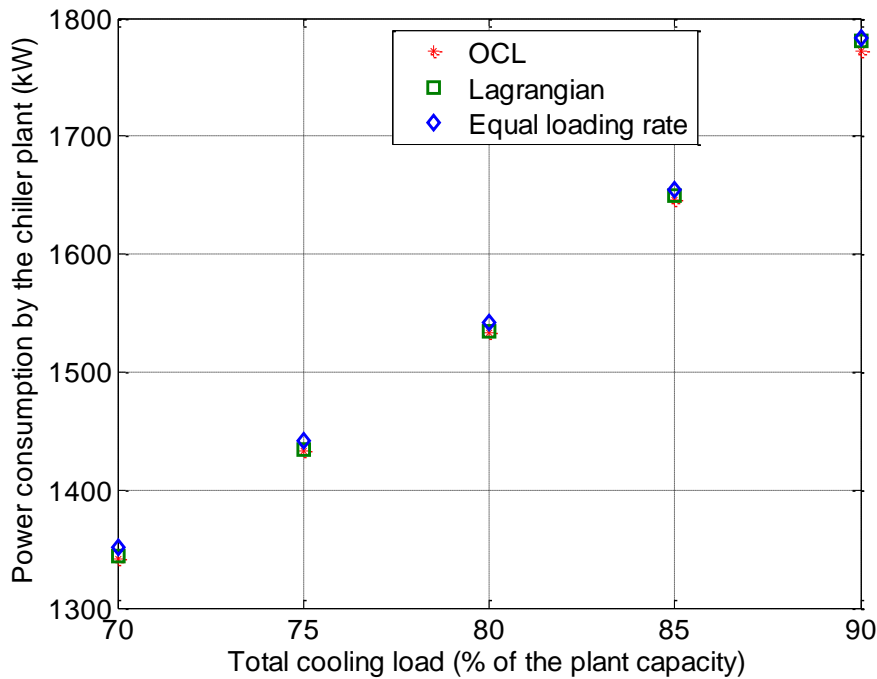


Figure 3.4: Comparison of power consumption in System 1 from different chiller loading methods

Figures 3.4 and 3.5 show the comparison of total power consumed by the plant from using the three chiller loading methods discussed in the previous section in System 1 and System 2 respectively. While the results show minor energy savings for System 1,

significant savings are observed for System 2 (Figure 3.5). For each data point, in both System 1 and System 2, the optimal chiller loading is observed to be the best in terms of energy efficiency while the equal loading rate method is the worst. As discussed in [7], Lagrangian method results in reduced power consumption by maximizing the sum of individual chiller COPs. However it is suboptimal because the objective function in this case is not directly related to the total power consumption.

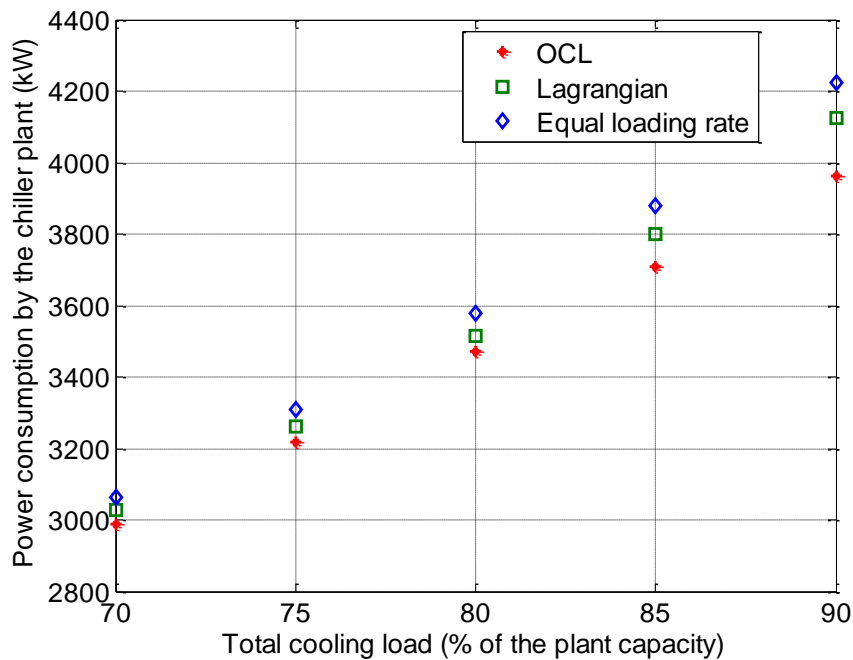


Figure 3.5: Comparison of power consumption in System 2 from different chiller loading methods

Figure 3.6 shows that the percentage energy savings for System 2 from using optimal chiller loading over equal loading rate method increases with total cooling load. It can go as high as over 6% for the cooling load of 5625 tons, which is 90% of the plant cooling capacity.

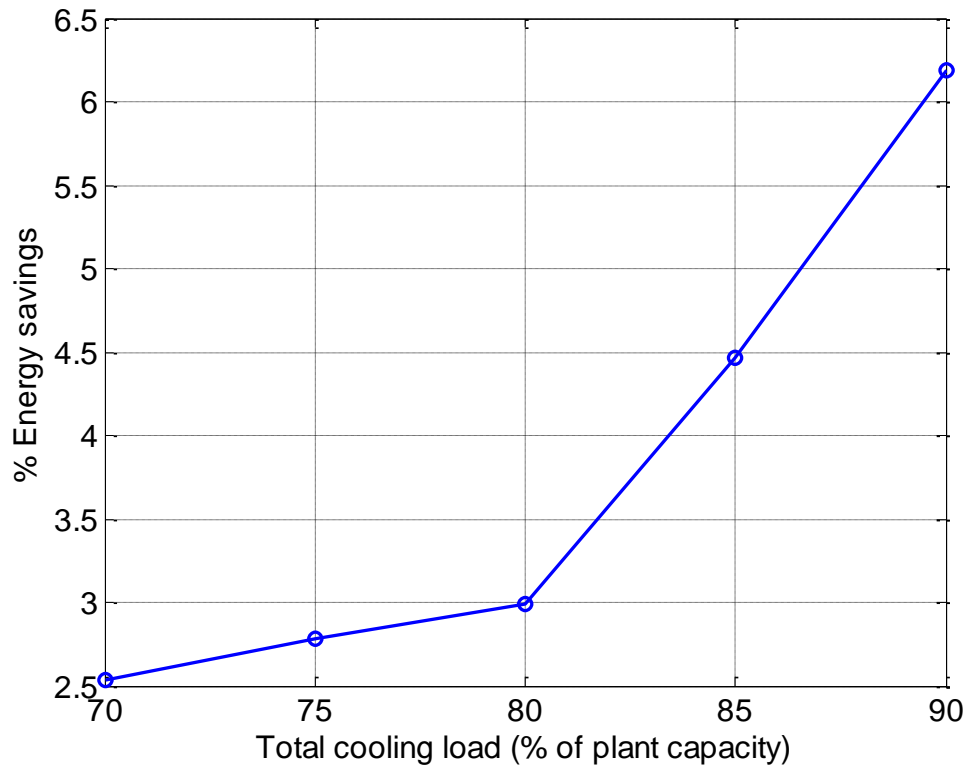


Figure 3.6: Estimated percentage energy savings from using OCL over ELR in System 2

These three methods follow the same order in terms of their computational complexity as they did for their effectiveness in optimizing power. While OCL needs to be solved using a numerical solver, Lagrangian method requires solving Equation 3.7 analytically and ELR method computes the cooling load for all chillers by one simple division. However, the computational requirement for OCL is not an issue since the optimization problem of this size can be solved in a fraction of a second using Microsoft Excel solver.

3.5 OPTIMIZATION VERSUS INTUITIVE COOLING LOAD DISTRIBUTION

In most chiller plants, the cooling loads are assigned based on operators' intuition which comes from comparing various chillers in terms of their energy efficiencies. This

section explains why optimal chiller loading can be essential even when intuitively the choice of the most efficient chiller is perfectly clear. This analysis is based on the System 2 results presented in Table 3.4.

It is clear from Figure 3.3 that Chiller 1 is the most efficient chiller over the entire cooling range. So, intuition and common sense would suggest that at large loads, Chiller 1 should be used at its maximum capacity (1250 tons). But the optimal chiller loading results suggest something else. For 90% cooling load (5625 tons), the optimization results are presented in Table 3.5.

Chiller number	Cooling load (tons)	kW/ton	Power (kW)
1	1182.1	0.592173	700.0071
2	1097.3	0.774919	850.3187
3	996.8	0.802267	799.6998
4	1213.8	0.674106	818.2304
5	1135	0.701266	795.9364
	Total = 5625	Average = 0.708	Total = 3964.2

Table 3.5: Optimal chiller loading results for System 2 at 90% cooling load

These cooling load values (approximated) and respective kW/ton values are marked in Figure 3.7.

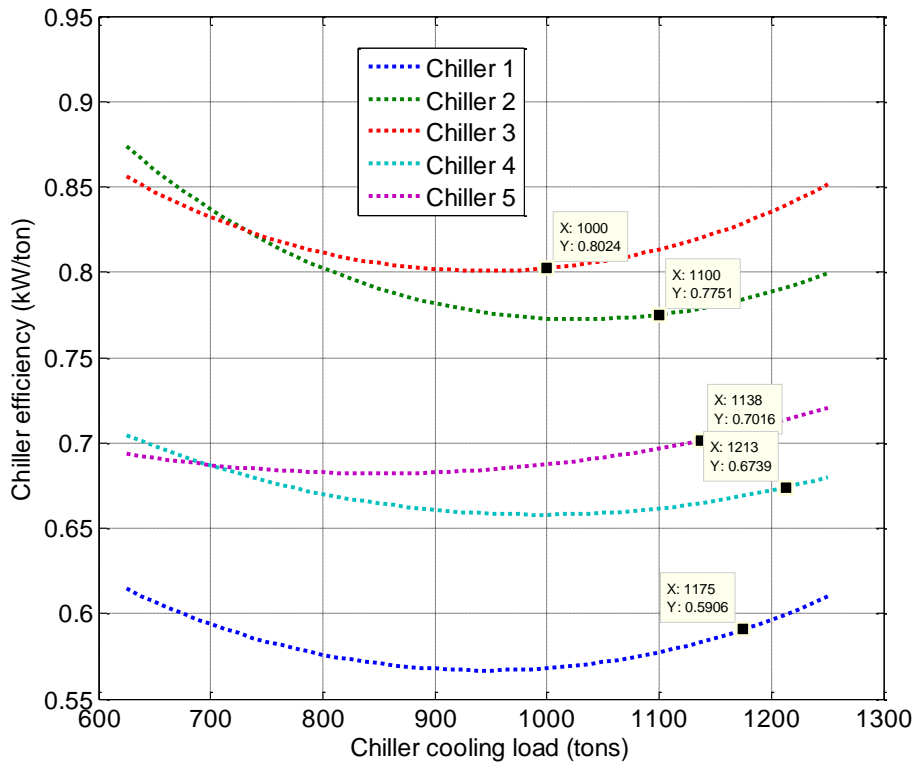


Figure 3.7: The optimal solution marked on energy efficiency curves

The optimal solution goes against the intuition as the most efficient chiller (Chiller 1) is not being used at its maximum capacity. It can be noticed from chiller efficiency curves and chiller models that the energy efficiency of Chiller 1 varies with the cooling load. If the cooling load is increased from 1182 tons to 1250 tons, the kW/ton rises from 0.59 to 0.61. Even though the kW/ton for Chiller 1 is still lower than that of any other chiller irrespective of the cooling load, the most amount of cooling load is not allocated to this chiller in the optimal solution presented. The reason behind this is explained in the paragraphs below.

Shifting some load from less efficient chillers to Chiller 1 would save us some energy (let's say E1). But the associated rise in kW/ton of Chiller 1 will increase the

energy consumption by say E2. It was observed that E1 is always less than E2 if we move away from the given optimal solution. Consider the following example to further illustrate this counter intuitive behavior.

[Note 1: since the problem was solved for just one point in time, the terms energy and power are used interchangeably.]

This problem was solved for a second case (called suboptimal case). The cooling load on Chiller 1 was fixed at 1250 tons and rest of the cooling load was divided among other chillers using OCL. The results obtained are presented in Table 3.6 and marked in Figure 3.8.

Chiller number	Cooling load (tons)	kW/ton	Power (kW)
1	1250	0.609999	762.4983
2	1083.73	0.774022	838.8311
3	979.90912	0.801504	785.4008
4	1198.3136	0.671876	805.1185
5	1113.0473	0.698396	777.348
	Total = 5625	Average = 0.711	Total = 3969.2

Table 3.6: Suboptimal chiller loading results for System 2 at 90% cooling load

By shifting 68 tons from Chillers 2, 3, 4 and 5 to Chiller 1, we saved E1 ~ 68 * (average difference in kW/ton). This gives an approximate number for E1 because we are taking average over the 4 less efficient chillers.

$$E1 \sim 68*(0.74-0.61) = 8.8 \text{ kW}$$

On the other hand, Chiller 1 efficiency drops by about 0.02 kW/ton and we lose E2 amount of power due to that.

$$E2 \sim 1182*(0.61-0.592) = 21 \text{ kW}$$

The loss in efficiency is higher because of a large cooling load (1182 tons) being affected by it. Therefore, this load distribution increases the overall power consumption as compared to the optimal solution presented.

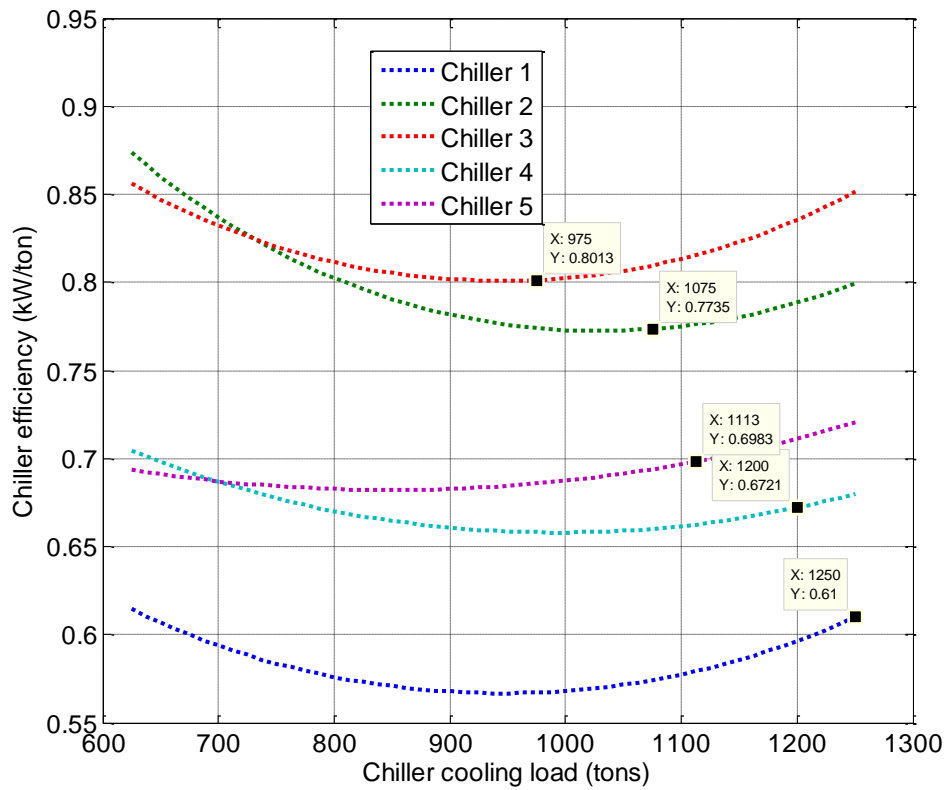


Figure 3.8: The sub-optimal solution marked on energy efficiency curves

[Note 2: The calculations presented in the above example are approximate and aimed at showing why the most efficient chiller being operated at its maximum capacity may not be the best solution.]

In conclusion, this example highlights the complexity of optimal chiller loading problem and signifies why OCL should be used even in cases where the most efficient and least efficient chillers are clearly distinguishable from one another.

3.6 CONCLUSIONS

This chapter discusses in detail various methods used to determine an appropriate cooling load distribution in a multi-chiller plant. Optimal chiller loading (OCL) is defined as a constrained optimization problem and it differs from the one resulting in Lagrangian method [7] in broadly two ways. First, OCL is an MINLP formulation while Lagrangian method was developed from an NLP formulation. Second, the sum of individual chiller power consumptions is used as the objective function for OCL while the sum of individual chiller COPs was maximized to derive the Lagrangian method. Since COP and chiller power are not linearly related, the two objective functions cannot be considered equivalent to each other. This conclusion was supported by the difference in optimization results obtained from OCL and Lagrangian method.

Equal loading rate method [27], Lagrangian method [7] and optimal chiller loading were compared with emphasis on improving the overall plant energy efficiency. Case studies were performed on two distinct actual multi-chiller systems in Taiwan using the chiller models that were available in [7]. Optimal chiller loading resulted in lowest total power consumption in each system proving it to be a better alternative to both Lagrangian method and equal loading rate method. Percentage energy savings resulting from OCL were shown to increase with the total cooling load. For the total cooling load being 90% of the plant capacity, OCL achieved energy savings more than 6% over equal loading rate method.

This work demonstrates the application of optimal chiller loading for energy efficient cooling operation. However, it uses simple quadratic correlations, which are entirely empirical in nature, as working chiller models. Most real chiller operations are complex and hence require more versatile models (such as those detailed in Chapter 2) to accurately characterize chiller energy efficiency. Chapter 4 combines the concepts

covered in Chapter 2 and Chapter 3 and illustrates the formulation and execution of optimal chiller loading problem for more complex cooling systems based on the models developed from large amount of real cooling data.

Chapter 4: Energy Optimization of Large Cooling Systems through Multi-period Optimal Chiller Loading

4.1 INTRODUCTION

Large cooling systems differ from one another in terms of their size, layout and individual chiller properties. Therefore, the optimization problem to minimize each such system's power consumption needs to be formulated separately using applicable models and constraints. This work studies two real cooling systems in detail to reveal some of the general complexities present in them.

Chillers can be used in conjunction with thermal energy storage (TES) to further improve system efficiency and reduce costs. Thermal energy storage is the storage of thermal energy (hot or cold) in some medium. Hot storage is used in applications such as district heating systems, where warm water is stored in large tanks, or in concentrating solar power system, where solar energy is stored in the form of molten salts or synthetic oils. Cold storage is most commonly used for cooling buildings or district cooling networks where the cooling energy is stored as chilled water or ice. Thermal storage has been identified as a cost-effective way to reduce required thermal or electric equipment capacities (such as chillers or turbines) [29,30] and to reduce annual energy costs [31-33]. TES is also known to effectively shift cooling loads from peak hours to non-peak hours, thus resulting in reduced peak energy demand [34-36].

Modeling and optimizing a system that has both a large number of chillers or boilers and TES leads to complex optimization problems with binary or integer variables. For example, Tveit et al. [37] optimized a system that included long-term thermal storage in a district heating system. The problem was solved as a multi-period mixed integer nonlinear program (MINLP). Söderman [38] considered the design and operation of a

district cooling system with thermal energy storage in the form of cold water. He used linear models and was able to formulate and solve the problem as a mixed integer linear program (MILP).

The current chapter demonstrates the application of optimal chiller loading (OCL), as discussed in Chapter 3, as part of an hourly chiller loading strategy. The proposed strategy, also referred to as multi-period optimization, involves solving independent OCL problems for the current cooling load demand after regular time intervals (an hour). This work on two case studies has been demonstrated in this chapter. In the first case study, the cooling system of the UT Austin campus is modeled and optimal chilling loads are determined. Because the modeling is based on real data, the optimal results are able to be benchmarked against an actual operating strategy in order to accurately assess the potential of the optimization scheme. The optimization formulation includes a penalty term to account for the cost of switching chillers on and off. Additionally, this work is unique in that it also considers the benefits of using a thermal energy storage system to perform optimal load shifting in a wholesale electricity market using actual wholesale market prices. The second case study solves the problem of multi-period optimal chiller loading for one of the chiller plants working at Texas Instruments Inc., Dallas. This case is unique and interesting because of the hybrid (a mix of series and parallel) arrangement of chillers in the plant.

4.2 SYSTEM OVERVIEW

Case study 1 focuses on modeling and optimization of the cooling system (System 1) at The University of Texas at Austin. UT Austin has its own independent cogeneration based power plant which generates power typically at about 6¢/kWh.

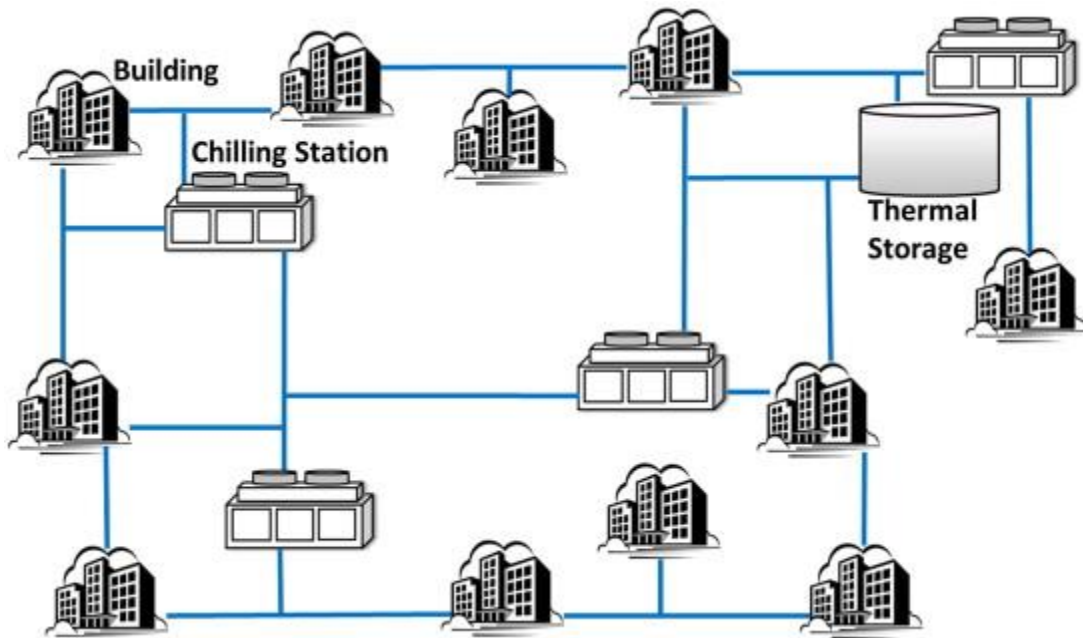


Figure 4.1: District cooling network at the University of Texas at Austin campus [24]

About a third of the power generated by the power plant is used by the cooling system; primarily by chillers, cooling towers and pumps. UT Austin has a large district cooling network (see Figure 4.1) to meet the cooling demands of the entire campus. The cooling system includes three chiller plants (also called cooling stations) and a 4 million gallon (15,100 m³) chilled water thermal energy storage tank. This tank has a storage capacity of 39,000 ton-hr (494 GJ). The tank can be filled with chilled water during the night and then discharged during the day when demand for cooling is highest. This cooling system serves over 160 buildings with approximately 17 million square feet (1.6 million m²) of space. The three active cooling stations are numbered as Station 3, Station 5 and Station 6 (stations 1, 2, and 4 have either been decommissioned or are not currently in use). Each station includes three centrifugal chillers, a set of cooling towers, condenser water pumps and chilled water pumps. Station 6 has variable frequency drives installed on all equipment. The chillers in any Station X are named as X.1, X.2 and X.3. The set of

cooling towers and pumps for each station is collectively referred to as auxiliary equipment. The power consumed by any station X is a sum of power consumed by Chiller X.1, Chiller X.2, Chiller X.3 and its auxiliary equipment. Hence, the energy efficiency of cooling towers and pumps in each station plays an important role in the formulation of OCL problem for this system.

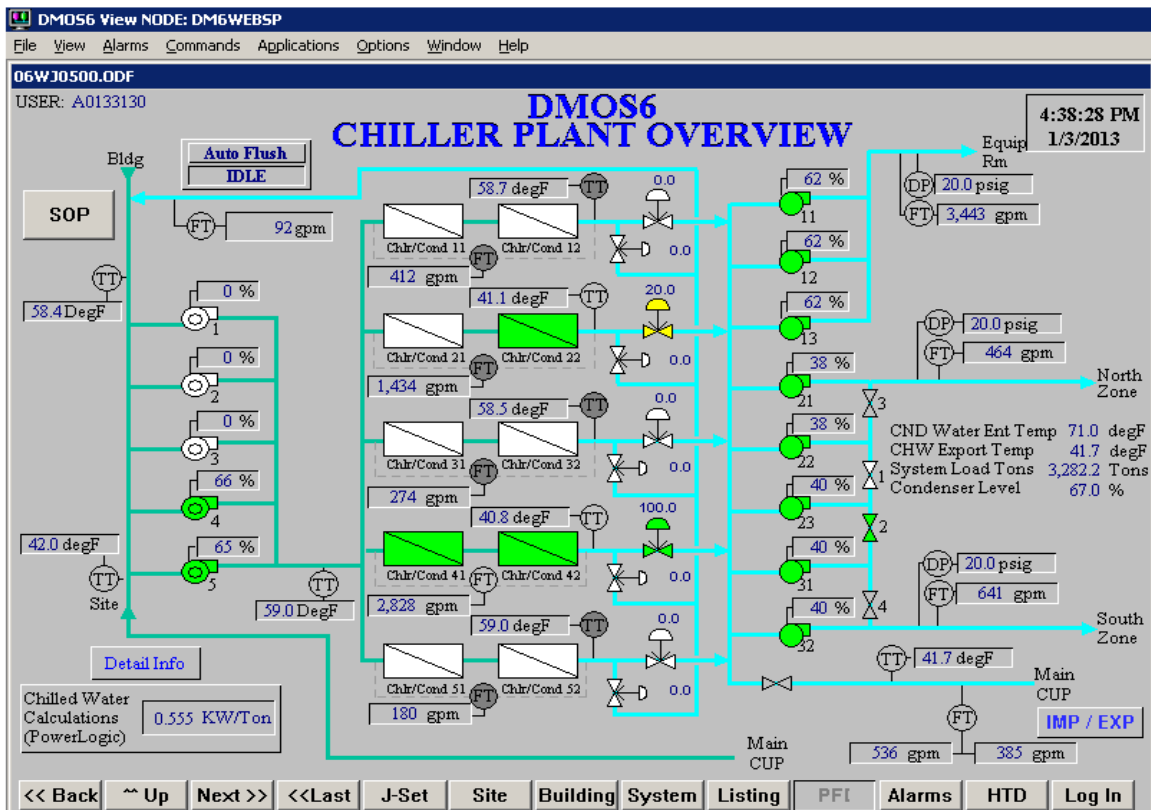


Figure 4.2: Screenshot from the chiller plant at fab DMOS6 (TI, Dallas)

Case study 2 considers a different chiller system (System 2) which operates with a semiconductor manufacturing factory (fab) and provides chilled water primarily to keep the fab tools from reheating. Data from the chiller plant at DMOS6, which is one of the fabs operating at Texas Instruments Inc. site in Dallas, was collected for the purpose of

modeling and optimization. Figure 4.2 is a snapshot of the chiller plant showing ten chillers along with several pumps and valves as part of the assembly. There are five parallel streams of chilled water flow in the plant, each of which passes through two chillers arranged in series. For such a parallel stream X, the chillers are named as Chiller X1 and Chiller X2, where X varies from 1 to 5. However, due to lack of data for Chiller 42, only nine chillers are assumed to be part of the system for the purpose of this study. All chillers of this plant are connected to the same set of auxiliary equipment. Therefore, the auxiliary power consumption adds to the objective function for OCL problem only as a constant for a fixed plant cooling load and hence is assumed to be insignificant in affecting the chiller loading decision.

4.3 MODEL DEVELOPMENT

A model of the cooling system was developed with the purpose of determining an expression for the power consumed by the cooling system in terms of several independent variables. These variables include the individual chiller loads, the ambient weather conditions and the chilled water temperature set point. The individual chiller loads are the decision variables in the OCL problem. The chilled water temperature set point (T_e) was assumed at a constant value of 39 °F (based on plant data) for System 1. For System 2, T_e assumes constant but different values for different chillers because of their hybrid arrangement. The ambient dry bulb temperature and relative humidity are variable. Hence, their forecasted estimates are used as model inputs for optimization. While only the chillers were modeled in System 2, modeling of System 1 involved correlations that evaluate the auxiliary power consumption as well. All auxiliary equipment in each station, i.e., the cooling towers and pumps, are lumped together for modeling purposes. Hence, there are nine chillers and three auxiliary equipment models

for System 1 as described in the following subsections. All variables in the model equations are assumed to be in SI units.

4.3.1 Chiller models

Chillers account for about 60 to 70% of the total power consumption of any cooling station. Modified Gordon-Ng model 1 (Equation 4.1) was used along with a correlation (Equation 4.2) between $T_{c,i}$ and $T_{WB,i}$ to fit the plant data through minimization of least squares and model parameters are estimated for each chiller. The parameters represented in bold font in Equations 4.1 and 4.2 are the model parameters. In comparison to the MGN1 model equations presented in Chapter 2, some of the variables in following equations have been associated with one or two subscripts in order to maintain consistency with the OCL formulation presented further in this chapter.

$$\frac{1}{COP_{ij}} = -1 + \frac{T_{c,i}}{T_e} + \left(\frac{1}{X_{ij}}\right) \left(\frac{q_{e,j}T_{c,i}}{T_e} - q_{c,j}\right) + \left(\frac{1}{X_{ij}}\right) \left(\frac{q_{e,j}}{\mathbf{M}_{c,j}T_e}\right) \left(\frac{q_{e,j}T_{c,i}}{T_e} - q_{c,j}\right) + \left(\frac{X_{ij}}{T_e}\right) \frac{T_{c,i}}{T_e} \left(\frac{1}{\mathbf{M}_{c,j}} + \frac{1}{\mathbf{M}_{e,j}}\right) + \frac{\frac{q_{c,j}}{\mathbf{M}_{e,j}} + \frac{q_{e,j}T_{c,i}}{T_e\mathbf{M}_{c,j}} + \left(\frac{T_{c,i}q_{e,j}}{T_e} - q_{c,j}\right) \left(\frac{1}{\mathbf{M}_{c,j}} + \frac{1}{\mathbf{M}_{e,j}}\right)}{T_e} \quad (4.1a)$$

$$q_{e,j} = \mathbf{q}_{e_mj} + \mathbf{a}_j * X_{ij} \quad (4.1b)$$

$$q_{e,j} = \mathbf{q}_{c_mj} + \mathbf{b}_j * X_{ij} \quad (4.1c)$$

$$P_{ij} = X_{ij} * \left(1/COP_{ij}\right) \quad (4.1d)$$

$$T_{c,i} = \boldsymbol{\theta}_1 + \boldsymbol{\theta}_2 * T_{WB,i} + \boldsymbol{\theta}_3 * T_{WB,i}^2 \quad (4.2)$$

Coefficient of performance (COP_{ij}) of a chiller is defined as the ratio of its cooling load to its power consumption.

Data from nine chillers of System 1 were individually fitted to the above models. Table 4.1 shows the mean and range of absolute percentage errors for these chillers.

Figure 4.3 shows the variation of the power consumed by chiller 6.1 both as predicted by the model and as measured by the plant.

Chiller	Range of absolute error (%)	Mean absolute error (%)
3.1	0 – 8.40	1.70
3.2	0 – 12.70	1.88
3.3	0 – 12.38	2.25
5.1	0 – 12.16	2.00
5.2	0 – 5.98	0.95
5.3	0 – 11.13	1.70
6.1	0 – 15.19	1.82
6.2	0 – 20.46	1.17
6.3	0 – 10.42	1.19

Table 4.1: Error analysis for centrifugal chiller modeling (System 1)

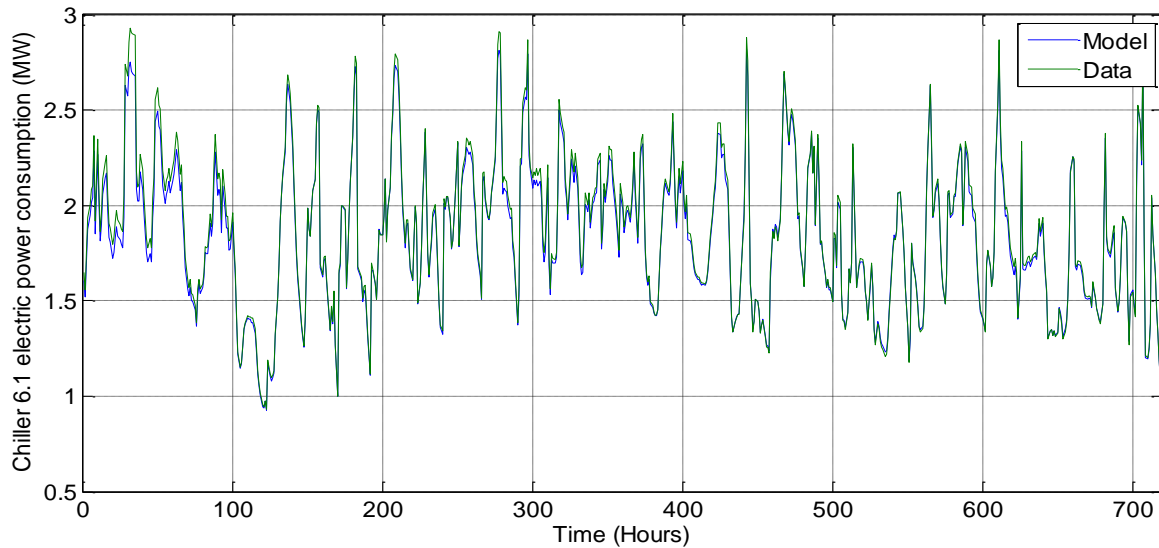


Figure 4.3: Electric power consumed by Chiller 6.1 (System 1) in the month of September– Model vs. data

For System 2, as discussed previously in Chapter 2, some of the chillers followed two different modes of operation named as series and parallel. Therefore, separate sets of fitting parameters were obtained for the two modes for every such chiller, i.e., Chiller 12, Chiller 22, Chiller 32 and Chiller 52. Table 4.2 illustrates the same error statistics for System 2.

Chiller model	Range of absolute error (%)	Mean absolute error (%)
11	0 – 17.39	1.08
12 (series)	0 – 14.37	0.90
12 (parallel)	0 – 6.48	0.65
21	0 – 24.84	4.28
22 (series)	0 – 13.99	0.72
22 (parallel)	0 – 21.63	10.12
31	0 – 13.94	1.07
32 (series)	0 – 12.31	0.75
32 (parallel)	0 – 7.80	0.70
42	0 – 13.98	0.90
51	0 – 10.20	1.02
52 (series)	0 – 18.34	0.94
52 (parallel)	0 – 25.66	8.69

Table 4.2: Error analysis for centrifugal chiller modeling (System 2)

Energy efficiency curves were plotted for all chillers (assuming series mode) in System 2 for two distinct values of wet bulb temperature using their MGN1 models. Figure 4.4 shows these plots for $T_{WB,i} = 270$ K while Figure 4.5 plots energy efficiency

curves for $T_{WB,i} = 300$ K. These curves help in visualizing the dependence of energy efficiency of a chiller on its cooling load. Comparing Figures 4.5 and 4.6, it is interesting to notice that as weather conditions change, i.e., as $T_{WB,i}$ changes, the chiller efficiencies change individually and also relative to one another. The change in the relative position of Chiller 51 in terms of its efficiency is fairly clear in these two figures, where the WBT values are different. This observation highlights the importance of using MGN1 models for these systems over the quadratic correlations that were described in Chapter 3.

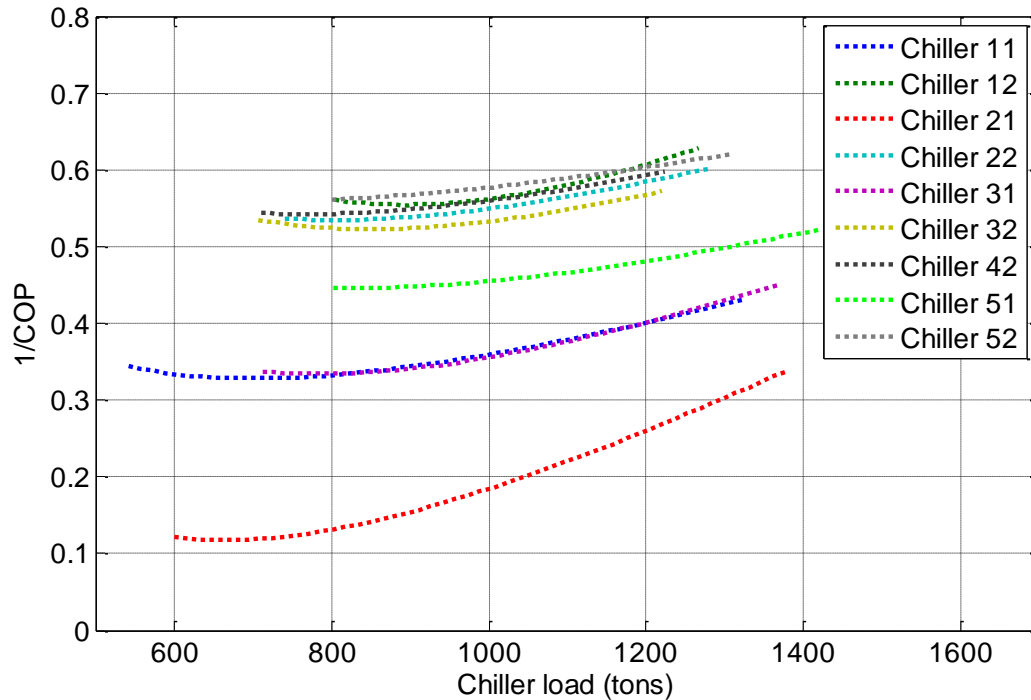


Figure 4.4: Fitted energy efficiency curves for chillers in System 2 at $T_{WB,i} = 270$ K

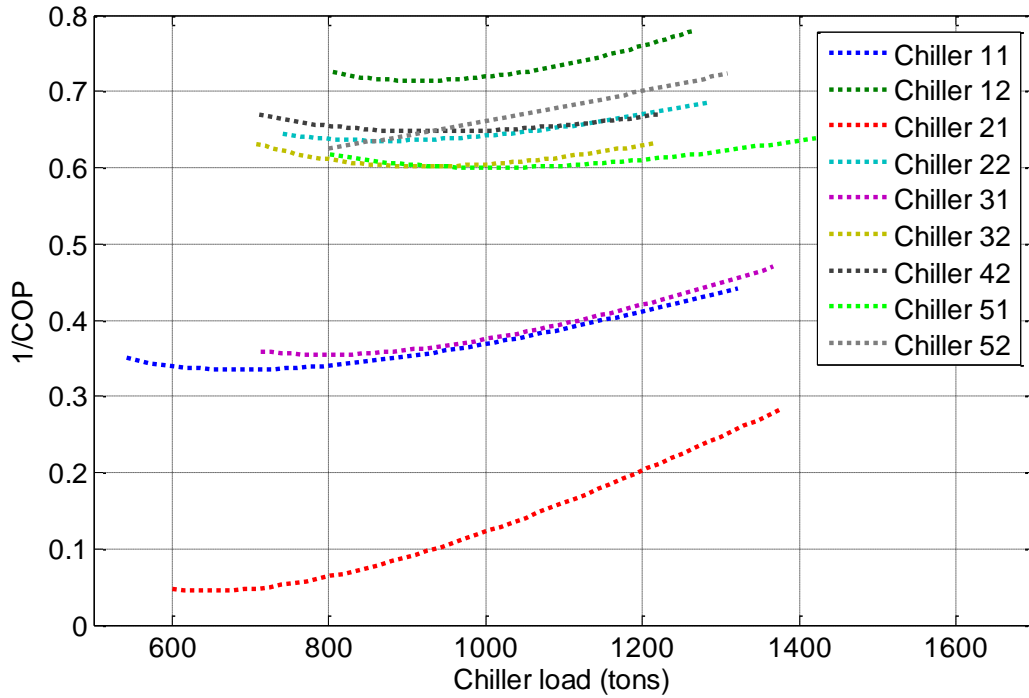


Figure 4.5: Fitted energy efficiency curves for chillers in System 2 at $T_{WB,i} = 300$ K

4.3.2 Auxiliary equipment models

Auxiliary equipment are modeled only for System 1. They include the components of a chilling station other than chillers, i.e., cooling towers, chilled water pumps, and condenser water pumps. Each station has a number of auxiliary components to distribute the chilled and condenser water flow in the best way. The total cooling load at a station has great impact on the auxiliary power consumption and hence on the total station power consumption value. Therefore, to determine the optimal chiller loading on a campus level, it is important to model the auxiliary power consumption at each station as a function of ambient weather conditions and station load. Because flow rates, pressures, and power consumption for each pump and cooling tower are not available, all auxiliary components in one station are lumped together and modeled as a single second order

polynomial function (Equation 4.3a). A second order polynomial is chosen in order to ensure a good model fit while keeping the model simple enough for optimization. For each station, a different set of model parameters (β_1 to β_{10}) is obtained by fitting the year round power consumption data collected at hourly time steps from the power plant historian.

$$P_{AUX,ik} = \beta_{1,k} + \beta_{2,k} * DBT_i + \beta_{3,k} * DBT_i^2 + \beta_{4,k} * RH_i + \beta_{5,k} * RH_i^2 + \beta_{6,k} * SL_{ik} + \beta_{7,k} * SL_{ik}^2 + \beta_{8,k} * SL_{ik} * DBT_i + \beta_{9,k} * DBT_i * RH_i + \beta_{10,k} * RH_i * SL_{ik} \quad (4.3a)$$

$$SL_{ik} = \sum_{j=m_{(k-1)}+1}^{m_k} \delta_{ij} X_{ij} \quad (4.3b)$$

By minimizing the sum of the squared error, the models show good agreement between the model's predicted values and the data obtained from the plant (Figure 4.6), with Station 3 being the least accurate model with an average absolute error of less than ten percent. The mean and range of absolute percentage errors between the data and model predictions are shown in Table 4.3.

Station Number	Range of absolute error (%)	Mean absolute error (%)
3	0 – 40.81	9.96
5	0 – 20.31	2.17
6	0 – 23.67	6.98
Total	0 – 26.48	5.85

Table 4.3: Error analysis for auxiliary component modeling

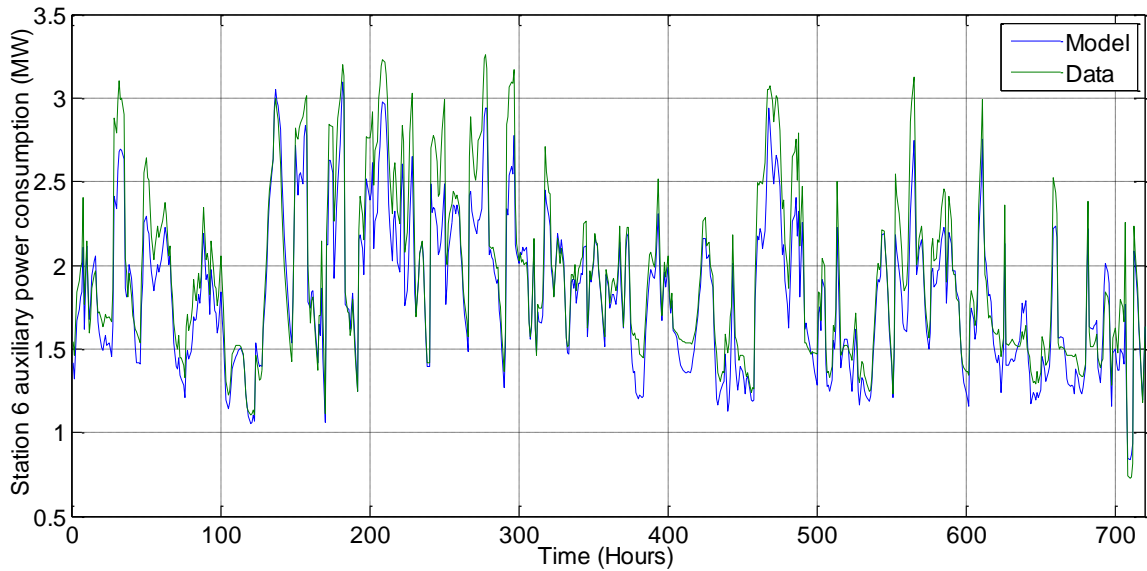


Figure 4.6: Total power consumed by the auxiliary equipment in the cooling station 6 – Model vs. data

The total power consumption by a cooling station in System 1 as a function of the cooling load distribution and ambient weather conditions is obtained by adding Equations 4.1 and 4.3:

$$P_{Station} = P_{AUX} + \sum_{i=1}^m (P_{CH})_i \quad (4.4)$$

4.4 MULTI-PERIOD COOLING SYSTEM OPTIMIZATION

Even though most cooling systems end up using computationally simple chiller loading methods such as the equal loading rate method, some of them do employ more sophisticated techniques to improve their efficiency. Different chiller plants in one network may use different techniques depending on the types of equipment installed in them. For example, the existing strategy for operating two out of the three chiller plants at UT Austin (plant 3 and plant 5), which do not have motors with variable speed drives, is based on heuristics and operators' discretion, and hence may be suboptimal. On the

other hand, chiller plant 6 has variable speed drives (VSD) installed on all its equipment and the decisions regarding its chiller loads are based on equal marginal performance principal (EMPP) [29]. EMPP is an unconstrained gradient-based optimal control strategy. Therefore, the optimal chiller load values at an instant are expected to be dependent on the previous operating values of chiller loads. Moreover, the decision to turn chillers on and off is taken based on the rise and fall in cooling demand and not on the varying efficiencies of individual chillers.

It is proposed in this work that independent optimization problems solved at regular intervals with wisely chosen initial conditions and satisfying constraints should give better results for all chiller plants, as compared to the current operating strategy. The optimal chiller loading problem is formulated differently for the cooling systems at two campuses considered in this chapter, i.e., UT Austin and DMOS6 (TI, Dallas). The problem formulations are presented in the following subsections.

4.4.1 Case study 1 – UT Austin cooling system

Due to the flexibility of using thermal energy storage at UT Austin, the multi-period optimization problem was formulated in two ways. First, it was solved as hourly independent steady state optimization problems where the cooling system is considered without any thermal storage. Next the thermal storage is included as part of the cooling system, and the time span of one optimization problem is expanded to 24 hours in order to take advantage of the flexibility to shift cooling loads.

4.4.1.1 Cooling system optimization without storage

Optimal chiller loading is solved as a multi-period static optimization problem. The objective of this problem is to minimize the total power consumed by the cooling system. This objective is achieved by optimizing the cooling load distribution among

various chillers operating in parallel. There are two decision variables for each chiller – the individual chiller load and a binary variable defining the chiller state, i.e., on or off. Therefore, for a total of M chillers, the static optimization problem has $2M$ decision variables, half of which are binary. The optimization problem also includes an inequality constraint requiring the chillers to satisfy the total cooling load. Mathematically, the static optimization formulation for any i^{th} hour can be represented with the following set of equations:

$$\min_{X_{ij}, \delta_{ij}} \sum_{k=1}^r \left(\sum_{j=m_{(k-1)}+1}^{m_k} \delta_{ij} P_{ij}(X_{ij}) + P_{AUX,ik}(\delta_{ij}, X_{ij}, k) \right) \quad (4.5a)$$

$$s. t. \sum_{j=1}^M \delta_{ij} X_{ij} - D_i \geq 0 \quad (4.5b)$$

$$L_j \leq X_{ij} \leq U_j \quad \forall i \in \{1, 2, \dots, n\} \text{ and } j \in \{1, 2, \dots, M\} \quad (4.5c)$$

$$\delta_{ij} \in \{0,1\} \quad (4.5d)$$

In equation 4.5a, P_{ij} and $P_{AUX,ik}$ are defined by Equations 4.1d and 4.3a respectively.

For a system of M chillers, the total number of possible δ_{ij} sets at a given time (constant i) is $(2^M - 1)$. For any fixed set of δ_{ij} , the objective function can be written as quadratic programming (QP) formulation, i.e., in the form of the following equation, due to the nature of models.

$$\min_{X_i} X_i^T H X_i + F^T X_i \quad (4.6)$$

The hessian of matrix H was verified to be positive definite for all possible cases. Hence, the optimization problem (Equation 4.5 with a fixed set of δ_{ij}) was a nonlinear convex formulation. It was solved for each of the $(2^9 - 1 = 511)$ possible sets of δ_{ij} in MATLAB using the sequential quadratic programming (SQP) algorithm to obtain a unique global solution always. The case resulting in the least value of the objective

function was accepted as the optimal solution. The total time taken by the MATLAB algorithm in solving this QP for 511 cases in order to obtain the optimal solution varied between 1 and 2 seconds.

4.4.1.2 Cooling System Optimization with Storage

Another goal of this research is to determine the advantage of using thermal energy storage (TES) with a large scale cooling system. Thermal storage is used to shift cooling load between different hours of the day. The extra chilled water generated during a given low-demand hour is sent to the storage tank and is retrieved during a high-demand hour to satisfy the extra cooling demand. The use of TES gives flexibility to shift cooling load across time periods and hence to use the most efficient chillers more often and the least efficient chillers less often. The addition of storage also makes the optimization problem dynamic because the current state of the storage depends on previous states. Optimal operation of the cooling system with storage should lead to additional energy savings.

Apart from savings on energy cost, the use of TES may benefit the chiller plant operation by flattening the cooling load profile over a day. Typically the total cooling load is at a lower level during the night and increases after sunrise and when occupants arrive on campus. After reaching a peak load, it again decreases in the evening. Depending on the fluctuations in the ambient temperature and building occupancy, this cooling load profile sometimes undergoes many fluctuations during the day (Figure 4.7). These fluctuations in the cooling load profile translate to frequent switching on and off of chillers, cooling towers and pumps. There are energy losses or inefficiencies associated with the transient operation of chiller plant equipment. These losses are not accounted for while solving the static multi-period hourly chiller optimization problems, which are

assumed to be independent from each other. Fluctuations in the cooling load profile also cause greater wear on chillers in addition to heat losses. However, while solving an optimization problem with thermal energy storage, we can address the issue of frequent cold starts in plant operation by adding a penalty cost to the objective function. This penalty cost is proportional to the sum of absolute difference between the total plant cooling load values at any two consecutive hours. It is added to the objective function to limit the amount of fluctuation in the cooling load profile in the optimal solution. Hence, it is expected to reduce the number of times any chiller is turned on or off.

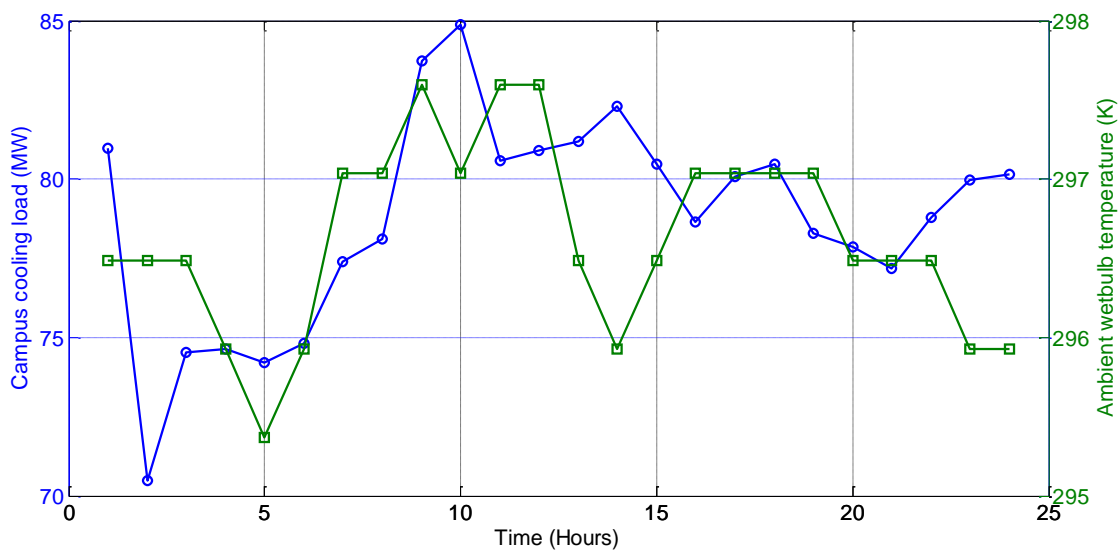


Figure 4.7: Hourly campus cooling load values (left axis) and ambient wetbulb temperature values (right axis) over 24 hour period. This data is from 11th July 2012. It serves as an example for days with more than one maxima in the cooling load profile.

Therefore, optimization with thermal energy storage aims at two improvements in the energy efficiency by reducing the energy cost associated with a) operating the chillers, and b) frequent cold starts.

The optimization problem formulation for a time span over n hours can be represented mathematically as follows:

$$\min_{X_{ij}, \delta_{ij}} \sum_{i=1}^n \gamma_i \left(\sum_{k=1}^r \left(\sum_{j=m_{(k-1)}+1}^{m_k} \delta_{ij} P_{ij}(X_{ij}) + P_{AUX,k}(\delta_{ij}, X_{ij}, k) \right) \right) + \alpha \sum_{i=2}^n \left| \sum_{j=1}^M \delta_{ij} X_{ij} - \sum_{j=1}^M \delta_{(i-1)j} X_{(i-1)j} \right| \quad (4.7a)$$

$$\text{s. t. } R_{max} \geq \sum_{j=1}^M \delta_{ij} X_{ij} - D_i \geq E_i - E_{i-1} \geq -R_{max}, \text{ for } i = 1 \text{ to } n \quad (4.7b)$$

$$E_1 = E_0 = 0 \quad (4.7c)$$

$$E_i \geq 0, \quad \text{for } i = 2 \text{ to } n \quad (4.7d)$$

$$E_i \leq E_{max}, \quad \text{for } i = 2 \text{ to } n \quad (4.7e)$$

$$L_j \leq X_{ij} \leq U_j \quad \forall i \in \{1, 2, \dots, n\} \text{ and } j \in \{1, 2, \dots, M\} \quad (4.7f)$$

$$\delta_{ij} \in \{0, 1\} \quad (4.7g)$$

An important thing to note is that the objective of this problem (Equation 4.7a) is to minimize the total cost (\$) of power. On the other hand, the objective of the optimization problem without storage (Equation 4.5a) was to minimize the total power consumed (kWh) by the cooling system.

This optimization problem is solved in two stages [24]. In the first stage, the total cooling load is optimally distributed among n discrete time periods (hours), while satisfying the cooling demand at each hour with the help of thermal energy storage. In the second stage, the cooling load on i^{th} hour is optimally distributed among M independent chillers having different model characteristics, which is equivalent to the optimization problem without storage. Hence, the optimization problem with storage consists of n number of static optimization problems without storage.

4.4.2 Case study 2 – DMOS6, Texas Instruments Inc., Dallas

The chiller plant at DMOS6 employs the chillers in a different configuration than any of the chiller plants at UT Austin. The chiller arrangement at DMOS6, as shown in Figure 4.2, is a mix of series and parallel arrangements and hence is referred to as hybrid arrangement. A simpler schematic of System 2 (Figure 4.8) is drawn for a case when all nine chillers are operating. All red streams in Figure 4.8 represent hot streams entering the chiller plant (typically at $T_H \approx 58$ °F). All blue streams represent the chilled water streams exiting the chiller plant (typically at $T_e \approx 40$ °F). Intermediate streams between any two chillers arranged in series are colored orange and are typically at $T \approx 48$ °F, according to the data obtained from DMOS6 chiller plant for the year 2012.

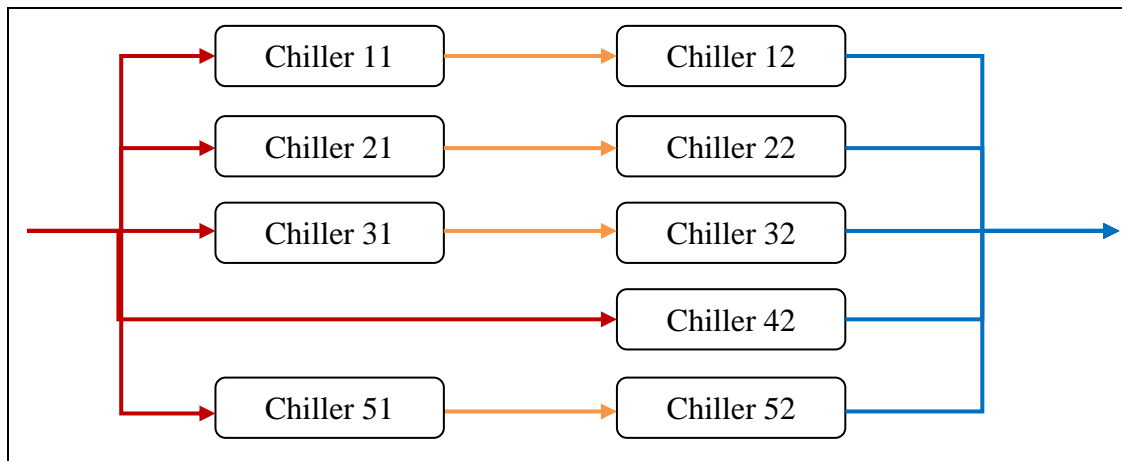


Figure 4.8: Schematic of chiller layout in System 2

The optimal chiller loading problem for System 2 was solved for two scenarios, i.e. real and hypothetical, as described in the following subsections.

4.4.2.1 OCL – Part 1

In part 1, OCL problem was solved for a hypothetical scenario in which all nine chillers of System 2 operate in parallel, just like in System 1 except that all chillers in System 2 belong to a single chiller plant. The plant cooling load is divided among all chillers by distributing the chilled water flow rate into parallel streams, while keeping the same temperature drop across all operating chillers. Hence, the chilled water outlet temperature for all chillers, which is a constant set point, is assumed to be equal to the outlet temperature of chiller plant, i.e. $T_e = 40$ °F. Due to System 2 sharing a common layout with any chiller plant in System 1, the OCL formulation is similar to Equation 4.5. However the expression of objective function given in Equation 4.5a was modified for System 2. The set of equations defining the OCL problem for this scenario is given below:

$$\min_{X_{ij}, \delta_{ij}} \sum_{j=1}^M \delta_{ij} P_{ij}(X_{ij}) \quad (4.8)$$

$$s. t. \sum_{j=1}^M \delta_{ij} X_{ij} - D_i \geq 0 \quad (4.5b)$$

$$L_j \leq X_{ij} \leq U_j \quad \forall i \in \{1, 2, \dots, n\} \text{ and } j \in \{1, 2, \dots, M\} \quad (4.5c)$$

$$\delta_{ij} \in \{0,1\} \quad (4.5d)$$

MGN1 model for each chiller was used to substitute the expression for $P_{ij}(X_{ij})$ in Equation 4.8. Models for parallel mode of operation were used for Chiller 12, Chiller 22, Chiller 32 and Chiller 52.

4.4.2.2 OCL – Part 2

While the optimization problem formulation in OCL – Part 1 simulates the most common chiller operation strategy (all chillers in parallel), it does not represent the real scenario at DMOS6 chiller plant. Also, since the chiller models were developed from real

plant data, they would work best for those operating conditions. This section formulates the OCL problem after learning about the chiller operation in DMOS6 chiller plant (System 2) from real data. The OCL – Part 2 is formulated as a separate optimization problem and not in continuation with OCL – Part 1.

The System 2 plant cooling load is divided among its chillers in two ways (see Figure 4.8). First, its chilled water flow rate is divided into five parallel streams. Second, the total temperature drop across any stream, i.e. $\Delta T = T_H - T_e$, is divided among its chillers that are arranged in series. Some patterns were noticed from the year long plant data regarding certain chiller operations. These patterns were modeled in the form of additional constraints for the OCL problem in addition to the set of equations used OCL – Part 1. Parameter modifications and additional constraints included in OCL – Part 2 as compared to OCL – Part 1 are listed below:

- (i) Two values of chilled water supply temperatures were used in chiller models:
 - a. $T_{e,1} = 49$ °F for chillers 11, 21, 31 and 51
 - b. $T_{e,2} = 40$ °F for chillers 12, 22, 32, 42 and 52
- (ii) Every pair of chillers arranged in series experiences the same flow rate. Hence, cooling load values on the chillers in a series pair are equal, if both the chillers are turned on at the same time. This led to four additional equality constraints.
- (iii) For every pair of chillers arranged in series, first chiller can only work in conjunction with the second chiller and not independently. Second chiller can however be turned on even if the first chiller is off. Therefore, chillers 11, 21, 31 and 51 would be on only when chillers 12, 22, 32 and 52 (respectively) were on.
- (iv) Two separate models were used for chillers 12, 22, 32 and 52 depending on whether they were operated in series with another chiller or independently. This was determined by the on/off status of chillers 11, 21, 31 and 51 respectively.

Due to the additional set of constraints used to represent the real chiller data, OCL – Part 2 is a more complex form of OCL – Part 1.

4.5 RESULTS AND DISCUSSION FOR SYSTEM 1

This section discusses the optimization results from several different cases. The cooling process system optimization problem was solved for the duration of a year. The problem of optimization without storage was solved hourly while optimization with storage was solved daily.

Hourly static optimization problems were solved for a year for the cooling system without storage. The model's predicted optimal power consumption values were compared against real data collected from the UT chiller plants. The results predict energy savings as high as 40% for a single time step which is of one hour. The average energy savings over 8784 hours of a year is predicted to be 8.57%. In absolute sense, the static optimal chiller loading could save about 8.1 GWh (~ \$486,000) over the year in 2012. In the current operation, the cooling loads for six out of nine chillers (stations 3 and 5) are determined based on operators' discretion and some heuristics that are easy to follow but not based on optimal operation. The cooling loads for chillers in Station 6 are determined based on a gradient based control strategy [29], which is expected to converge at the nearest local minima. On the other hand, the proposed optimal chiller loading method is based on solving independent hourly optimization problems with deterministic models for individual components. Therefore, with a little computational effort and minimal capital investment, we are able to see significant savings in the energy consumption by the cooling system.

With the objective of adding more degrees of freedom to the optimization, thermal energy storage was included in the system for the next study. Assuming $n = 24$ (hours), daily optimization problems were solved for a year for the cooling system with storage (i.e., a total of 366, which is the total number of days in 2012). At first, the problem was solved assuming an arbitrary constant price of electricity. This assumption eliminated the variable γ_i from the objective function expression. It also made the objective function equivalent to minimizing the total power consumption (kWh) in a day for the case when $\alpha = 0$. Midnight was chosen to be the initial time for each problem after iterating over other possible initial times. The 24-hour cooling load profiles are compared for two chosen days in the month of September, named as Day 1 and Day 2 (Figures 4.9 and 4.10 respectively). Figure 4.9 presents the comparison among various distributions of the optimal cooling load from the stage 1 of dynamic optimization, i.e., the redistribution of cooling load among several hours. Figure 4.10 presents similar results for Day 2, which has less frequent cooling load variations as compared to Day 1. For each day, the optimization problem was solved for different values for the penalty coefficient, $\alpha = 0, 0.1$ and 0.5 \$/kW. It is clearly visible from the Figures 4.9 and 4.10 that the usage of thermal energy storage provides flexibility to shift cooling load across time and hence to opt for alternate cooling load profiles for a chosen time horizon (24 hours in this case). This flexibility comes with the opportunities to save energy and/or to reduce fluctuations in the cooling load profile. These figures show various cooling load profiles for different optimization parameters, each profile independently satisfying the hourly cooling demand constraints.

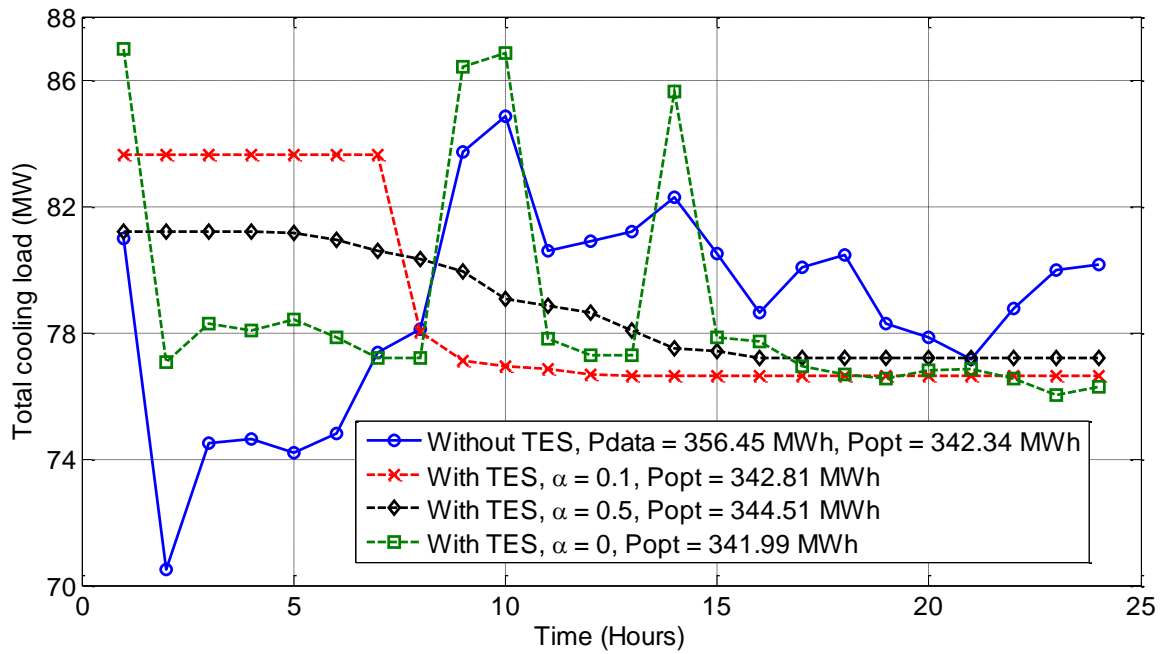


Figure 4.9: Cooling load distribution among 24 hours (Day 1) from different optimization conditions for System 1

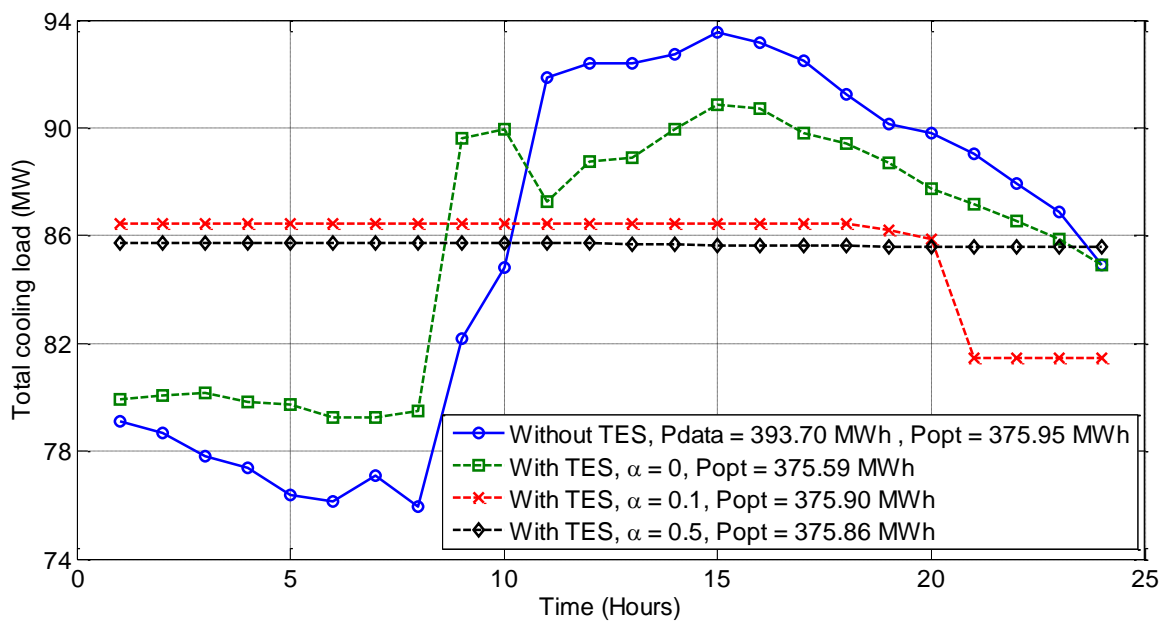


Figure 4.10: Cooling load distribution among 24 hours (Day 2) from different optimization conditions for System 1

Figure 4.11 compares the electricity consumption by the overall cooling system, as predicted by the proposed optimization strategies and as gathered from the historical data of the power plant. The comparison is done between the daily cost values of electricity. Since a constant electricity price is assumed for this section, the electricity consumption is compared between the plant data and the optimization results with and without storage for a total of 366 data points over a year. Figure 4.11 summarizes the results for the year by showing the system's electricity consumption for 50 representative days over the year.

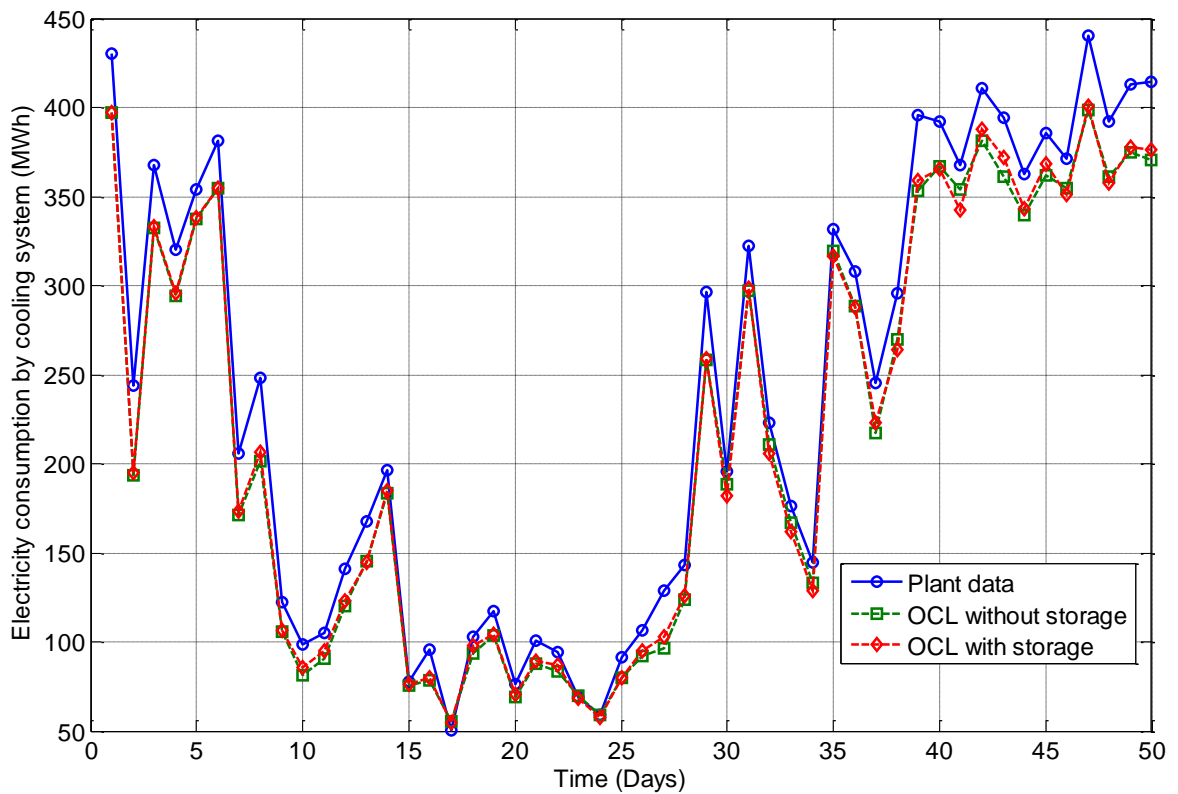


Figure 4.11: Comparison of power consumption values from a) plant data, b) static optimization and c) dynamic optimization for System 1

It can be observed from Figure 4.11, that solving OCL with storage does not seem to predict significant energy savings as compared to solving OCL without storage. The results from 366 days of the year 2012 predict a maximum of 6.3% of daily energy savings from using TES as compared to OCL without TES. On an average day, the usage of TES could save about 1.5% of energy consumed by the cooling system. This study does not take into account the heat losses associated with transporting chilled water to and from the storage tank. Hence, in reality the savings are expected to be less than the predictions from the above mentioned optimization study. This is in agreement with other work that has demonstrated minimal energy savings for TES in the Austin, Texas, climate [30]. Because the wet bulb temperature is nearly constant during the summer time (the standard deviation of the wet bulb temperature from June through August is less than 2°C), there is little opportunity to gain efficiency improvement through the shifting of loads.

However, an interesting observation is made from the above results (Figures 4.9 and 4.10) about the effect of optimization on the reduced amount of fluctuations of cooling load profile over 24 hours. It can be seen qualitatively that as α increases, the optimal use of thermal storage generates a closer to flat cooling load profile for the 24 hours at no or negligible extra energy consumption. Therefore as the value of the penalty coefficient α is increased, the resultant optimal cooling load profile would require fewer events of turning chillers on or off. This effect is quantitatively studied for day 1 (Figure 4.9). A variable N_i is defined as the number of chillers operating during the i^{th} hour. The difference between the values of N_i for any consecutive hours represents the number of turning on/off events occurring between those two hours. It is assumed that between any two hours, either some chillers are turned on (rise in cooling load) or some chillers are turned off (drop in cooling load) and not both.

Table 4.4 and Figure 4.12 show the results from the abovementioned study for Day 1. The number of times a chiller is turned on or off over a period of 24 hours is compared for different cooling load profiles resulting from different optimization parameters, i.e., the usage of TES and the penalty coefficient α . As α is increased, the penalty cost in the objective function due to the cooling load variation increases. Hence, the optimal cooling load profile seems to be more flat qualitatively and demonstrates less of a need to turn on/off chillers. Since the introduction of the penalty coefficient moves the focus of optimization from minimizing the energy consumption, there is a small cost of energy to be paid for a less fluctuating cooling load profile. For example, for Day 1, by increasing the value of α from 0 to 0.1, the number of chiller turning on/off events can be reduced from 5 to 1 for a rise in energy consumption as little as 0.24% (Table 4.4). It comes out as an interesting trade-off situation where determining an optimal value of α can be another optimization problem.

Cooling load profile	Number of chiller turning on/off events in 24 hours	Total power consumption in 24 hours (MW)
Plant data	4	356.45
OCL Without storage	4	342.34
OCL With storage, $\alpha=0$	5	341.99
OCL With storage, $\alpha=0.1$	1	342.81
OCL With storage, $\alpha=0.5$	0	344.51

Table 4.4: Effect of OCL with thermal energy storage on the frequency of cold starts

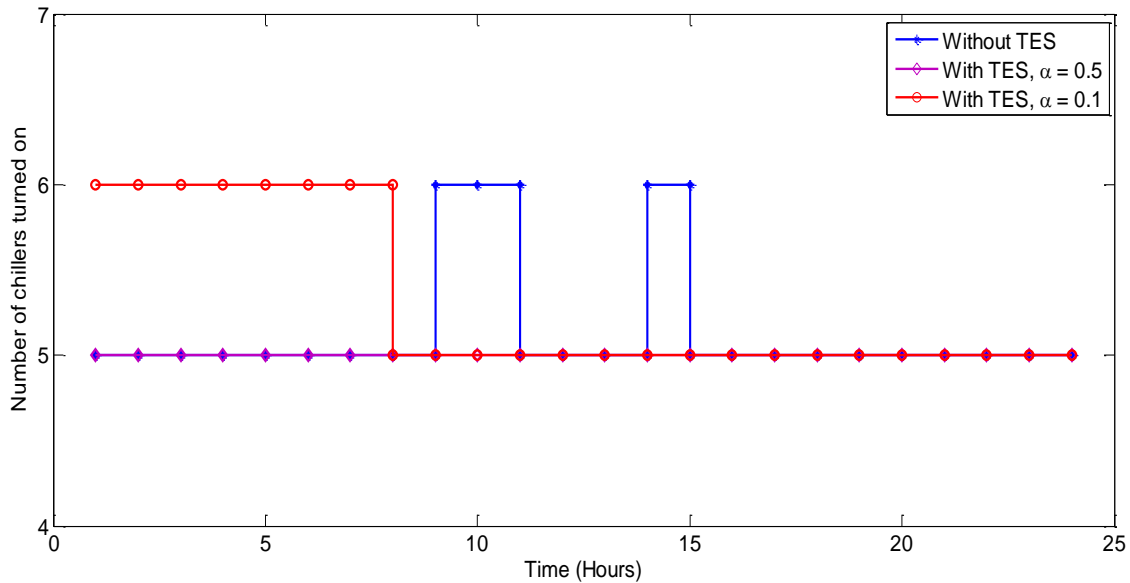


Figure 4.12: Comparison of the variations in the total number of operating chillers under different cooling load profiles (System 1)

4.5.1 Time-varying electricity prices

This section evaluates the advantages of using thermal storage in a scenario where electricity prices vary hourly. Real-time market prices from the Austin Load Zone in the Electricity Reliability Council of Texas (ERCOT) market from 2012 were used for the analysis of optimization results. Such a variable cost scenario highlights the advantage of using thermal energy storage. The market price data (Figure 4.13) shows that prices do vary hourly and sometimes quite dramatically, i.e., by orders of magnitude. A huge cost saving opportunity lies in shifting the cooling load from high cost hours to low cost hours with the help of energy storage.

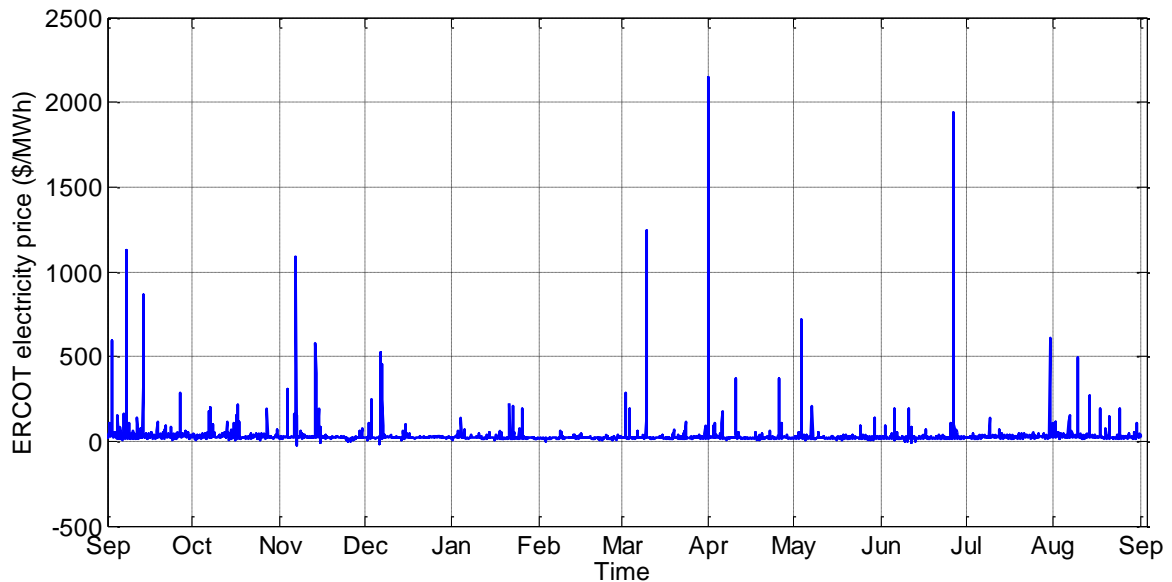


Figure 4.13: Variation in the hourly real-time prices in the ERCOT wholesale market over the year 2012 in Austin, TX

For the purpose of studying the effect of using TES in the case of time varying prices, the value of α was assumed to be zero while solving the optimization problem with storage. Possible savings from using TES in this case were simulated for 366 days of the year 2012 by solving 366 optimization problems. The daily optimal cost (with TES) is compared with the daily estimated cost (without TES) based on real hourly cooling load values and the variable price of electricity from ERCOT. The days with large variation in the electricity price demonstrate large savings in the cost of cooling. The percentage savings in the cooling cost for an hour are predicted to be up to 42.2% with a mean of 13.45%. In absolute sense, it translates to a sum total of \$400,000 saved over a year for a large system such as UT Austin.

Figure 4.14 shows the comparison between daily cost to cool the campus, with and without using thermal energy storage. For the purpose of clarity, this figure shows

the results for only 75 consecutive days from the year 2012. The energy cost savings through the optimal usage of thermal storage is more pronounced in days with high electricity price fluctuation. On a day with high electricity price fluctuations, all or most of its cooling load is spread over hours with low cost and the least amount of chiller operation occurs during the peak cost hours. The excess chilled water generated during the low cost hours is sent to the thermal storage tank. This chilled water is used to satisfy the campus cooling demand during the peak cost hours. Therefore, a significant amount of money can be saved just by using the already existing thermal storage tank in an optimal fashion.

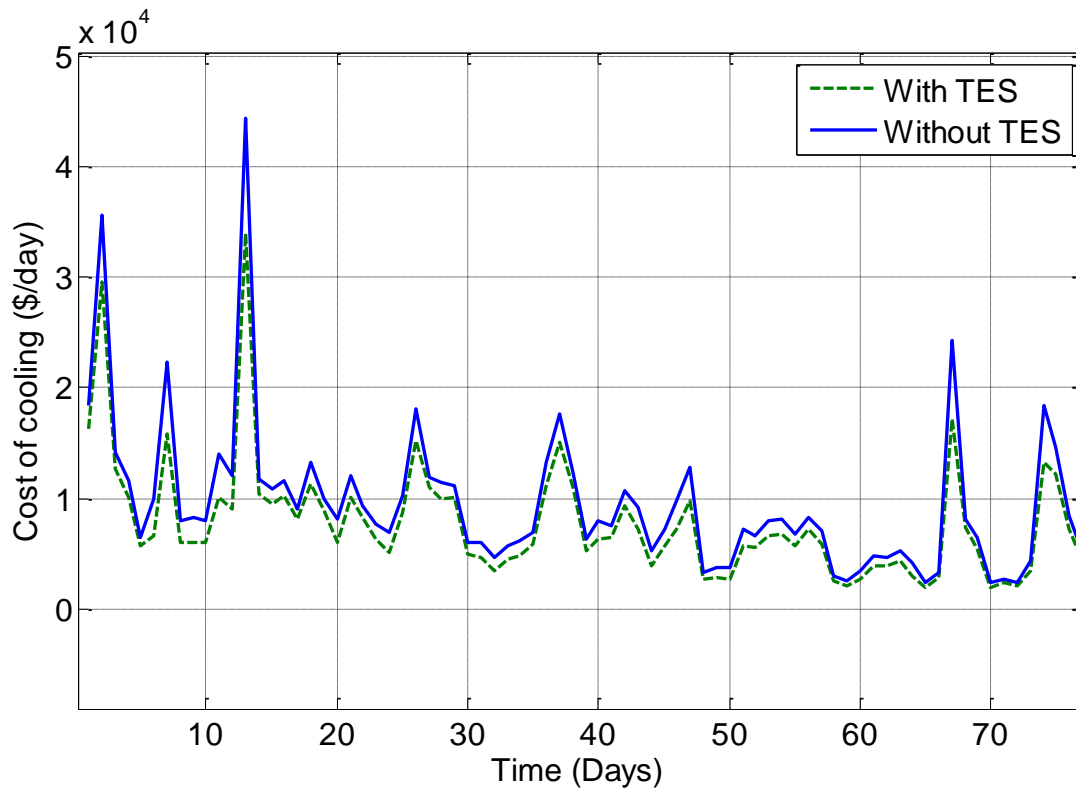


Figure 4.14: Comparison of the cooling cost in case of time varying electricity prices – With TES ($\alpha = 0$) vs. without TES (System 1)

4.6 RESULTS AND DISCUSSION FOR SYSTEM 2

System 2 is smaller than System 1 with lesser number of energy consuming components considered. The possibility of utilizing thermal energy storage has also not been included in its analysis. However, System 2 is complex in a unique way by virtue of its hybrid chiller arrangement and several additional operational constraints imposed because of that. Therefore, the optimal chiller loading problem was solved for this system for two different scenarios, named as OCL – Part 1 and OCL – Part 2.

Figure 4.15 compares the multi-period optimization results obtained from solving OCL – Part 1 against the hourly power consumption values from data. Figure 4.16 plots the hourly percentage energy savings from OCL – Part 1 against time. It is clear from both figures that the OCL solved for hypothetical scenario estimates significantly high savings (on an average ~25%) in energy cost as compared to the current chiller loading strategy.

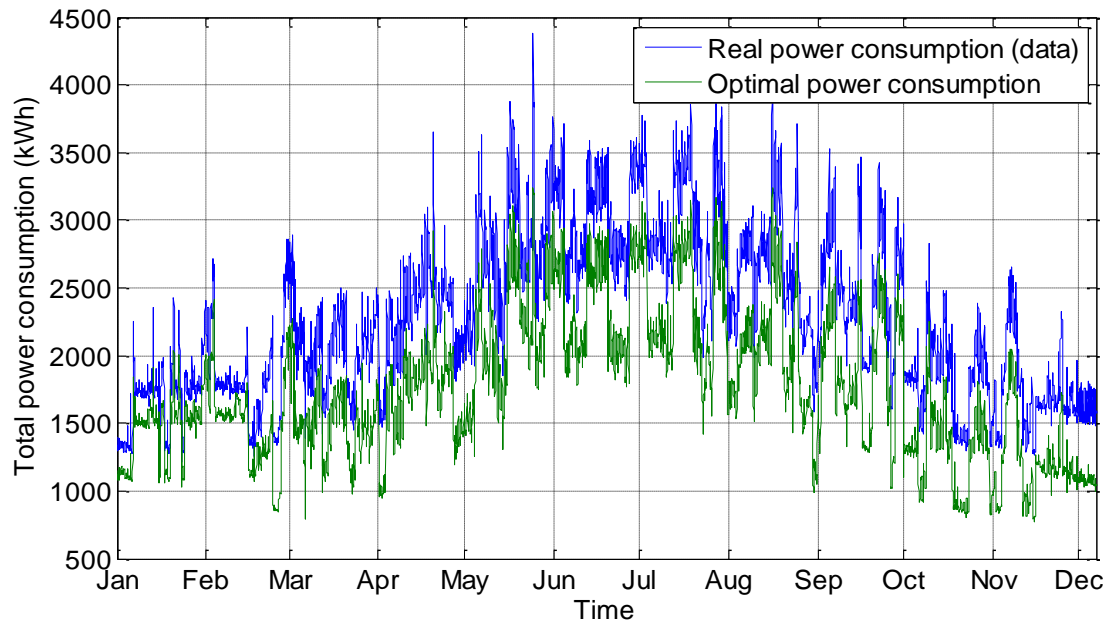


Figure 4.15: Comparison of hourly power consumption values over the year 2012 from
a) plant data, b) OCL – Part 1 for System 2

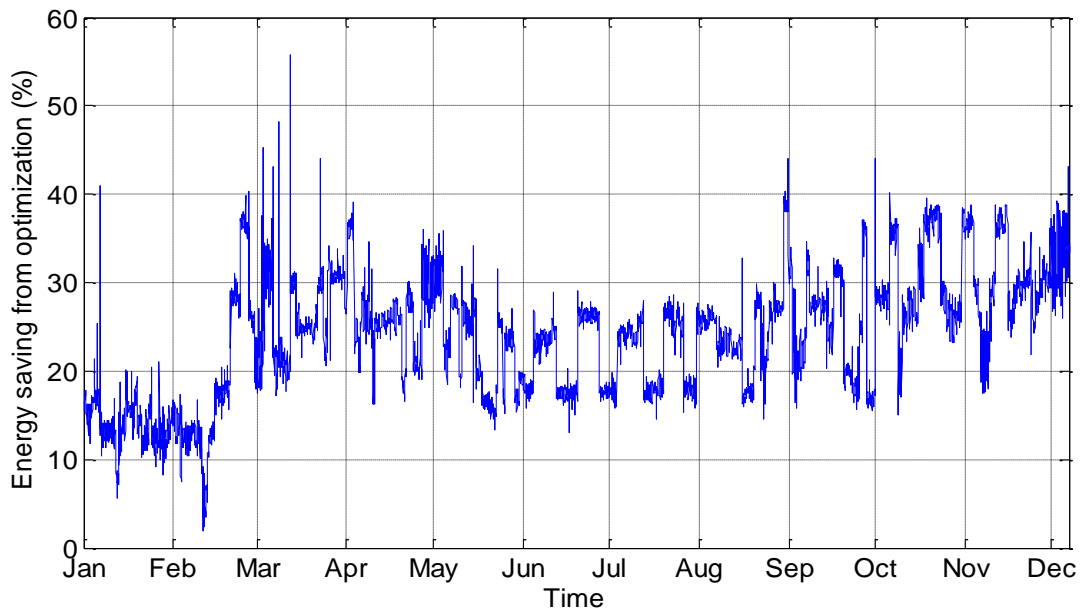


Figure 4.16: Predicted hourly energy savings from OCL – Part 1 for System 2

The difference between the real power consumption and OCL – Part 1 resulted optimal power consumption can be attributed to two factors (in addition to optimal chiller loading):

Modeling error: Models for chillers 11, 21, 31 and 51 might not be suitable to be used in the optimization set up defined by OCL – Part 1. These models were developed using real operation data for these chillers. The real operating conditions for these chillers were different from the hypothetical scenario used in this problem in two ways.

First, chillers 11, 21, 31 and 51 always operated in the series mode in System 2 while the hypothetical scenario assumed an operation in which all chillers operated in parallel to one another. It has been illustrated in Chapter 2 through examples that chillers demonstrate different energy efficiencies when operated in different modes because of differences in internal heat losses arising from chilled water flow rate. Separate MGN1 models may characterize a chiller’s efficiency curve in series and parallel mode. Models

developed using data of series mode of operation were used to optimize a scenario of parallel mode of operation.

Second, the hypothetical scenario assumed a constant value of $T_e = 40$ °F for all chillers. However, models developed for chillers 11, 21, 31 and 51 were based on data in which these chillers always assumed $T_e \approx 48$ °F due to being operated in series with other chillers (see Figure 4.8).

While a broader range of data was available for chillers 12, 22, 32 and 52 so that separate models for series and parallel mode of operation could be developed; this was not the case for chillers 11, 21, 31 and 51. Hence, significant errors could have arisen from using unsuitable models.

Energy saving from parallel mode of operation: Using separate series and parallel mode models based on real data for chillers 12 and 32, it has been demonstrated in Chapter 2 that these chillers worked more efficiently in parallel mode than in series mode for a constant $T_e = 40$ °F. By extrapolation, this can be assumed true for all other chillers with the same chilled water outlet temperature, i.e., chillers 22 and 52.

In the real System 2 plant operation, more than three-fourth of the time chillers 12, 22, 32 and 52 are operated in series mode which has been shown to be more energy consuming. In the hypothetical scenario though, these chillers were always assumed to be running in parallel mode. This could be one of the reasons behind OCL – Part 1 resulting in high energy savings as compared to real data.

Figure 4.17 compares the multi-period optimization results obtained from solving OCL – Part 2 against the hourly power consumption values from data. Figure 4.18 plots the hourly percentage energy savings from OCL – Part 2 against time. While at certain times, this optimization results in energy savings of over 35%, average of percentage savings over the year 2012 is 3.86%. This is much lower than the estimated savings from

OCL – Part 1 and the static optimization results for System 1 due to a much restricted chiller operation.

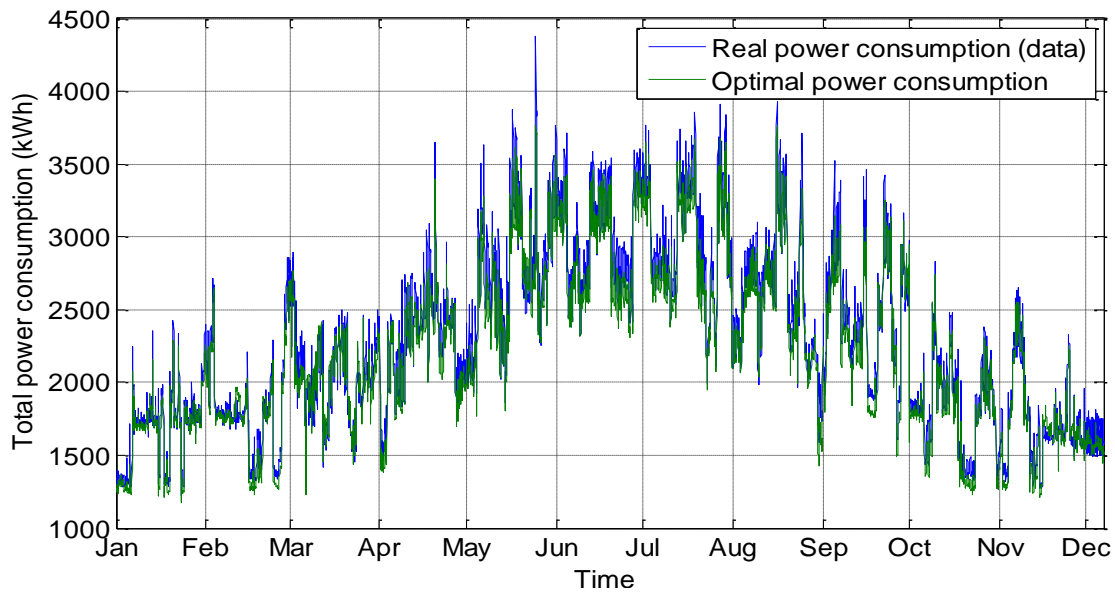


Figure 4.17: Comparison of hourly power consumption values over the year 2012 from a) plant data, b) OCL – Part 2 for System 2

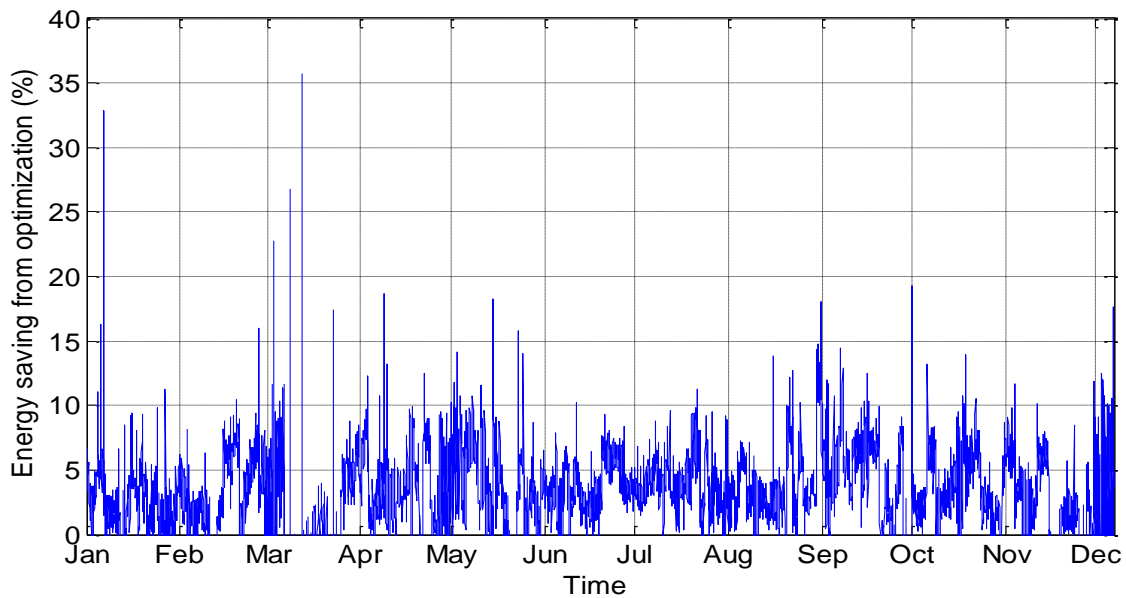


Figure 4.18: Predicted hourly energy savings from OCL – Part 2 for System 2

Even though the resultant savings seem to be relatively small, the decisions to use certain chillers resulting from OCL – Part 2 are significantly different from the chiller loading strategy used in the real chiller plant. The total number of hours (n) for which the multi-period optimization problem was solved is equal to 8183, i.e. $i = 1$ to 8183. For a system of nine chillers, there were nine decisions to be taken every hour regarding turning or keeping any chiller on or off (decision variables are δ_{ij}). Out of a total of 73647 decisions, 34742 decisions (47%) were recommended by OCL – Part 2 to be changed from the existing operation.

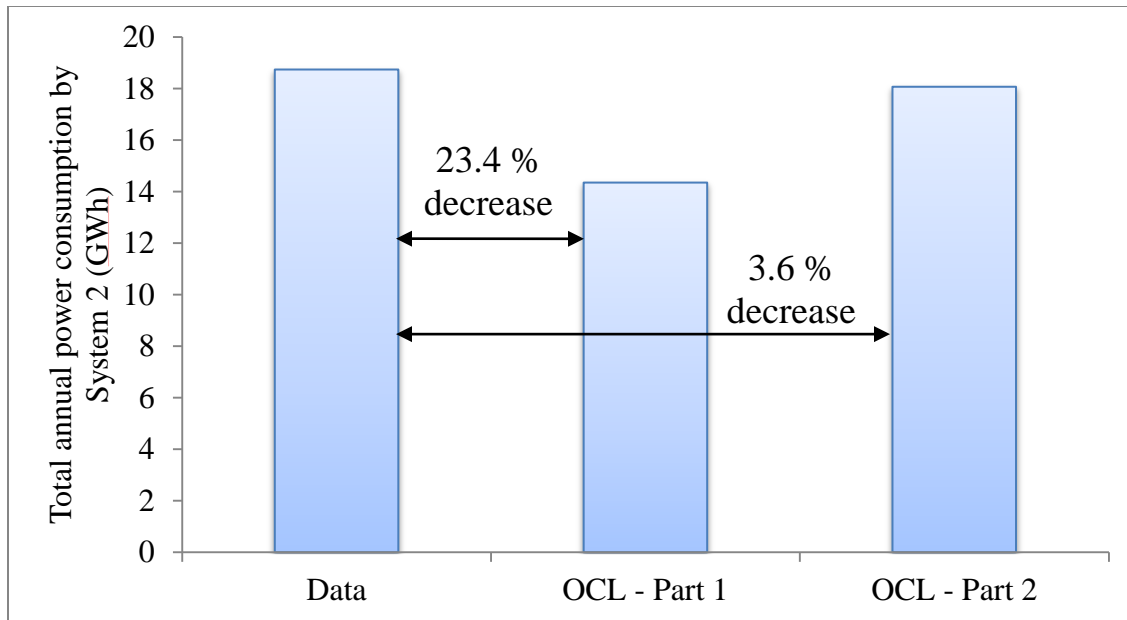


Figure 4.19: Comparison of the total annual power consumption of System 2 from data, OCL – Part 1 and OCL – Part 2

Figure 4.19 compares the resultant total annual power consumption obtained from OCL – Part 1 and OCL – Part 2. Clearly, the former (hypothetical arrangement) results in much more energy savings as compared to the latter (real arrangement). As discussed previously, there are three primary reasons behind this. One, OCL – Part 1 could be

partially wrong in predicting these results due to possible modeling errors. Two, chillers 12, 22, 32 and 52 are more efficient when operated in parallel mode than in series mode while the chilled water outlet temperature is same for these chillers in both cases. Three, the real arrangement imposes additional physical constraints regarding certain chiller operations.

4.7 CONCLUSIONS

In the current work, two distinct large scale cooling systems, referred to as System 1 and System 2, were separately optimized using various MINLP formulations. System 1 is part of a district cooling network at the UT Austin campus. System 2 is a chiller plant providing chilled water to one of the semiconductor fabs (DMOS6) at TI, Dallas. Both systems are different from each other in many ways and were modeled and optimized independently.

The System 1 optimization results were compared against the hourly real plant data from UT Austin chiller plants spanning over one year. Multi-period static optimal chiller loading yielded energy savings up to 40% for a time period (one hour). Assuming a constant electricity cost of 6 cents/kWh, annual savings of \$486,000 were estimated for the year 2012. Hence, optimal chiller loading emerges as an effective way to reduce electrical energy consumption. Since the cooling system at UT Austin consumes over 30% of the annual total power generation, efficient operation of cooling system will reduce the load on power generation equipment.

Addition of thermal energy storage to the cooling system provides additional flexibility in its operation. A multi-period optimization problem over a larger time horizon (24 hours) was solved to study the effect of using TES on power consumption

and operational stability. The results in this case did not translate to significant energy savings. Moreover, the objective function did not include the heat losses associated with the use of TES. Therefore in a real situation, the energy savings from using TES are expected to be somewhat lower. However, for a hypothetical scenario of time varying electricity prices, shifting of cooling load with the help of TES predicted economic savings up to 42.2% for a day.

The optimal operation of cooling system with TES was also shown to have a significant positive impact on the chiller plant operations in terms of the frequency of cold starts. Because of the added flexibility to adjust the cooling load profile, the cooling system with TES was able to generate a less fluctuating operating strategy with the help of the proposed optimization routine. It was shown that the number of occurrences of turning a chiller on or off over a period of 24 hours can be reduced from 4 to 0 by using thermal storage. It is expected to even reduce the energy losses further that occur during the transient phase of a chiller operation. Additionally, with a smoother cooling operation, the equipment wear is also expected to be reduced.

The System 2 optimization results were compared against the hourly real plant data from the DMOS6 chiller plant spanning over one year. Optimization for the chillers in System 2 was solved for two different scenarios – real (OCL – Part 2) and hypothetical (OCL – Part 1). The hypothetical scenario in which all chillers operated in parallel estimated greater savings on total annual power consumption (23.4%) as compared to OCL with real scenario (3.6%). All chiller models were developed from real plant data which was valid for certain operating conditions. It was assumed for OCL – Part 1 that models extrapolate for the hypothetical arrangement as well. Therefore, the results from OCL – Part 1 may also include some modeling error which could not be verified due to lack of relevant data. In order to improve the model accuracy for OCL – Part 1, data

should be generated to replicate the hypothetical arrangement by modifying the operating conditions and should be used to update the models.

The current System 2 chiller plant arrangement has too many physical constraints which restrict the chillers from attaining optimal loads and lead to only 3.6% savings on annual power consumption. This figure could be improved by redefining some of the additional constraints listed in OCL – Part 2 as soft constraints rather than hard constraints or as inequality constraints rather than equality constraints to have a larger feasible region. Apart from the physical constraints present in the System 2 chiller plant, even though it was shown that the parallel mode of operation is more energy efficient for certain chillers than the series mode of operation, more than 75% of the time in year 2012 those chillers were operated in series mode. Therefore, in addition to employing the OCL strategy in making decisions for cooling load distribution, design of an optimal layout of the chiller plant was also recommended to improve its energy efficiency. Chapter 5 discusses some of the factors important in designing an optimal chiller arrangement for an energy efficient chiller plant.

The findings from System 1 study suggest that optimal chiller loading is an effective energy saving operating strategy for large scale cooling systems with multiple chillers sharing a common cooling load. The installation and operation of thermal energy storage (TES) is marginally beneficial to save energy costs where the cost of electricity is constant with time. On the other hand, the use of TES can minimize the fluctuations in cooling load profile. In situations where time varying electricity prices are used, TES is shown to be quite useful in reducing electricity bills. The current study can be further extended in many ways. The choice of time horizon of the optimization problem with TES can have a significant impact on improving the cooling operation. The starting point of one optimization cycle was assumed to be midnight in the current study, assuming an

empty TES tank at that time. Different starting points also need to be considered in order to expand the proposed study. For systems like UT Austin, shifting of cooling loads with the help of TES can also shift loads on the power generation equipment. Variable efficiency curves of turbines suggest another possible optimization problem to minimize the total natural gas consumption by the power plant.

Chapter 5: Energy Efficient Chiller Configuration – A Design Perspective

5.1 INTRODUCTION

Multi-chiller plant design can be a fairly complex problem depending on its size. Several factors affect the way chillers are arranged in the plant relative to one another. The chiller arrangement decision normally depends on the peak and average cooling load demand, chilled water flow rate, chilled water supply temperature, chilled water return temperature and chiller design capacity. This chapter discusses the different ways in which chillers can be arranged in a plant followed by the study illustrating the effect of chiller plant design on its overall energy efficiency. The energy efficiency of a chiller plant does not only depend on the distribution of its cooling load among chillers (Chapter 3), but also on the way its chillers are arranged.

Since the decisions regarding a chiller plant design are taken much less frequently than the operational decisions, it is important to solve the problem of optimal chiller configuration while focusing on minimizing the energy costs. The analysis presented in this chapter compares the several ways in which chiller arrangement can affect the plant energy efficiency. It is based on models developed from real chiller data obtained from the semiconductor fab DMOS6 at Texas Instruments, Inc. (Dallas). The advantages and disadvantages from using any kind of chiller configuration are pointed out and quantified using these models. This knowledge in addition to the capital installation costs can significantly aid the process of designing an energy efficient multi-chiller system.

5.2 CHILLER ARRANGEMENTS

Chillers in any multi-chiller plant can be configured in three possible ways – series, parallel and hybrid. In a hybrid configuration, a set of chillers are arranged in

series while operating in parallel with another set of chillers. While majority of the chiller plants have chillers operating in parallel, a number of plants do use hybrid or series arrangement. In the following section, series and parallel chiller arrangements are discussed in detail using a two chiller system as an example.

5.2.1 Chillers in series

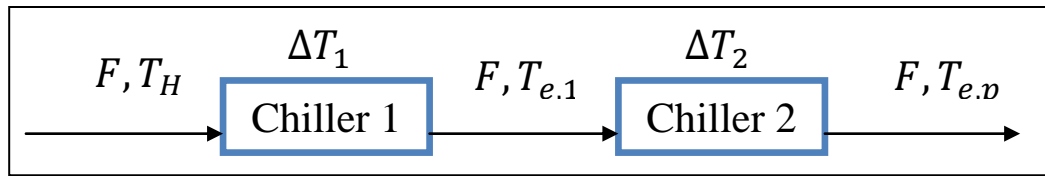


Figure 5.1: Schematic of a two-chiller system in series configuration

Figure 5.1 shows a schematic of a simple two-chiller system arranged in series. In such an arrangement, a common stream of chilled water passes through the chillers sequentially. Hence, flow rate of the chilled water is constant across all the chillers in series. But the temperature drop for the chilled water across each chiller can be different. The temperature of the chilled water stream is lowered from T_H to $T_{e,p}$ in two stages – (i) from T_H to $T_{e,1}$ by Chiller 1, and (ii) from $T_{e,1}$ to $T_{e,p}$ by Chiller 2. Cooling load for each of the series chillers can be expressed as:

$$Q_{1,series} = F * (T_H - T_{e,1}) \quad (5.1a)$$

$$Q_{2,series} = F * (T_{e,1} - T_{e,p}) \quad (5.1b)$$

By adding Equations 5.1a and 5.1b, the following relation is obtained for the total cooling load of the chiller plant:

$$Q_{Total,series} = F * (T_H - T_{e,p}) \quad (5.1c)$$

From Equation 5.1c, it can be inferred that the total cooling load in the case of series chillers depends only on the properties of the chilled water stream (flow rate and

temperature) entering and leaving the system. The cooling load is independent of state of intermediate streams (chilled water at stages in between the series chillers).

5.2.2 Chillers in parallel

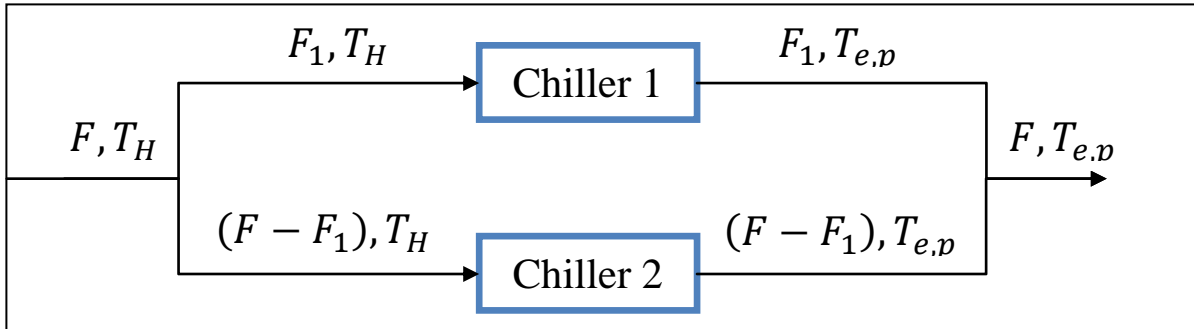


Figure 5.2: Schematic of a two-chiller system in parallel configuration

Schematic of a two-chiller system in parallel configuration is depicted in Figure 5.2. For all the chillers in parallel arrangement, the input and output streams of chilled water have the same temperature (T_H and $T_{e,p}$ respectively) and hence the temperature drops across the chillers are identical. But the flow rate of chilled water may vary across chillers. . In a two chiller parallel arrangement, the input chilled water flow F is divided into two parallel streams with flow rate F_1 and $(F - F_1)$ respectively. Each stream passes through a separate chiller where it is cooled from T_H to $T_{e,p}$. Cooling load for each chiller in this system is given by the following equations:

$$Q_{1,parallel} = F_1 * (T_H - T_{e,p}) \quad (5.2a)$$

$$Q_{2,parallel} = (F - F_1) * (T_H - T_{e,p}) \quad (5.2b)$$

By adding Equations 5.1a and 5.1b, the following relation is obtained for the total cooling load for this system:

$$Q_{Total,parallel} = F * (T_H - T_{e,p}) \quad (5.2c)$$

Even though the Equations 5.1c and 5.2c are derived for a two-chiller system, they can be assumed true for any number of chillers as the resultant expressions are independent of the number of chillers. It is evident from comparing these two equations that the total plant cooling load is a function of the flow rate and temperatures of the input and output chilled water streams, irrespective of the chiller arrangement in the plant (series, parallel or hybrid).

5.3 COMPARISON OF ENERGY EFFICIENCY – SERIES VERSUS PARALLEL

The way of distributing cooling load in a chiller plant is strongly connected to its chiller arrangement. As discussed in the previous section, the chilled water flow rate is divided among chillers if they are arranged in parallel. On the other hand, the chilled water temperature drop ($\Delta T = T_H - T_e$) is divided among the chillers in a series configuration. In case of a hybrid arrangement, first the chilled water flow rate is divided among the number of total parallel streams and then each stream consisting of more than one chiller is treated like an independent series arrangement.

Even though the cooling capacity of a chiller is irrespective of its configuration (series/parallel or hybrid), its power consumption is not. In other words, for the same cooling load, chilled water outlet temperature and condenser water inlet temperature, the power consumed by a chiller may vary with its relative position in the overall plant arrangement. Hence, the total power consumed by a plant for a given total cooling load depends on two main factors – (i) cooling load distribution among its chillers, and (ii) chiller arrangement in the plant. While the former is an operational decision which is to be taken several times in a day, the latter is a design decision which is taken either when a new plant is designed or when an existing plant undergoes retrofitting. Optimal chiller

loading, as discussed in Chapters 3 and 4, aims at making the decision of cooling load distribution to maximize the overall plant energy efficiency for a fixed chiller arrangement. However, the current chapter presents a study that compares energy efficiency of a chiller plant in series and parallel arrangements.

5.3.1 Difference in chilled water flow rate

The key difference between operating conditions of a chiller working in series or parallel configuration is its chilled water flow rate and ΔT for a particular cooling load. As described in the previous section, chilled water flow rate is higher when a chiller is working in series as compared to parallel (where the overall flow rate gets distributed among the chillers), assuming same cooling load in both cases. By making modifications to the Gordon-Ng model for centrifugal chillers (Equations 2.7 and 2.8 of MGN2 model in Section 2.3.2), it has been proposed and validated that the chiller power consumption increases with chilled water flow rate. This implies that a chiller will consume more power in series mode than in parallel mode for the same amount of cooling load. The difference in chiller power consumption in series and parallel mode was quantified by analyzing MGN1 chiller models for Chiller 12 and Chiller 32 (DMOS6, TI Dallas). Separate MGN1 model parameters for series and parallel mode of these chillers were obtained from Tables 2.1 and 2.2 (Section 2.5.2).

Chiller power consumption was plotted against cooling load for Chiller 12 (Figure 5.3) and Chiller 32 (Figure 5.4) in both operating modes – series and parallel). The values of T_e and T_c were kept constant for this analysis at 278 K and 295 K respectively. The calculations predict 9.13% to 9.62% of energy savings for Chiller 32 by switching from series to parallel mode of operation whereas Chiller 12 (DMOS6) can save between 5.97% and 7.97% of its energy usage by switching the mode.

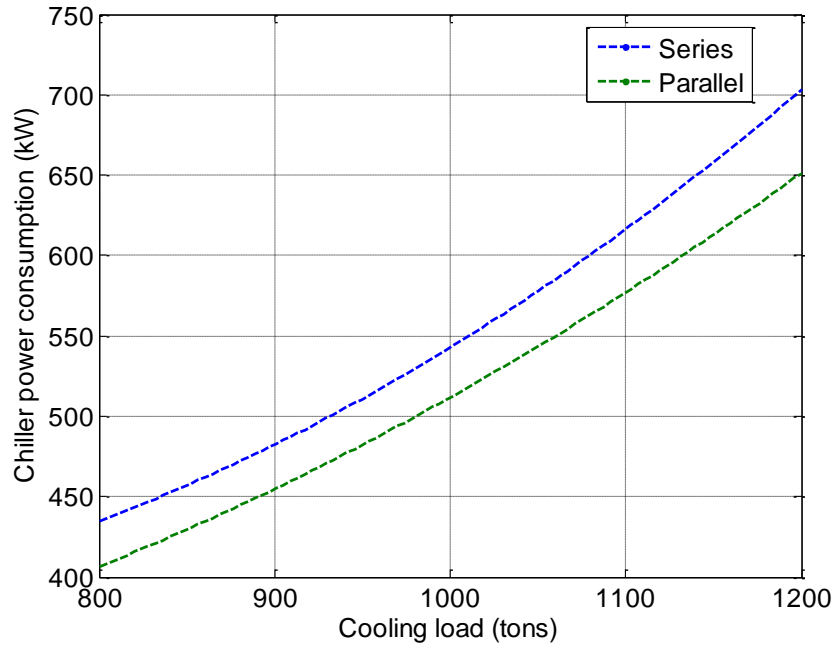


Figure 5.3: Chiller power variation with cooling load (series vs. parallel) for Chiller 12

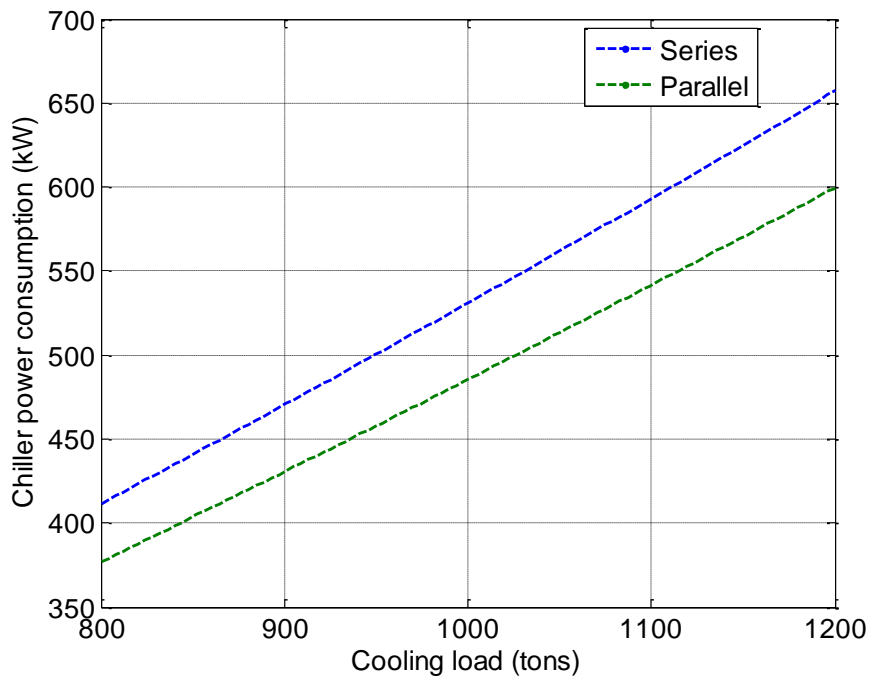


Figure 5.4: Chiller power variation with cooling load (series vs. parallel) for Chiller 32

The above analysis using real year-long data from DMOS6 chiller plant illustrates the extent by which energy efficiency of a chiller can vary by simply changing its mode of operation from series (high F , low ΔT) to parallel (low F , high ΔT).

5.3.2 Difference in chilled water outlet temperature

This section illustrates the effect of chiller arrangement on chilled water outlet temperature for each individual chiller and how the outlet temperature in turn affects the energy efficiency.

Taking the two chiller system in Figure 5.1 as an example, it is observed that the value of T_e differs among chillers in a series arrangement. While Chiller 2 (the last chiller) generates chilled water with $T_e = T_{e,p}$, Chiller 1 has $T_e = T_{e,1}$ where $T_{e,1} > T_{e,p}$. By extrapolation, the following relation is established for a series of m chillers where $T_{e,j}$ is the chilled water outlet temperature for the j^{th} chiller.

$$T_H \geq T_{e,1} \geq T_{e,2} \geq \dots \geq T_{e,j} \geq \dots \geq T_{e,(m-1)} \geq T_{e,p} \quad (5.3)$$

On the other hand, all chillers in a parallel arrangement have a common value of $T_{e,j} = T_{e,p}$. Therefore, for each chiller j , the following relation holds.

$$T_{e,j}(\text{series}) \geq T_{e,j}(\text{parallel}) \quad (5.4)$$

The dependence of a chiller's COP on its T_e was studied using Gordon-Ng model (Equations 2.3) and can be represented in the form of following equation.

$$\frac{1}{COP} = \gamma_0 + \gamma_1 * \frac{1}{T_e} + \gamma_2 * \frac{1}{T_e^2} \quad (5.5a)$$

$$\gamma_0 = -1 + \left(\frac{1}{Q}\right)(-q_c) \quad (5.5b)$$

$$\gamma_1 = \left(T_c - \frac{q_c}{M_c}\right) \left(1 + \frac{q_e}{Q}\right) \quad (5.5c)$$

$$\gamma_2 = \left(\frac{q_e}{Q} + 1\right) \frac{q_e T_c}{M_c} + T_c * (Q + q_e) \left(\frac{1}{M_c} + \frac{1}{M_e}\right) \quad (5.5d)$$

Because of positive values attained by heat transfer coefficients, rates of internal energy losses, cooling load and condenser water temperature, γ_2 is always positive (Equation 5.5d). Additionally, from the model fitting parameters of chillers at DMOS6 and at UT Austin it was observed that the order of magnitude of q_c/M_c is 10^0 whereas T_c is of the order of magnitude of 10^2 . From Equation 5.5c, this implies that the value of γ_1 is also positive. Therefore, chiller efficiency increases as T_e increases if all other factors are kept constant. To simulate this effect, Chiller 11 (DMOS6) power consumption was plotted against its cooling load for $T_e = 277K$ (parallel mode) and $T_e = 282K$ (series mode) in Figure 5.5. It shows clearly that Chiller 11 is more energy efficient at a higher T_e setpoint. This analysis estimated that by changing the value of T_e from 282 K to 277 K, the COP drops and hence the power consumption rises by 11.96% to 12.26%. Combining this result with Equation 5.4, this section concludes that a series arrangement adds to the plant energy efficiency by using higher chilled water outlet temperature for most chillers.

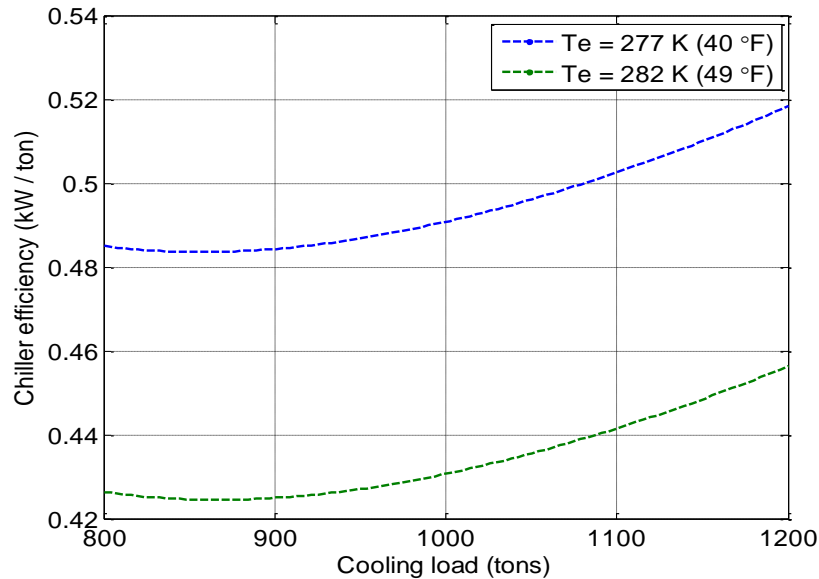


Figure 5.5: Chiller efficiency variation with cooling load for Chiller 11 for constant T_e

5.4 CONCLUSIONS

This chapter discussed different types of chiller arrangements that can be employed in a multi-chiller plant – series, parallel and hybrid. These configurations are referred to as different modes of operation from the perspective of each individual chiller. Series and parallel chiller configurations are discussed in detail and their benefits with respect to overall plant energy efficiency compared. The effects of two main differences between series and parallel arrangements (flow rate and temperature difference across individual chillers) on chiller power consumption are analyzed for this purpose.

Data obtained from DMOS6 fab for Chiller 11, Chiller 12 and Chiller 32 along with their respective models were used to validate and quantify the effect of chiller arrangement on energy efficiency. Separate models developed for series and parallel operations for both Chiller 12 and Chiller 32 (discussed in Chapter 2) are used to illustrate the effect of high chilled water flow rate on the chiller power consumption. For the systems studied in this chapter, the switch from parallel mode to series mode increases the chilled water flow rate by almost 100% which adversely affected the energy efficiency. The analysis showed that the power consumption of a chiller can rise by 9.6% by switching its mode of operation from parallel to series, while keeping the cooling load, chilled water outlet temperature and condenser water inlet temperature constant. This extra energy is lost in the form of viscous dissipation which increases with increase in volumetric flow rate of chilled water through evaporator tubes. Hence, this particular study highlighted the energy cost associated with using a series arrangement in a multi-chiller plant.

The study also revealed that the type of chiller arrangement has a significant impact on the chilled water outlet temperature setpoints (T_e) for individual chillers. Each chiller in a parallel arrangement has a common value of T_e which is the required output

chilled water temperature from the plant. Whereas in a series arrangement, T_e gradually decreases from the first chiller in series to the last chiller, taking certain values in the range $[T_{e,p}, T_H)$. It was shown by using the Gordon-Ng model equations that a higher T_e value increases the chiller efficiency. Model parameters for Chiller 11 were used to quantify the change in energy efficiency by switching its mode of operation. The chiller efficiency was plotted against cooling load for two distinct values of T_e , each corresponding to a mode of operation. This analysis showed that efficiency of Chiller 11 can drop by 12.26% by switching its mode of operation from series (current) to parallel (hypothetical).

In summary, the study revealed that series and parallel arrangements have their own pros and cons. In series configuration, the high chilled water flow rate adversely affects the efficiency, but the relatively higher chilled water outlet temperature (T_e) reduces the power consumption. However as shown in this work, the magnitude of impact on energy efficiency depends on several factors such as the model parameters of each chiller, total cooling load requirement, the number of parallel streams in a parallel or hybrid chiller plant and the number of chillers in each series arrangement. Based on the abovementioned studies, it is clear that a trade off is involved in making the decision on optimal configuration. There is no clear winner for the best chiller arrangement which would work across all chiller plants. Therefore, for every chiller plant, optimal chiller configuration should be formulated and solved as a complex optimization problem to attain the lowest possible power consumption.

Chapter 6: Conclusions and Future Work

This study illustrated various ways to model and to optimize the processes involved in large scale cooling systems in order to reduce the overall power consumption. The two main factors which affect energy efficiency of cooling systems - (i) system design and (ii) operation strategy – were both analyzed in detail. Data obtained from the chiller plants at UT Austin campus and a semiconductor fab at TI (Dallas) were used to simulate the optimal energy consumption. The optimization results obtained were then compared with the real power consumption at both sites over the year 2012.

A major part of this dissertation discusses optimizing the operation of multi-chiller plants that employ electric centrifugal chillers. Optimal chiller loading (OCL) is used to minimize the chiller plant power consumption by optimizing its cooling load distribution at regular time intervals. Formulation of OCL as a constrained optimization problem utilizes a cooling system model which evaluates the total power consumption as a function of ambient weather conditions and the cooling load distribution. Since the optimization results are based on model predictions, the accuracy and robustness of the cooling system model is paramount. Since chillers consume about 60% to 70% of the overall cooling system power consumption, this work was mainly focused on developing chiller models.

Chapter 2 describes the development and performance of three different models that compute the power consumption of an electric centrifugal chiller. The Modified Gordon-Ng 1 (MGN1) model was conceptualized by redefining the rates of internal energy losses in the Gordon-Ng model equation as variables that depend linearly on the chiller cooling load. This modification led to much better fits to a wider range of chiller data. Moving one step further, the Modified Gordon-Ng 2 (MGN2) model was proposed

to have a single model characterizing the operation of a chiller that operates in series as well as in parallel with other chillers. The MGN2 model considers the rates of internal energy losses to vary with the cooling load as well as the chilled water flow rate linearly. The model fitting results showed that MGN2 model can be used to describe a chiller's efficiency curve irrespective of its mode of operation. Further, the implicit chiller model was developed in order to compute the chiller power consumption without having to know or guess the condenser water temperature (T_c). This model uses a combination of MGN1 model, Stoecker's correlation, and energy balance around the condenser water loop of a chiller plant.

The MGN1 and MGN2 models evaluate the power consumed by each independent chiller separately. Since the objective function in an OCL problem is total power consumed by the cooling system, individual chiller model equations are added to obtain the complete system model. In multiple chiller systems, modeling errors associated with each model can accumulate, which may cancel each other to some extent if carrying opposite signs or may produce larger errors if carrying same signs. The implicit chiller model models the entire assembly of the cooling system by establishing overall energy balance equation instead of independently modeling separate components, which could reduce the total modeling error. The results showed the implicit chiller model to be fairly accurate as compared to the real plant data for most of the operating range. However, this model was shown to have certain limitations, especially during unsteady chiller operation and at high cooling loads. Addition of dynamic equations to the implicit chiller model could be explored as part of future research to overcome its shortcomings.

Chapter 4 illustrated the formulation and execution of optimal chiller loading problem for complex cooling systems based on the models developed from a large

amount of real system cooling data. Multi-period static optimal chiller loading for the UT Austin cooling system yielded annual energy savings of \$486,000 for the year 2012 assuming a constant electricity cost of 6 cents/kWh. Addition of thermal energy storage (TES) yielded a less fluctuating cooling profile and even further reduction in energy cost in case of time varying electricity prices. This research can be further continued to improve the energy efficiency of a more complex plant system, as described below.

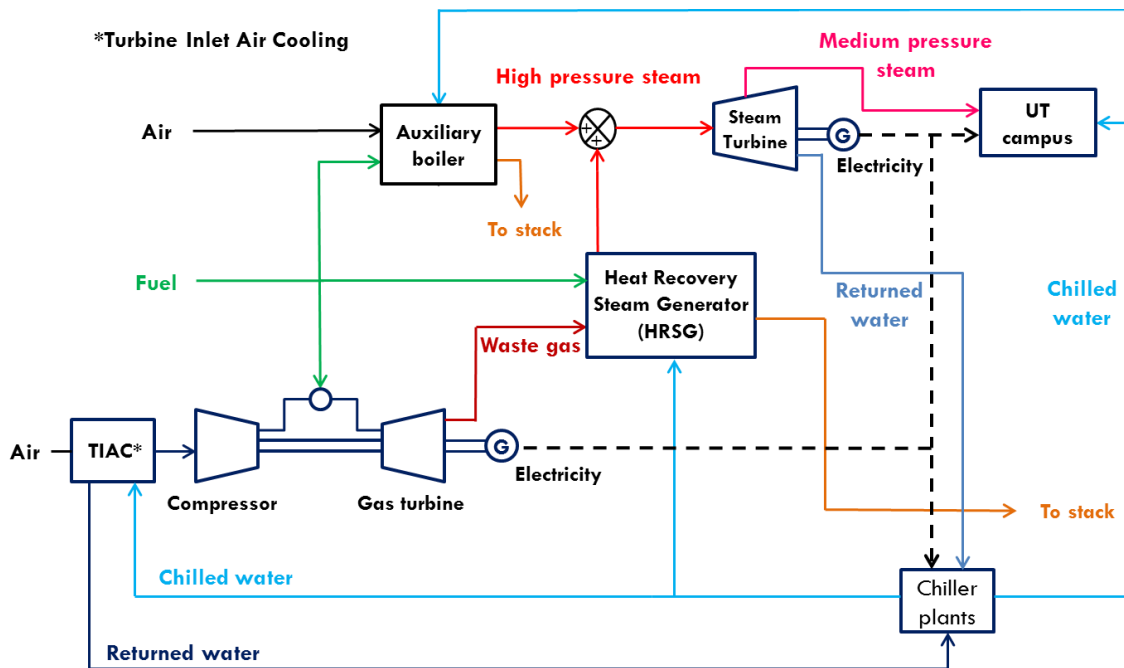


Figure 6.1: Simplified schematic of the Hal C. Weaver power plant complex at UT Austin [39]

At UT Austin, the electricity, heat and cooling networks are inter-connected to each other (Figure 6.1). Hal C. Weaver power plant produces electricity based on a combined heat and power (CHP) cycle. While part of the steam generated by the boiler and heat recovery steam generator (HRSG) is used to generate electricity, the rest of the

steam is used to provide heating to the campus. Over 30% of the annual total power generation is used to run the chiller plants that provide cooling to the entire campus. Hence, the energy efficiency of the cooling operation and the total cooling load at UT Austin has a direct impact on the electricity load of the power plant. Chapter 4 results illustrated that OCL can improve the energy efficiency of cooling operation and that addition of TES can even transform the cooling load profile. This provides an opportunity to optimize the cooling load profile with the help of TES in order to maximize the overall energy efficiency of the power plant [40].

However, the campus-wide optimal chiller loading problem can be expanded further and made more realistic by including geographical complexities to the formulation. The different locations of buildings and chiller plants in a widespread campus have a significant impact on the pumping costs, which are accountable for about 20% of the total cooling cost. Geography of buildings and chiller plants entails their relative positions and elevations. The optimal cooling load distribution among various chiller plants should result from a more complex optimization problem that includes considerations regarding distances and elevations of different areas in a campus.

Hourly power consumption values resulting from OCL were also simulated for a chiller plant at the DMOS6 fab (TI, Dallas). OCL for this system was solved for two independent scenarios – real and hypothetical. The real scenario modeled the chiller arrangement and operational constraints at DMOS6 as studied from the year-long data. The hypothetical scenario, all chillers operating in parallel, estimated greater savings on total annual power consumption (23.4%) as compared to OCL with the current configuration (3.6%). This striking difference in results obtained from the two scenarios was attributed to the possibility of modeling error in the hypothetical scenario and to the many additional physical constraints associated with the chiller plant operation in the real

case. This observation leads to two main conclusions. First, real data should be generated for the hypothetical arrangement by modifying the operating conditions and later used to update the models. Second, a parallel arrangement of all chillers (as in the hypothetical scenario) provides more flexibility in terms of the cooling load distribution and hence may result in higher energy savings as compared to a hybrid arrangement (as in the current case).

The analysis in Chapter 5 revealed that even if the difference in physical constraints is ignored, the energy efficiency of a chiller plant depends on its layout and that series and parallel arrangements have their own pros and cons. In the series configuration, the high chilled water flow rate adversely affects the efficiency, but the relatively higher chilled water outlet temperature (T_e) reduces the power consumption. However, the magnitude of impact on energy efficiency depends on several factors such as the model parameters of each chiller, total cooling load requirement, the number of parallel streams in a parallel or hybrid chiller plant and the number of chillers in each series arrangement. Optimal configuration of a chiller plant is an important design decision. It is clear that a trade-off is involved in making this decision because of the complex ways in which a configuration may affect the plant efficiency. The current research concludes that the optimal chiller configuration should be formulated and solved as an independent optimization problem for every chiller plant. However, further analysis on various chiller configurations can provide valuable guidelines which can potentially be used as basic design rules for chiller plants.

References

1. DOE. Energy Efficiency Trends in Residential and Commercial Buildings. Oct. **2008**.
2. Naughton, P.; Schrecengost, R. Cleanroom Energy Optimization Methods. Fourteenth Symposium on Improving Building Systems in Hot and Humid Climates **2004**, 5-18. Richardson, TX: SESA.
3. Hu, S.C.; Chuah, Y.K. A Study of energy and electricity consumption for high-tech industry-focused on the semiconductor industry in Taiwan area. *Report of NSC*. **2000**, 89-TPC-7-02-002.
4. Henze, G.J. Evaluation of optimal control for ice storage systems, Ph.D. dissertation, University of Colorado, Boulder, CO: Department of Civil, Environmental and Architectural Engineering, **1995**.
5. Gordon, J.M.; Ng, K.C.; Chua, H.T. Optimizing chiller operation based on finite-time thermodynamics: universal modeling and experimental confirmation. *Int. J. Refrig.* **1997**, *20*, 191-200.
6. Gordon, J.M.; Ng, K.C.; Chua, H.T. Centrifugal chillers: Thermodynamic modeling and a diagnostic case study. *Int. J. Refrig.* **1995**, *18*, 253-257.
7. Chang, Y.C. A novel energy conservation method - optimal chiller loading. *Electric Power Systems Research* **2000**, *69* (2-3), 221-226.
8. American Standard Inc. *Refrigeration Compressors*. Retrieved from NJATC: <http://www.njatc.org/downloads/trc004en.pdf>

9. Browne, M.W.; Bansal, P.K. Steady-state model of centrifugal liquid chillers: Modèle pour des refroidisseurs de liquide centrifuges en régime permanent. *Int. J. Refrig.* **1998**, *21*, 343-358.
10. Le, C.V.; Bansal, P.K.; Tedford, J.D. Three-zone system simulation model of a multiple-chiller plant. *Appl. Therm. Eng.* **2004**, *24*, 1995-2015.
11. Yik, F.H.W.; Lam, V.K.C. Chiller model for plant design studies. *Build. Serv. Eng. Res. Technol.* **1998**, *19*, 233-41.
12. Cui, J.; Wang, S. A model-based online fault detection and diagnosis strategy for centrifugal chiller systems. *Int. J. Therm. Sci.* **2005**, *44*, 986-99.
13. Reddy, T.A.; Niebur, D.; Andersen, K.K.; Pericolo, P.P.; Cabrera, G. Evaluation of the suitability of different chiller performance models for on-line training applied to automated fault detection and diagnosis (RP-1139). *HVAC Res.* **2003**, *9*, 385-414.
14. Reddy, T.A.; Andersen, K.K. An evaluation of classical steady-state off-line linear parameter estimation methods applied to chiller performance data. *HVAC Res.* **2002**, *8*, 101-24.
15. Hydeman, M.; Gillespie, K.L. Tools and techniques to calibrate electric chiller component models. *ASHRAE Trans.* **2002**, *108*, 733-41.
16. Hydeman, M.; Sreedharan, P.; Webb, N.; Blanc, S. Development and testing of a reformulated regression-based electric chiller model. *ASHRAE Trans.* **2002**, *108*, 1118-27.
17. Swider, D.J. A comparison of empirically based steady-state models for vapor-compression liquid chillers. *Appl. Therm. Eng.* **2003**, *23*, 539-56.

18. Monfet, D.; Zmeureanu, R. Ongoing commissioning of water-cooled electric chillers using benchmarking models. *Appl. Energy* **2012**, *92*, 99-108.
19. Katipamula, S.; Brambley, M.R. Methods for fault detection, diagnostic, and prognostics for building systems – a review, Part I. *HVAC Res* **2005**, *11*, 3–25.
20. Gordon, J.M.; Ng, K.C. Thermodynamic modeling of reciprocating chillers. *J. Appl. Phys.*, **1994**, *75*, 2769-2774.
21. Gordon, J.M.; Ng, K.C. A general thermodynamic model for absorption chillers: theory and experiment. *Heat Recovery Systems & CHP*, **1995**, *15*, 73-83.
22. Lee, T.-S.; Liao, K.-Y.; Lu, W.-C. Evaluation of the suitability of empirically-based models for predicting energy performance of centrifugal water chillers with variable chilled water flow. *Appl. Energy* **2012**, *93*, 583-595.
23. Ng, K.C.; Chua, H.T.; Ong, W.; Lee, S.S.; Gordon, J.M. Diagnostics and optimization of reciprocating chillers: theory and experiment. *Appl. Therm. Eng.* **1997**, *17*, 263-276.
24. Powell, K.M.; Cole, W.J.; Ekarika, U.F.; Edgar, T.F. Optimal chiller loading in a district cooling system with thermal energy storage. *Energy* **2013**, *50*, 445-453.
25. Stoecker, W. F. Procedures for simulating the performance of components and systems for energy calculations. *ASHRAE* **1976**. Atlanta.
26. Supervisory Control strategies and optimization. *ASHRAE* handbook; **1999** [Chapter 40].
27. Hackner, R.; Mitchell, J.; Beckman, W. HVAC system dynamics and energy use in buildings. *Part I, ASHRAE Trans.* **1984**, *90*, 523-535.

28. Hartman, T. Designing efficient systems with the equal marginal performance principle. *ASHRAE* **2005**, 47.
29. Ehyaei, M.A.; Mozafari, A.; Ahmadi, A.; Esmaili, P.; Shayesteh, M.; Sarkhosh, M.; Dincer, I. Potential use of cold thermal energy storage systems for better efficiency and cost effectiveness. *Energy Build.* **2010**, 42, 2296-2303.
30. Cole, W.J.; Powell, K.M.; Edgar, T.F. Optimization and advanced control of thermal energy storage systems. *Rev. Chem. Eng.* **2012**, 28, 81-99.
31. Cole, W.J.; Rhodes, J.D.; Powell, K.M.; Edgar, T.F. Turbine inlet cooling with thermal energy storage. *Int. J. Energy Res.*, in press.
32. Deng, K.; Sun, Y.; Chakraborty, A.; Lu, Y.; Brouwer, J.; Mehta, P.G. Optimal scheduling of chiller plant with thermal energy storage using mixed integer linear programming. *American Control Conference* **2013**, Washington, DC, USA.
33. Dincer, I.; Rosen, M.A. Thermal Energy Storage: Systems and Applications. *John Wiley & Sons*, **2002**.
34. Hittinger, E.; Whitacre, J.F.; Apt, J. What properties of grid energy storage are most valuable? *Journal of Power Sources* **2012**, 206, 436-449.
35. Hasnain, S.M. Review on sustainable thermal energy storage technologies, Part II: cool thermal storage. *Energy Conversion and Management* **1998**, 39, 1139-1153.
36. Rismanchi, B.; Saidur, R.; Masjuki, H.H.; Mahlia, T.M.I. Cost-benefit analysis of using cold thermal energy storage systems in building applications. *Energy Procedia* **2012**, 14, 493-498.
37. Tveit, T.-M.; Savola, T.; Gebremedhin, A.; Fogelholm, C.-J. Multi-period MINLP model for optimising operation and structural changes to CHP plants in district

- heating networks with long-term thermal storage. *Energy Convers. Manag.* **2009**, *50*, 639-647.
38. Söderman, J. Optimisation of structure and operation of district cooling networks in urban regions. *Appl. Therm. Eng.* **2007**, *27*, 2665-2676.
39. Kapoor, K.; Powell, K.M.; Cole, W.J.; Kim, J.S.; Edgar, T.F. Improved large scale process cooling operation through energy optimization. *Processes* **2013**, *1*, 312-329.
40. Powell, K.M.; Kim, J.S.; Kapoor, K.; Mojica, J.; Hedengren; J.D.; Edgar, T.F. Dynamic optimization of a district energy system with combined heat and power and thermal energy storage. *Submitted to Applied Energy*.